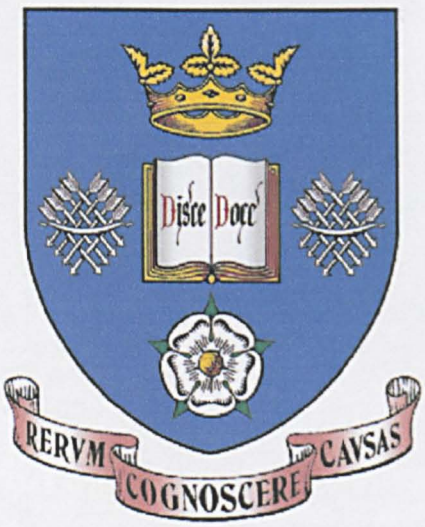

The role of PARP-1 and XRCC1 in Homologous Recombination

Kayan Marie Parker

A thesis submitted for the degree of

Doctor of Philosophy

Institute for Cancer Studies
Division of Genomic Medicine
University of Sheffield
December 2006

I hereby declare that no part of this thesis has previously been submitted for any degree or qualification of this, or any other, University or Institute of learning.

ACKNOWLEDGEMENTS

I would like to thank my supervisor, Thomas Helleday, for all the help and encouragement he has given me during the writing of this thesis, and also for the opportunity to study at the Institute for Cancer Studies.

I would also like to thank my partner, Richard Cooke, for all the support and understanding he has given me whilst studying for this PhD, and patience during the writing of this thesis. This thesis would have taken a lot longer to write without his encouragement.

A big thank you goes to my parents and family, who have always been very supportive and I know are proud of my achievements. In fact, I think everyone in Loughborough knows what I am studying! (Thanks mum).

I would like to thank Anu Kumari from the bottom of my heart for showing me all the lab techniques, and for being a really great friend. Likewise, a big thank you to the rest of 'the team', Helen Bryant, Nasrollah Saleh Gohari, Ponnari Gottipatti, Jarek Dziegielewski and Dan Flower, for good advice, looking after my cells when I was on holiday, and putting up with Radio 4.

A special thank you must go to Emma Bolderson for being a great listener and friend, and to Gordon McPherson and Jenny Shorto for always being in the tea room for a chat!

I must also thank other colleagues in the lab, Andy Platts (for all computer-related emergencies and locating great pubs), Gary Rodgers (for invaluable assistance with the microscope), Shelia Rodgers (being a great help with the PCR), Sarah Bottomley, Ian Brock, Sue Clark, and Jean Lazenby.

One person who deserves a very special mention is Helen Bryant, whose support and understanding has really helped me through. Thank you for letting me ask you the same stupid question over again, and also being a great friend.

Finally, thank you to Yorkshire Cancer Research who funded this research.

PUBLICATIONS EMERGED FROM THIS WORK

Bryant, H.E., Schultz, N., Thomas, H.D. Parker, K.M., Flower, D., Lopez, E., Kyle, S., Meuth, M., Curtin, N.J. and Helleday, T. (2005) Specific killing of BRCA-deficient tumours with inhibitors of poly(ADP-ribose) polymerase. *Nature,* 434, 913-917

Saleh-Gohari, N., Bryant, H.E., Schultz' N., Parker, K.M., Cassel, T.N. and Helleday, T. (2005) Spontaneous homologous recombination is induced by collapsed replication forks that are caused by endogenous DNA single-strand breaks. *Mol Cell Biol.,* 25 (16), 7158-69

AWARDS EMERGED FROM THIS WORK

Mutagenesis/OUP Poster award, European Environmental Mutagenesis Society Conference (2004) *Genes and Environment: Bridging the gap.*

LIST OF ABBREVIATIONS

3-AB	3-aminobenzamine
6tG	6-thioguanine (or 2-amino-6-mercaptopurine)
α-MEM	Alpha-modified eagle media
AMD	Auto-modification domain
AP	Apurinic-apyrimidinic site
APE	AP endonuclease-1
APS	Ammonium persulphate
ATM	Ataxia telangiectasia mutated protein
ATR	Ataxia telangiectasia related protein
BaP	Benzo(a)pyrene
BER	Base excision repair
BIR	Break-induced replication
BLM	Bloom's syndrome protein
BRCA1	Breast cancer gene-1
BRCA2	Breast cancer gene-2
BRCT I	Breast cancer protein 1 carboxyl terminous-1
BRCT II	Breast cancer protein 1 carboxyl terminous-2
BrdU	Bromodeoxyuridine
BSA	Bovine serum albumin
CE	Catechol oestrogen
CE-Q	Catechol oestrogen quinone
CE-SQ	Catechol oestrogen semiquinone
CHEF	Contour-clamped heterogeneous field
CPD	Cyclobutane photo-dimer
CPT	Camptothecin
CTD	C-terminal domain
DBD	DNA-binding domain
dCTP	Deoxyribose cytosine triphosphate
DNA	Deoxyribonucleic acid
DNA-PK	DNA-dependent proteinase kinase
DSB	DNA double strand break
DMEM	Dulbecco's modified eagle media
DMSO	Dimethyl sulphoxide
dT	Thymidine
EDTA	Ethylene diamine tetra acetic acid
EGF	Epidermal growth factor
EMS	Ethyl methylsulphonate
ERCC1	Excision repair cross-complementing protein 1
FBS	Foetal bovine serum
FEN1	Flap endonuclease-1
FITC	Fluoroscein isothiocyanate
G418	Geneticin
GSH	Glutathione
HAsT	Hypoxanthine azaserine thymidine medium
HJ	Holliday junction
HMG	Human motility group protein

HNE	4-hydroxynoenal
HPNCC	Hereditary non-polyposis colorectal carcinoma
HPRT	Hypoxanthine phosphoribosyl transferase
HR	Homologous recombination
HRR	Homologous recombination repair
HU	Hydroxyurea
ISQ	1,5, dihydroxyisoquinoline
LET	Linear energy transfer
LOH	Loss of heterozygosity
LTGC	Long tract gene conversion
MDA	Malondialdehyde
MNNG	N-methyl-N-nitro-nitrosoguanidine
MMS	Mis-match repair
MMS	Methylmethanesulfonate
MRN	Mre11/RAD50/Nbs1 complex
NAD	Nicotine adenine dinucleotide
NEAA	Non-essential amino acids
NER	Nucleotide excision repair
NHEJ	Non-homologous end-joining
NLS	N-laurylsarcosine
NLS	Nuclear localisation signal
PAH	Poly aromatic hydrocarbon
pADPr	Poly(ADP-ribose)
PARG	Poly(ADP-ribose) glycohydrolase
PARP-1	Poly(ADP-ribose) polymerase-1
PARP-2	Poly(ADP-ribose) polymerase-2
PARP-3	Poly(ADP-ribose) polymerase-3
PBS	Phosphate-buffered saline
PBS-T	Phosphate-buffered saline, with Tween-20
PCNA	Proliferating cell nuclear antigen
PCR	Polymerase chain reaction
PDGF	Platelet-derived growth factor
PFGE	Pulsed-field gel electrophoresis
PMSF	Phenylmethyl sulphonyl fluoride
RCS	Reactive carbonyl series
RDR	Recombination-dependent replication
RF	Replication fork
RNA	Ribonucleic acid
ROS	Reactive oxygen species
RPA	Replicating protein A
RT-PCR	Reverse transcriptase-PCR
SAM	S-adenosylmethione
SCE	Sister chromatid exchange
SCID	Severe combined immunodeficiency
SDS	Sodium lauryl sulphate
SSA	Single-strand annealing
STGC	Short tract gene conversion
TLS	Translesion synthesis

Top1	Topoisomerase-1
Top2	Topoisomerase-2
UV	Ultra-violet
WRN	Werner's syndrome protein
XPA	Xeroderma pigmentosa complementation group A
XPB	Xeroderma pigmentosa complementation group B
XPC	Xeroderma pigmentosa complementation group C
XPD	Xeroderma pigmentosa complementation group D
XPE	Xeroderma pigmentosa complementation group E
XPF	Xeroderma pigmentosa complementation group F
XPG	Xeroderma pigmentosa complementation group G
XRCC1	X-ray cross-complementation group-1
XRCC2	X-ray cross-complementation group-2
XRCC3	X-ray cross-complementation group-3
XRCC4	X-ray cross-complementation group-4

LIST OF FIGURES

SUMMARY

In this thesis, the role of PARP-1 and XRCC1 in camptothecin (CPT) induced homologous recombination (HR) has been elucidated. The aims of this study were to investigate the role of PARP-1 and XRCC1 in the repair of CPT-induced damage, to find out if PARP-1 was involved in single strand break (SSB) repair, and to investigate the role of PARP inhibitors in the repair of CPT-induced damage.

Cells lacking PARP-1, and wildtype cells treated with PARP inhibitors, were found to have increased sensitive to CPT. This increased sensitivity was found to correlate to an increased amount of DNA double-strand breaks (DSBs), and an increased number of cells containing RAD51 foci. This is an indication of an increased amount of HR in these cells.

Cells deficient in XRCC1 were also found to have an increased sensitivity to CPT, increased levels of DSBs and an increased number of cells containing RAD51 foci. A mutant XRCC1 cell line containing a disrupted BRCT I motif showed even further sensitivity to CPT. This motif interacts with PARP-1, and when disrupted, seems to inhibit the protein in some way.

We have concluded that in the absence of PARP-1 or XRCC1, the repair of SSBs is slower. These breaks are therefore more likely to encounter the replication machinery, where they become DSBs. These breaks are repaired by HR. Cells that lack both PARP-1 and XRCC1 may have even slower SSB repair, as they have an increased amount of cells containing RAD51 foci, which indicates increased HR. PARP inhibitors used in conjunction with CPT increases the cytotoxicity of CPT, which could help in chemotherapy. In the future, maybe inhibiting XRCC1 as well could further enhance this affect.

CHAPTER 1: INTRODUCTION

CHAPTER 1: INTRODUCTION

1.1 General Introduction

Our DNA is constantly bombarded by a combination of exogenous and endogenous DNA damaging agents (Friedberg *et al*, 1995). There are a number of different DNA lesions, each resulting from one of three main causes. These are environmental agents, such as ultraviolet (UV) light (Tornaletti & Pfeiffer, 1996), by-products of normal cellular metabolism, like reactive oxygen species (hydroxyl radicals, hydrogen peroxide and superoxide anions) (Clopton & Saltman, 1995), and spontaneous lesions, like the deamination and hydrolysis of nucleotide residues (Cadet, 1994). Eukaryotic cells have evolved highly conserved repair pathways to deal with all three types of damage.

1.1.1 DNA damage

During a human lifetime, the body's cells undergo approximately 10,000 trillion cell divisions. Even in an environment free of mutagens, there will be an estimated rate of 10^6 mutations per gene, per cell division. This is due to inaccuracies during DNA replication and repair. Therefore, during that lifetime, it is likely that every single gene will have undergone mutation on about 10 billion separate occasions. Among the resulting mutant cells, it could be expected that many would show defects in genes that regulate cell division, and could therefore become cancerous. The fact that 100% of the population does not have cancer seems to be evidence that a single mutation is not enough to make a healthy cell into a cancerous one. A series of sequential mutational

events have to occur in order for normal cells to alter to a state of uncontrolled proliferation, which leads to tumour formation.

The human cell cycle can be divided into four stages, G1, S, G2 and M. In order for cells to produce exact copies of themselves, this process is strictly regulated by checkpoints. Therefore, there is a checkpoint just before DNA replication (the G1/S checkpoint), during replication (the intra-S checkpoint) and before entering mitosis (the G2/Mcheckpoint). If damage to the DNA is discovered during one of these checkpoints, the cell cycle is arrested while repair is carried out. When the damage is repaired, the cell cycle continues. If the damage is too extensive, the cell goes through programmed cell death (apoptosis) (van Gent *et al*, 2001).

DNA damage initiates a chain of phosphorylation events to activate downstream effectors. Double-stranded breaks in the DNA are processed by the MRN complex which cause ATM to become phosphorylated (Uziel *et al*, 2003). The ATM protein then phosphorylates p53 (Nakagawa *et al*, 1999). The p53 protein then activates p21 which binds to a cyclin-cdk heterodimer and inhibits the CDK protein kinase activity. This blocks the cell cycle from progressing. If the DNA damage occurs in during G1, it is the cylinE-cdk2 heterodimer that is inhibited (Koff *et al*, 1992). If the DNA damage occurs in the G2 phase of the cell cycle, it is the cyclin A/B-cdk1 heterodimer that is inhibited (Draetta *et al*, 1989). ATM can also phosphorylate Chk1 and Chk2, two proteins involved in cell cycle arrest at the G2/M checkpoint .

ATM is not only responsible for downstream arrest of the cell cycle. ATM also phosphorylates BRCA1 in response to DNA double-strand breaks (Cortez *et al*, 1999). BRCA forms foci with Rad51 and has a role in repair of DNA double strand breaks (DSBs). ATM also has a role in apoptosis. By phosphorylating p53, it prevents the binding of Mdm2, the negative inhibitor of p53. This increases the transcriptional activation of p53 for pro-apoptotic factors, FAS, PUMA and BAX which lead to the death of the cell.

1.2 Factors that lead to DNA damage

There are many factors both intrinsic to the human body and in the environment that surrounds us, which could lead to a mutation within a cell. Mutations can be inherited that either cause cancer or predispose a person to developing cancer. Endogenous factors, such as mistakes during DNA synthesis, also play a role, as do exogenous factors, such as radiation or genotoxic chemicals, which can enter the body and cause mutations.

1.2.1 Endogenous factors

The vast majority of mutations in the body are of endogenous origin (De Bont & van Larebeke, 2004; Jackson & Loeb, 2001). These are caused by processes such as hydrolysis, exposure to reactive oxygen species, free radical production by oestrogens, methylation, deamination, poor proofreading by DNA polymerases, and carboxyl stress.

1.2.2.1 Hydrolysis

The glycosidic bond between DNA bases and the deoxyribose sugar is labile under certain conditions, such as heating, alkylation of the bases, or activation of N-glycosylases (Lindahl & Barnes, 1992). The cleavage of these bonds leads to the formation of abasic sites, or apurinic-apyrimidinic (AP) sites, which are among the most common lesion found in DNA. There are an estimated 10,000 AP sites formed, per human cell, per day (Lindahl, 1993).

Typical AP sites induce base pair substitutions, usually an AP site is converted to thymine, but can also sometimes induce a frameshift mutation. AP sites are mutagenic due to the preferential incorporation of adenine opposite abasic sites by DNA polymerase during replication.

1.2.1.2 Oxidative DNA damage

Reactive oxygen species (ROS) are generated constantly by the body as a consequence of metabolic and biochemical reactions, and cause the majority of the DNA damage in a cell (Jackson & Loeb, 2001). ROS are produced through a variety of endogenous processes, such as mitochondrial respiration, and neutrophil and macrophage activation. ROS include superoxide (O_2^-), hydrogen peroxide (H_2O_2), hydroxyl radicals (OH^+), and singlet oxygen ($^1O_2$). Neutrophils produce oxygen bursts of superoxide and hydrogen peroxide, which interact to form hydroxyl radicals, whilst macrophages produce superoxide and nitric oxide. These ROS oxidise DNA, which can lead to oxidised bases and single- and double strand breaks. In fact, many studies have found a relationship

between inflammatory diseases, where these white blood cells are activated, and cancer. The oxidation of bases by ROS can lead to mispairing during replication., For example, one oxidative DNA adduct, 8-oxodeoxyguanine, pairs preferentially with cytosine instead of guanine and causes GC to TA transversions.

1.2.1.3 Lipid oxidation

The polyunsaturated fatty acids of phospholipids are very sensitive to oxidation, and form lipid hydroperoxides. These are quickly reduced to unreactive fatty acid alcohols or react with metals to produce aldehydes, such as 4-hydroxynoenal (HNE) and malondialdehyde (MDA). These can then form exocyclic adducts, which damage DNA by blocking the base-pairing region. For example, HNE reacts with DNA and modulates the expression of genes that are involved in cell cycle control and apoptosis.

1.2.1.4 Endogenous oestrogens

Several oestrogen metabolites can cause DNA damage directly or indirectly, through redox recycling processes that generate reactive radical species (Yager & Liehr, 1996). Oestrogen metabolites, particularly catechol oestrogens (CEs), are involved in the initiation process through oxidative DNA damage, and also enhance cell proliferation, which leads to tumour promotion. Oestrogen-induced direct or indirect DNA damage includes single-strand breaks, 8-hydroxylation of guanine bases, bulky DNA adducts, estradiol-induced MDA adducts and oestrogen-DNA adducts (Liehr, 2000).

Direct DNA damage is caused by CEs that have been oxidised to semiquinones (CE-SQ) or quinones (CE-Q) by redox cycling. CEs are formed by the oxidation of oestrogens, and are inactivated by specific enzymes. If this process is incomplete the CEs may be oxidised to CE-SQ or CE-Q. CE-Q is inactivated by conjunction with glutathione, or reduction to CE. If either of these inactivation processes are incomplete, the CE-2,3-Q can interact with DNA and form adducts, that remain in the DNA unless repaired. These adducts are lost from the DNA by cleavage of the glycosidic bond, which leaves an AP site.

Indirect DNA damage can be caused by redox cycling generated by the enzymatic reduction of CE-Q to CE-SQ, and subsequent autoxidation back to CE-Q by oxygen, as this leads to the formation of superoxide and hydroxyl radicals. Oestrogens also cause the proliferation and activation of macrophages, which produce superoxide and nitric oxide.

1.2.1.5 Endogenous alkylating agents

Endogenous methylating agents, such as S-adenosylmethionine (SAM) betaine and choline, have a role in the regulation of gene expression by contributing to enzymatic DNA methylation (Holliday & Ho, 1998). However, non-enzymatic methylation can also occur, which can generate mutagenic adducts such as 7-methylguanine, 3-methyladenine and 0^6-methylguanine. These adducts can lead to the formation of mutagenic abasic sites (7-methylguanine) or block replication (3-methyladenine). 0^6-methylguanine causes GC to AT transitions during replication.

1.2.1.6 Hydrolytic deamination

DNA bases, particularly cytosine and 5-methylcytosine, are susceptible to hydrolytic deamination (Lindahl, 1993), which is when the exocyclic amino group of the base is lost. The deaminated form of cytosine is uracil, and this is rapidly excised by uracil-DNA glycohydrolase to generate a base-free site, which is then repaired. The deaminated form of 5-methylcytosine is thymidine, and forms a GT base pair, which is corrected by mismatch repair. However, this is a slow process, and often causes a GC to AT transition.

Figure 1.2.1.6 Deamination of DNA bases

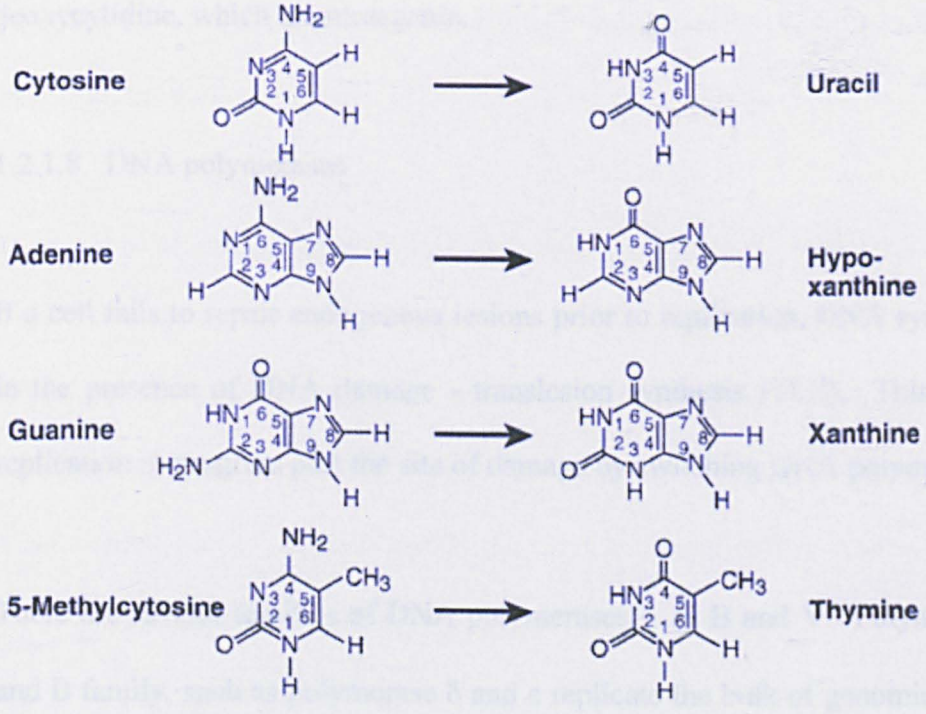

Guanine and adenine are deaminated to xanthine and hypoxanthine respectively, but at a much lower frequency than cytosine (Karran & Lindahl, 1980). Hypoxanthine pairs with C rather than T and as hypoxanthine can cause a mutagenic lesion. Xanthine pairs with C, so is less mutagenic; however the xanthine-deoxyribose bond can be easily hydrolysed, generating an AP site.

1.2.1.7 Carbonyl stress

Reactive carbonyl species (RCS) are formed by endogenous chemical processes, such as lipid peroxidation and glycation (Roberts et al., 2003), and mediate cellular carbonyl stress. RCS include glyoxal and methylglyoxal, which are reactive aldehydes formed as the result of glucose metabolism. These form DNA adducts such as glyoxalated deoxycytidine, which are mutagenic.

1.2.1.8 DNA polymerases

If a cell fails to repair endogenous lesions prior to replication, DNA synthesis proceeds in the presence of DNA damage - translesion synthesis (TLS). This process allows replication to progress past the site of damage by switching DNA polymerases.

There are several families of DNA polymerases – A, B and Y. Polymerases of the A and B family, such as polymerase δ and ε replicate the bulk of genomic DNA and have been streamlined for processivity and accuracy – they have a proofreading ability of < 20 errors per million bases. These polymerases fit the DNA substrate tightly into

their active site, where the replicating base pair is enclosed by the finger domain. They use a system called the induced-fit mechanism to check the fidelity of replication – the fingers can only close when the correct base is incorporated into the DNA. If the wrong base is incorporated, the polymerase undergoes conformational distortion of its active site, which causes it to pause replicating. The polymerase then proofreads the wrong base and removes it so that synthesis can resume.

Polymerases from the Y family, such as polymerases ι and η, have less good proofreading than A/B family DNA polymerases and have a high error rate when replicated non-damaged DNA. They can also synthesise DNA across and past a variety of template lesions (Eckert & Opresko, 1999). Y-family DNA polymerases have a unique carboxyterminal domain which forms a spacious active site, allowing the DNA substrate through a few largely non-specific contacts. Therefore they can tolerate DNA substrate distortions.

During translesion synthesis, the A/B family polymerase comes across an impassable lesion, such as an abasic site, and pauses. It then switches with a Y-family polymerase, which simply bypasses the lesion, inserting a base opposite, which is the Watson-Crick partner to the base 5' to the abasic site. This usually results in -1 frameshift mutation or a base substitution. The A/B family polymerase then switches place with the Y-family polymerase to resume replication (Lehmann, 2002).

1.2.2 Exogenous factors

1.2.2.1 Ionising radiation

Ionising radiation involves high energies and as electrons are ejected from molecules charged particles - ion pairs – are formed. These often break down to form highly reactive free radicals. There are two classes of ionising radiation – particulate (involving β particles, neutrons and α particles), and electromagnetic (involving x-rays and γ rays). Both classes produce ionisation, but the way in which it is produced, and the patterns are different.

Sets of ion pairs can be spaced close together or far apart, and the average energy released per unit distance is called linear energy transfer (LET). The LET depends on the energy and charge of a particle – the greater the charge and lower the velocity, the greater the LET. High LET radiation (α particles or neutrons) produces dense sets of ion pairs, and is more potent than low LET radiation (β particles, x-rays or γ rays) because of its more disruptive effects on proteins, RNA and DNA.

The free radicals produced by ionising radiation can cause single and double strand breaks in the DNA. These radicals can oxidise guanine to 8-hydroxyguanine, and generate abasic sites or strand breaks in the DNA, which result in miscoding if left unrepaired. Radiation is very effective at producing breaks in chromosomes (Carrano and Wolff, 1975). These breaks often lead to chromosome translocations, which can lead to the activation of certain oncogenes.

1.2.2.2 Non-ionising radiation

Non-ionising radiation, which includes ultraviolet light (UV), microwaves and radio waves, does not produce ions, but causes molecular excitations such as vibrations and electron movement. This form of radiation is not as potent as ionising radiation, but UV light can still cause damage to DNA. When DNA absorbs a UV photon, it forms an extra chemical bond between two adjacent pyrimidines, resulting in thymidine-thymidine, cytosine-cytosine, or thymidine-cytosine dimers. These can be in the form of cyclobutane pyrimidines dimers, where bonds are formed between the C5 and C6 carbons of the two bases, or a 6-4 photoproduct, where a single bond is formed between the C6 carbon of one base, and the C4 carbon of the other.

Figure 1.2.2.2 The formation of pyrimidine dimers and 6-4 photoproducts

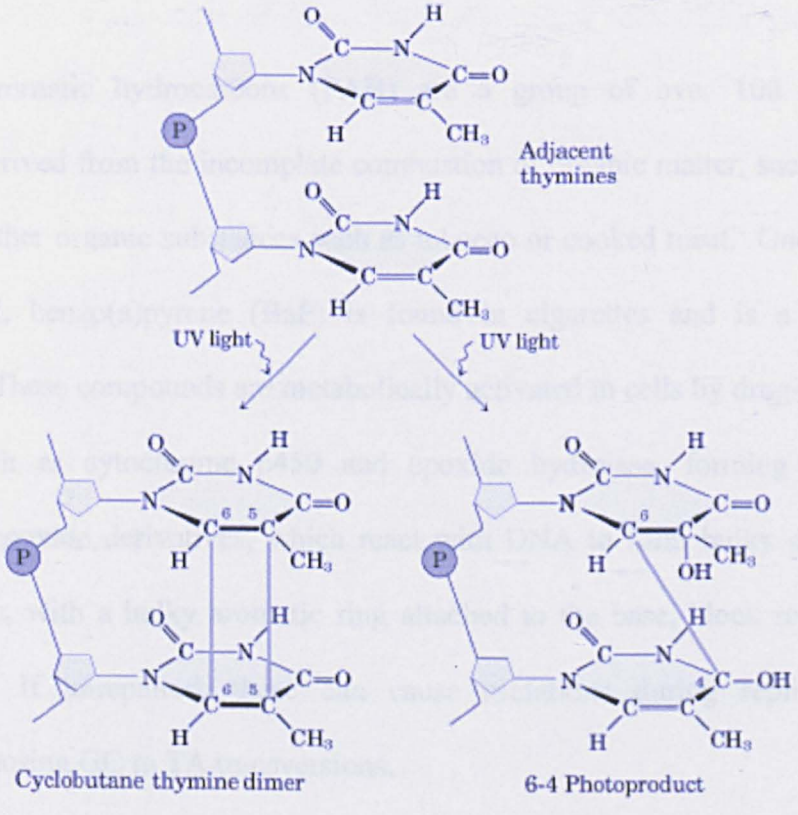

C-T transitions are formed if a cytosine is a component of the dimer, as it is read as a thymidine, and an adenine is matched with a cytosine dimer, instead of a guanine. If this mutation occurs inside a gene that regulates cell division, the cell could become prone to malignancy.

1.2.2.3 Genotoxic compounds

The genotoxic compounds can be grouped into four major classes, polycyclic aromatic hydrocarbons, aromatic amines, nitrosamines and alkylating agents. These all act by forming covalent adducts with DNA bases, which distort the DNA structure and disrupt DNA replication.

1.2.2.3.1 Polycyclic aromatic hydrocarbons

Polycyclic aromatic hydrocarbons (PAH) are a group of over 100 carcinogenic chemicals, derived from the incomplete combustion of organic matter, such as coal, oil and gas, or other organic substances such as tobacco or cooked meat. One extensively studied PAH, benzo(a)pyrene (BaP) is found in cigarettes and is a potent lung carcinogen. These compounds are metabolically activated in cells by drug-metabolising enzymes such as cytochrome p450 and epoxide hydrolase, forming electrophilic dihydrodiol epoxide derivatives, which react with DNA to form bulky adducts. The DNA adducts, with a bulky aromatic ring attached to the base, block replication and transcription. If unrepaired, these can cause mutations during replication, most commonly causing GC to TA transversions.

1.2.2.3.2 Aromatic amines

Aromatic amines include phenols, hydroquinones, and catechols, which are found in hair dye, fungicides, rubber, food and cigarette smoke. These can be converted to quinones by N-oxidation catalyzed by monooxygenase or peroxidase enzymes, such as hepatic cytochrome P450 or nonhepatic peroxidases, and in some cases molecular oxygen. Aromatic amine N-cation radicals formed by peroxidases were found to co-oxidise GSH or NADH and form reactive oxygen specie, which leads to DNA adduct formation.

1.2.3.3.3 Nitrosamines

Nitrosamines are commonly occurring agents, formed from their chemical precursors, amines and nitrosating agents via a simple chemical reaction. Nitrosamines are used as preservatives in processed foods to prevent the growth of toxic bacteria, and are also found in cigarette smoke. Nitrosamines, nitrite and nitrate salts all metabolise to form nitrous acid, which is a deaminating agent that accelerates the rate of base deamination in the cell.

1.2.2.3.4 Alkylating agents

Alkylating agents, such as N-methyl-N-nitro-nitrosoguanidine (MNNG) and methylmethanesulfonate (MMS), interfere with DNA by adding methyl groups onto DNA bases. MNNG and MMS add methyl groups to guanine to form O^6 methylguanine, causing G-C to A-T transitions. Alkylating agents belong to a family of anticancer drugs that inhibit cancer cell growth.

1.3 DNA damage-inducible cell signalling

1.4 DNA repair mechanisms

The DNA damage encountered by the genome does not go unchecked. The DNA in the cells is constantly monitored by DNA damage recognition proteins, which trigger a number of repair pathways to eliminate damage. When DNA lesions are detected, a cascade of events occurs in order to respond to and repair DNA lesions. Sensor proteins detect any damage and activate transducer proteins, which amplify and branch out the DNA-damage signals to trigger the proper response.

Dividing cells respond to DNA damage in the G1 or S-phase of the cell cycle stopping the advance of the cell cycle, preventing entry and progression in the S-phase. This provides time for DNA repair before the arrival of the DNA replication machinery. If DNA damage takes place in the G2-phase, progression into the M-phase is stopped in order to prevent mis-segregation of chromosome fragments (Zhou & Elledge, 2000; Khanna & Jackson, 2001). These points in the cell cycle are called checkpoints and are regulated by proteins such as p53 (Kuerbitz *et al.*, 1992). If the damage is too great to repair, the cell enters into an apoptotic cascade (Martin & Schwartz, 1997).

A single repair process cannot cope with all types of DNA damage, so mammalian cells have several overlapping DNA repair pathways, evolved to repair different types of damage. These are translesion synthesis (TLS), mismatch repair (MMR), base excision

repair (BER), nucleotide excision repair (NER), non-homologous end joining (NHEJ) and homologous recombination (HR).

1.3.1 Translesion synthesis

Translation synthesis (TLS) is a way for the cell to bypass mutations, such as cyclobutane pyrimidine dimers, and then either correct them or incorporate them into the daughter strands (Eckert & Opresko, 1999). In this process, replication is stalled by a mutated base, activating a second set of DNA polymerases known as the Y-family polymerases. These special polymerases can bypass the mutation but can cause errors in the new daughter strand, which can be either non-mutagenic or mutagenic. However, using the error prone polymerases can be a potential benefit to the cell because they allow replication to continue (Cox *et al.,* 2000) and sometimes tolerance of the DNA damage is preferable to cell death..

TLS occurs in two stages, first a nucleotide is inserted opposite the damaged base or bases, and then the DNA strand is extended beyond the lesion (Lehmann, 2002). The Y-family group lack exonuclease proofreading activity which is why they tend to be error-prone. These polymerases are able to bypass UV-induced cyclo-butane pyrimidine dimers (6-4) photodimers, 8-oxoguanine and O-6-methylguanine (Lehmann, 2002). One of the Y polymerases, DNA polymerase η (polη) is encoded by the XPV gene in humans and its mutation induces a variant form of Xeroderma pigmentosum (XP-V). XP-V patients are UV sensitive and susceptible to a high incidence of skin cancer (Yamada *et al.,* 2000).

1.3.2 Mis-match repair

When mismatched bases are incorporated into the DNA, they will lead to mutations in the cell, and potentially lead to the formation of a mutant cell. Therefore such errors have to be repaired. Errors can be repaired via MMR, which recognises and corrects mispairs and insertions that have occurred during DNA replication and recombination. MMR can correct non-Watson-Crick base pairing and small distortions produced by the incorrect alignment of DNA strands. There are two forms of MMR, long patch MMR and short patch MMR. Excision and resynthesis of more than 1 kb of DNA occurs in long patch MMR (O'Driscoll & Jeggo, 2002), whilst short patch MMR mechanism removes single base mismatches.

MMR happens in three stages. First the mismatch must be recognised, and in mammalian cells, this is done by the hMutSα or hMutSβ proteins (O'Driscoll & Jeggo, 2002). The hMutSα heterodimer is made up of hMsh2 and hMsh6 and is preferentially involved in single base repair mismatches. The hMutSβ complex includes hMsh6 and hMsh3, and deals with two or more mismatched bases. Secondly, the mismatched base, or bases, must be excised. Single base mismatches are probably excised by hExo1 and an unknown helicase removes the sequences containing two or more mismatch bases. Thirdly, the produced gap must be filled and religated. In humans, DNA ploymerase δ possibly fills the gap and DNA ligase I seals the generated nicks (Bennett *et al.*, 1997). Other proteins implicated in the MMR pathway are proliferating cell nuclear antigen (PCNA), which serves as cofactor for DNA polymerase δ, and replicating protein A (RPA) (Umar *et al.*, 1996).

1.3.3 Base excision repair

Base excision repair (BER) repairs nucleotides damaged by free radical oxidation, methylation, or hydroxylation, incorrect bases, and single strand breaks (SSBs). Left unrepaired, this damage may result in miscoding and mutations. Two of the most frequent spontaneous lesions are depurination and deamination. Depurination interferes with the glycosidic bond between the adenine or guanine and the deoxyribose sugar, resulting in the loss of the bases from the DNA. The deamination of cytosine results in the formation of uracil and the deamination of 5-methylcytosine forms thymine (Blount *et al.*, 1989).

The incorrect base is initially removed from the DNA backbone by an appropriate glycosylase, producing an abasic AP site. The deoxyribose phosphate 5' to the damaged base is then cleaved by AP endonuclease (APE1) creating a 3'-OH terminus. In the short-patch BER pathway, which is dominant in mammalian cells, the polβ enzyme removes the sugar residue and fills the one-nucleotide gap (Hoeijmakers, 2001). In long-patch BER, polβ, and polδ or polε, as well as PCNA, synthesise 2-10 base pairs and FEN1 removes the displacing DNA flap. Finally, the remaining nick is sealed by DNA ligase III or DNA ligase I in short-patch BER and long-patch BER, respectively.

1.3.4 Nucleotide excision repair

Nucleotide excision repair (NER) involves a large number of enzymes and removes any mismatched bases, UV-induced pyrimidine dimers, and bulky adducts. These forms of damage generally obstruct transcription and the normal replication progress, and interfere with base pairing. NER recognises damaged regions based on their abnormal structure and excises the DNA strand containing the damage, filling the gap by replication. In mammals, XPC (together with hRAD23α/β) recognises the lesion. Then, the XPB and XPD helicase subunits in the transcription factor TFIIH open up the base pairs around the lesion (Hoeijmakers, 2001) to create an open region of 20-30 nucleotides. This is then excised on the 3' side by the exonuclease, XPG and on the 5' side by another endonuclease, XPF, aided by ECCR1 (excision repair control component). After excision, the gap is filled by DNA polymerase δ or ε, DNA ligase and proliferation control nuclear antigen (PCNA). In the case of UV damage, XPE aids TFIIH in the repair process.

1.3.5 Recombinational repair

There are several types of lesions thought to induce recombinational repair, one-ended DNA strand breaks (DSBs), two-ended DSBs, and stalled replication forks (RFS) (*Figure 1.3.5*). The ways in which they are produced and the pathways that are triggered by each are discussed below in detail, but briefly these lesions are repaired by homologous recombination (HR) or non-homologous end-joining (NHEJ). These are two different and complementary mechanisms with overlapping roles in DNA repair.

The contribution of each pathway in DNA repair depends on the type of damage, and the phase of cell cycle. There is competition between the two pathways, for example, cells defective for NHEJ enzymes such as Ku protein had increased HR (Pierce *et al.*, 2001). Also if NHEJ fails, HR may take over and compensate for the repair (Frank-Vaillant & Marcand, 2002).

During late S and G2 phase both HR and NHEJ are active, while in other phases NHEJ predominates. Compared to wildtype cells, cells defective in HR proteins, such as RAD54 and XRCC2, show relatively unchanged levels of sensitivity to ionising radiation as they pass through the cell cycle as compared to wild type cells (Takata *et al.*, 1998). DNA damage caused by ionising radiation is mostly repaired by NHEJ, implying that NHEJ remains intact in all phases of the cell cycle. Late S and G2-phase are the only phases in which HR can be used because it is only then that sister chromatids are available to serve as donor templates (Arnaudeau *et al*, 2001).

Two-ended DSBs are caused by ionising radiation (X-rays and gamma rays) (*Figure 1.3.5a*). Free radicals during normal cellular metabolism may also cause two-ended DSBs. About 1% of the oxygen we breathe is converted into oxidative free radicals (Chance *et al.*, 1979). The DNA double helix breaks and the chromatin structure cannot keep the two DNA ends together. This particular lesion is deadly to the cell and must be repaired immediately. A single unrepaired chromosomal break is enough to kill a cell (Huang *et al.*, 1996).

Figure 1.3.5. Three possible substrates for recombination in mammalian cells

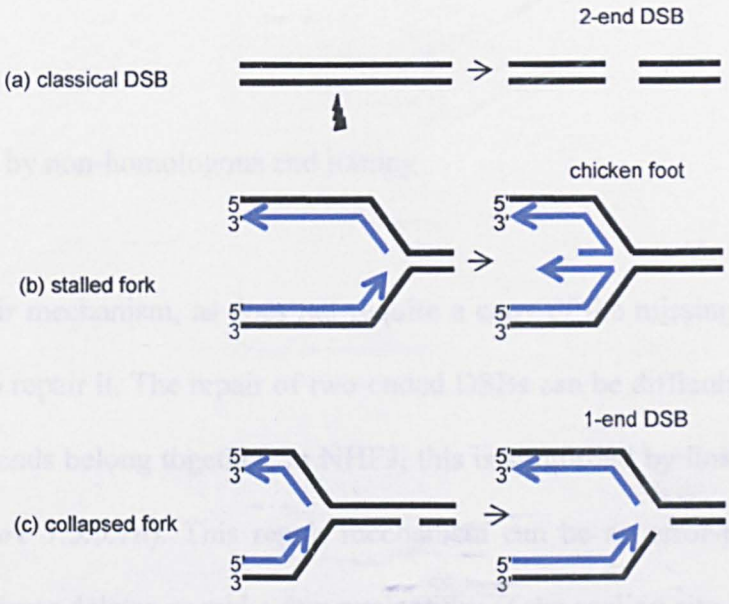

(a) DNA damage causes a break in both strands of DNA and leaves a classical DSB with two free ends. (b) Following the stall of the replication fork, the newly synthesized DNA strands reverse and form a chicken foot structure. (c) When replication machinery collides with a SSB, it causes the RF to collapse and creates a DSB with a single free end.

HR has been suggested to be associated with the repair of stalled RFs (Lundin *et al.*, 2002) (*Figure1.3.5b*). When a RF stalls, the newly synthesized DNA strands reverse and generate a structure called a chicken foot. This may serve as a substrate for HR (McGlynn and Lloyd 2002). As the DNA replication machinery encounters damage in the DNA template it may stall the RF (Kogoma *et al.*, 1996). A collision between the RF and a SSB can collapse the RF and change the lesion to a one-end DSB, which is also a substrate for HR (*Figure 1.3.5c*). Following the detection of a DSB, a cascade of

events is triggered resulting in cell cycle arrest and the activation of the repair machinery.

1.3.5.1 DSB repair by non-homologous end joining

NHEJ is a fast repair mechanism, as does not require a copy of the missing part of the sequence in order to repair it. The repair of two-ended DSBs can be difficult, as the cell has to know which ends belong together. In NHEJ, this is simplified by linking the two ends together (*Figure 1.3.5.1a*). This repair mechanism can be an error-prone repair pathway as it sometimes deletes or add a few nucleotides at the sealing site. During the repair process, the DNA bases at the DSB ends become damaged, and must be removed. The MRN (Mre11/RAD50/Nbs1) protein complex removes the damaged bases by endonuclease and exonuclease activity (D'Amours and Jackson 2002). The DSB ends must be held in proximity to each other (synapsis) to allow repair. In order to do this, two flexible colloid coils of RAD50 protein dimerise using a Zn^{2+} ion (Lieber *et al.*, 1988; Agrawal & Schatz, 1997) and act as arms to bring the two broken ends together.

Figure 1.3.5.1 DSB repair pathways.

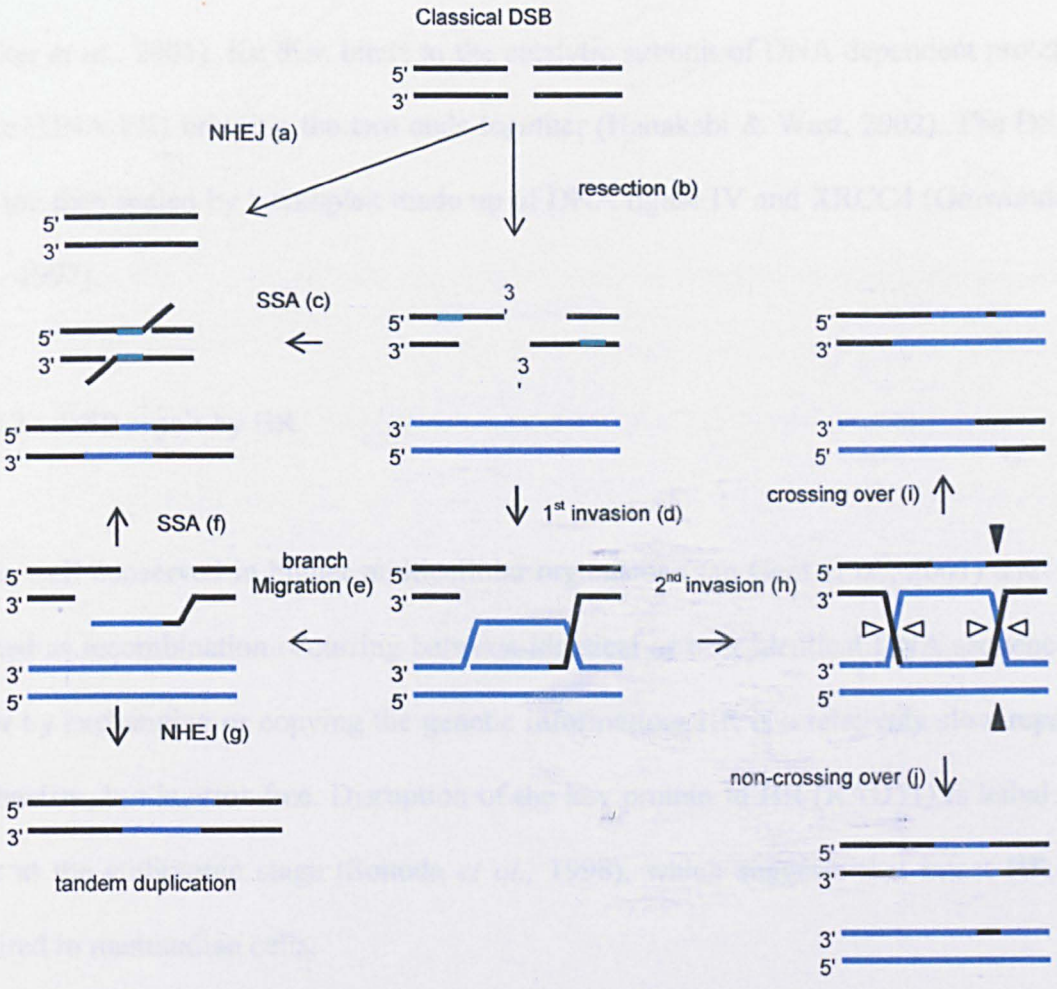

(a) The 2-ended DSB can simply be sealed by the NHEJ mechanism. (b) The DNA ends may be resected and generate 3' ssDNA overhangs. (c) Homologous sequences flanking the DSB ends can be uncovered and used for the SSA repair pathway. (d) One of the 3' overhangs may invade an intact homologous DNA duplex and elongate past the break site. (e) The produced Holliday junction (HJ) may migrate and release the extended 3' overhang (f) sharing homology for synthesis-dependent SSA repair. (g) Synthesis-dependent NHEJ can rejoin the wandered 3'overhang and leave tandem duplications. (h) If the second DNA end migrates, it forms another HJ. These HJs are dissolved either by crossing over (i) or non-crossing over (j).

The DNA ends at the DSB are then bound by the Ku protein, which is a heterodimer of Ku70 and Ku80. The hole in the Ku protein surrounds the broken DNA ends like a ring (Walker *et al.*, 2001). Ku then binds to the catalytic subunit of DNA dependent protein kinase (DNA-PK) bringing the two ends together (Hanakahi & West, 2002). The DSB ends are then sealed by a complex made up of DNA ligase IV and XRCC4 (Grawunder *et al.,* 1997).

1.3.5.2 DSB repair by HR

HR is well conserved in higher multicellular organisms (van Gent *et al.*, 2001) and is defined as recombination occurring between identical or near identical DNA sequences either by exchanging or copying the genetic information. HR is a relatively slow repair mechanism, but is error-free. Disruption of the key protein in HR (RAD51) is lethal in mice at the embryonic stage (Sonoda *et al.,* 1998), which suggests that intact HR is required in mammalian cells.

The first model for HR was suggested in fungi (Holliday 1964) and developed later to describe meiotic recombination in yeast (Szostak *et al.*, 1983). In *Saccharomyces cerevisiae*, most DSBs are repaired by HR (Game & Mortimer, 1974). The first model for HR in mammalian somatic cells was not proposed until later (Kanaar *et al.*, 1998). There are three main sub-groups of HR, single strand annealing (SSA), gene conversion (GC) and break-induced replication (BIR). All three processes start in the same way. Once DNA surveillance proteins detect a DSB, the MRE11/NBS1/XRS2 complex resects the ends, to generate long 3'-ended single strand DNA tails (*Figure 1.3.5.1b*).

1.3.5.2.1 Single strand annealing

Single-strand annealing (SSA) takes place between homologous sequences flanking both of the DSB-ends and was first reported to explain the results of intramolecular recombination in plasmid substrates (Lin *et al.*, 1990; Maryon & Carroll, 1991). SSA requires a number of enzymes that are also required for other types of recombinational repair. After the MRN complex resects the ends, the newly exposed single strands load recombination proteins that promote annealing. The RAD52 and RPA proteins then anneal the compatible single stranded sequences together (*Figure 1.3.5.1c*). The regions flipped out in between the repeats are removed by the XPF/ERCC1 complex (Sargent *et al.*, 2000). In this pathway, a lot of the sequence between the regions of homology is lost, making SSA a non-conservative pathway. SSA can occur in competition with gene conversion, which is a conservative HRR pathway.

1.3.5.2.2 Gene conversion

Gene conversion (GC) is the most accurate repair process, utilising the complementary sequence on the sister chromatid, to accurately copy the missing bases. This is not the same as sister chromatid exchange (SCE). This is reciprocal exchange of DNA sequences between a damaged and an intact chromatid within a single chromosome, whereas GC is simply copying DNA sequence information from the sister chromatid without any exchange. When sister chromatids are not available as GC templates, homologous chromosomes or sequence repeats, such as the Alu elements can be used. These elements are short (300 bp) and are spread throughout the genome (Schmid

1996). Because they are often far apart, a lot of the DNA sequence could potentially be lost. Therefore, using Alu sequences as a recombination template may compromise the integrity of the genome and predispose cells to cancer.

During GC, DNA ends are bound by RAD52, which protects them from endonucleases, and interacts with RAD51 (Van Dyck *et al*, 1999; Lundin *et al*, 2003). The RAD51 protein forms filaments, which bind along the unwound DNA, and facilitate strand invasion of a homologous sequence. Once the homologous sequence has been found, one strand is displaced to form a D-loop and new DNA synthesis can be initiated to fill in the missing sequence (Meselson & Weigle, 1961). DNA polymerase β then copies information from the undamaged partner, extending the 3' terminus of the damaged DNA strand. The ends are then ligated by DNA ligase I. The migration of one strand across the other causes the formation of a DNA crossover, or Holliday junction that is resolved by cleavage and ligation to create two intact molecules. A HJ may move (branch migration) and if it moves in the direction of RF, it can reverse the strand invasion and leaves a larger single stranded DNA (*Figure 1.3.5.1e*). This DNA end may be repaired through SSA sharing sequence homology with the other end (*Figure 1.3.5.1f*). This will result in gene conversion. Alternatively, the extended DNA end can be repair via NHEJ (*Figure 1.3.5.1g*), which will produce a tandem duplication (Helleday *et al.*, 2003).

It is possible that the second DNA strand could move toward the same homologous strand and forms a second HJ (*Figure 1.3.5.1h*). This structure, with two HJ, may resolve itself either by a crossing over (*Figure 1.3.5.1*i) or a non-crossing over (*Figure*

1.3.5.1j) repair pathway. Crossovers are frequent in meiotic recombination, but the association of this event is less frequent in somatic mammalian cells. This could be due to the fact that organisms containing large numbers of repetitive elements may have developed a stronger crossover suppression in order to maintain the integrity of the genome (Richardson *et al.,* 1998).

1.3.5.2.3 Break-induced replication

At the site of a difficult DNA lesion, the replication machinery may arrest causing the RF to stall. This may lead to complete separation of one branch of the fork end, which is called a one-ended DSB or a collapsed RF (Hanawalt, 1966) (*Figure 1.3.5.2.3b*). Collapsed RFs occur in most of the cells and the consequences of this event are catastrophic if not repaired. It has been estimated about 10 replication forks collapse or arrest per human cell replication cycle (Haber, 1999). This type of DSB can be a substrate for recombinational repair pathways (Marians *et al.,* 2000 and Cox *et al.,* 2001).

Figure 1.3.5.2.3 HR at stalled and collapsed replication forks

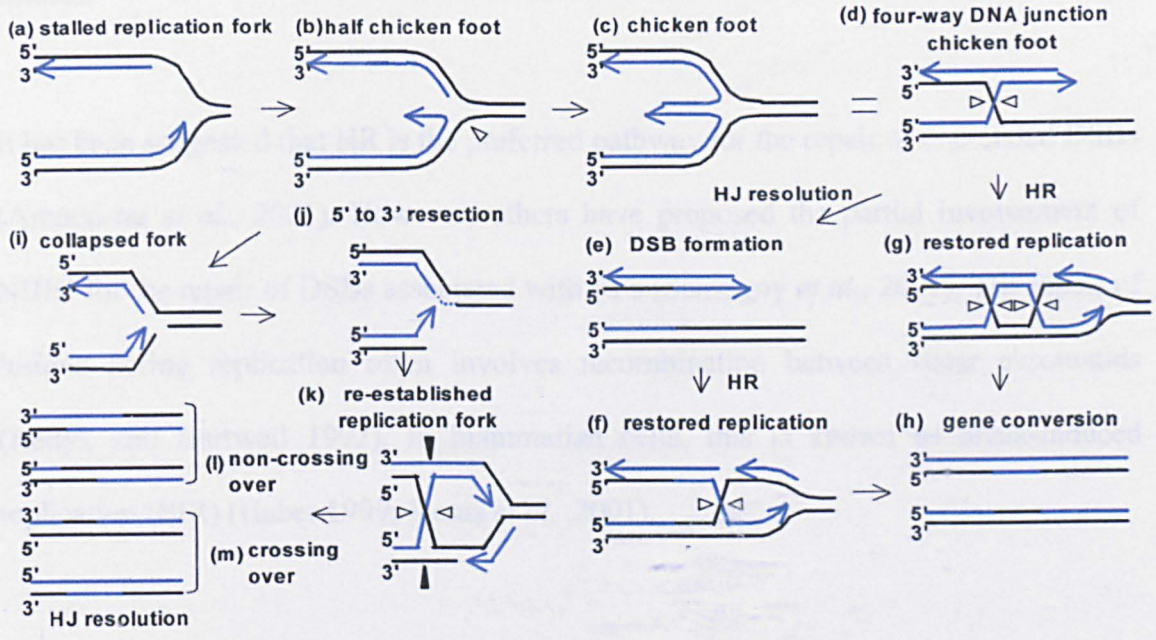

(a) HR at stalled and collapsed RFs. (b) One of the newly synthesized DNA strands has reversed and formed a half chicken foot. (i) This structure may be cleaved by endonucleases causing a collapsed RF. (c) If the second newly synthesized DNA strand reverses as well, a complete chicken foot will be generated. (d) This structure is the same as four-way HJ and its resolution results in a (e) DSB which can re-establish (g) RFs and leave a HJ. Cleavage of this HJ results in (h) gene conversion. Alternatively, (g) a second HJ may form at the chicken foot substrate avoiding the DSB. (h) Non-crossing over resolution of the two HJ results in gene conversion. (j) Endonucleases may resect the 1-end DSB from 5' to 3' to produce a 3' overhang and the single strand nick will be filled by polymerase activity. (k) Invasion of the 3' overhang forms a HJ and restores the RF. The HJ can be resolved either through (m) crossing over or (l) non-crossing over. Open arrowheads show non-crossing over and filled arrowheads designate crossing over. Arrows indicate the direction of DNA synthesis. Blue lines

demonstrate newly synthesized DNA strands and black lines designate template DNA strands.

It has been suggested that HR is the preferred pathway for the repair of one-ended DSBs (Arnaudeau *et al.,* 2001). However, others have proposed the partial involvement of NHEJ for the repair of DSBs associated with RFs (Saintigny *et al.*, 2001). The repair of lesions during replication often involves recombination between sister chromatids (Kadyk and Hartwell 1992). In mammalian cells, this is known as break-induced replication (BIR) (Haber 1999; Kraus *et al.* ,2001).

In BIR, the nick at the DNA template fills and the end of the DSB processes to produce a 3` end. This end then invades the intact DNA duplex template (*Figure 1.3.5.2.3d*) and establishes a RF (*Figure 1.3.5.2.3c*). This RF can progress all way to the end of the chromosome. The HJ left behind can be resolved through a crossing over or a non crossing over pathway (*Figure 1.3.5.2.3f*).

1.3.5.3 Repair of stalled RFs

RF damage can arise spontaneously or when it encounters damage in the DNA. For example, collisions between replication and transcription proteins might present obstacles to replication, which pauses the RF and causes it to stall (McGlynn & Lloyd 2000). RF arrest occurs in all organisms, and a lot of work has been done on the relationship between replication and recombination in bacteria. However, but very little is known about this relationship in mammalian cells (Rothstein *et al.*, 2000). There is

strong evidence that HR is the prominent pathway for RF repair in E-coli (Kogoma 1996; Cox *et al., 1*999) and it has also been reported that HR has a significant role in the repair of stalled replication forks in mammalian cells (Lundin *et al.*, 2002).

At stalled RFs, a nascent strand may reverse and make a half chicken foot (*Figure 1.3.5.2.3b*), which, in human cells, can be cleaved by the Mus81-EmI endonuclease (Ciccia, *et al.* 2003) and form a one-end DSB. This substrate is similar to the DSBs formed at collapsed RFs (Figure *1.3.5.2.3c*) and may be repaired through SCE (*Figure 1.3.5.3.3d*). If the second newly synthesized strand reverses, it makes a complete chicken foot with the first reversed-strand and forms a HJ at the four-way junction (*Figure 1.3.5.3.3e*) (Cox, 2001; McGlynn & Lloyd 2002). The stalled replication fork may reverse and form an intermediate chicken foot structure. Following DNA synthesis, both nascent strands can reverse and resume RF progression without recombination. However, it is also possible that HR could form two HJs before HJ cleavage and resume the RF (*Figure 1.3.5.3.3h*). The HJs may also be resolved through non-crossing over (Richardson *et al.,* 1998). The outcome following recombination involving a chicken foot structure is always gene conversion (Helleday *et al.*, 2003).

1.4 Poly(ADP-ribose) polymerase-1 (PARP-1)

Poly(ADP-ribose) polymerase (PARP) is a DNA damage detection protein. It is an abundant nuclear protein (10,000,000 molecules per cell), which is very well conserved in most mammalian cells (Herceg & Wang, 2001). PARP acts by attaching to DNA breaks, and catalysing a number of different events by the action of poly(ADP-ribosyl)ation. This is the addition of poly (ADP-ribosyl), (pADPr), subunits onto a protein substrate (D'Amours & Desnoyers, 1999).

1.4.1 The structure of PARP-1

PARP is made up of three domains, the DNA- binding domain, the automodification domain, and the catalytic domain (*Figure 1.4.1*). The PARP-1 protein has an N-terminal 46kDa DNA binding domain containing two large zinc fingers that bind to both DNA single-strand breaks (SSB) and DNA double-strand breaks (DSBs) (d'Adda di Fagagna, 1999; Lindahl, 1995). The DNA-binding domain has a high affinity with DNA because it contains a high proportion of basic residues. This domain also has a nuclear localisation signal (NLS). The catalytic domain is 54 kDa, and is responsible for catalysing the production of poly(ADP-ribose) polymers (pADPr) from nicotinamide adenine dinucleotide (NAD). pADPr subunits can be from a few, to 200 residues. After activation, PARP adds these to its substrates. The automodification domain is 22 kDa in size, and is the site upon which PARP regulates itself. During poly(ADP-ribosyl)ation, pADPr subunits bind here, and cause PARP to dissociate from the DNA. This is because pADPr subunits carry a negative charge, and PARP pulls away from negative

DNA because of electrostatic repulsion. Poly(ADP-ribose) glycohydrolase (PARG) then breaks the bonds between the pADPr polymers, allowing PARP to bind to DNA once again. The automodification domain also contains a BRCT module that allows PARP to bind to other proteins containing the same module. The zinc fingers, NLS and catalytic domain are the most highly conserved portions of the PARP protein. Of these, there are 50 amino acids that are 100% conserved in vertebrates (92% amongst all species). These are known as the PARP signature.

Figure 1.4.1 Structure of PARP-1

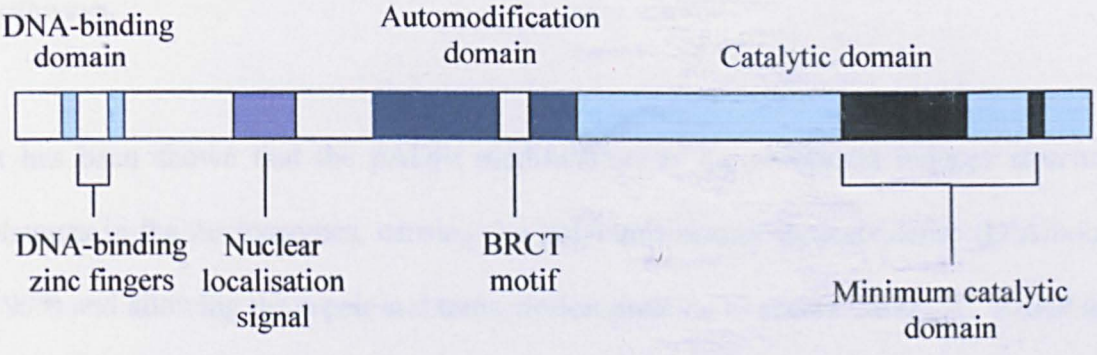

The activity of PARP-1 is triggered by its DNA binding activity and it adds pADPr to glutamine residues of itself and to surrounding histones (Smith *et al.*, 2001). The biochemical role for the pADPr modification of histones is unknown; however it is believed that the negative charge caused by the modification would change the local chromatin structure to allow access by DNA repair proteins.

PARP has been reported to regulate many cellular processes such as DNA repair, genomic stability, cell cycle progression, cell death and gene transcription (D'Amours, *et al.*, 1999; Shall & de Murcia, 2000) through the addition of pADPr polymers onto

acceptor proteins involved in these pathways. This pADPr modification affects their activity, possibly because of the negative charge of the pADPr polymers. .

1.4.2 The function of PARP-1 and its mechanism of catalysis

PARP has a role in many processes including chromatin structure, DNA replication, transcription, BER, DNA synthesis, and maintenance of telomere length (Dantzer et al., 1998; Muiras & Burkle, 2000; Herceg and Wang, 2001; d'Adda di Fagagna et al., 1999; D'Amours et al., 1999), through pADPr modification of acceptor proteins in these pathways.

It has been shown that the pADPr modification of the chromatin induces structural changes in the nucleosomes, causing the polynucleosomes to decondense (D'Amours, 1999) and allowing the repair and transcription proteins to access the DNA. PARP acts on several chromatin proteins, including histones, H1, H2A, H2B, H3, H4,H5, and the HMG proteins. Upon activation, PARP first shows preference for itself as a substrate, however, preference gradually changes in favour of the chromatin proteins, especially H1 and H2B. The chromatin remains decondensed until the DNA is repaired. PARP also has a role in transcription. It has an enzymatically inactive role through interaction with RNA polymerase II, by acting as a transcription factor and can also form part of the pre-initiation complex. PARP also, regulates transcription when the DNA is damaged, by decreasing RNA polymerase II activity. Proteins involved in transcription are modified by pADPr polymers and cannot bind to the DNA. Therefore, PARP can be a positive and negative regulator of transcription.

1.4.3 The role of PARP in homologous recombination

Although, PARP-1 binds to DSBs, it is not required for the repair of DSBs via homologous recombination (HR), as RAD51 foci form in response to hydroxyurea in PARP-$1^{-/-}$ cells. Also, PARP-1 does not co-localise to RAD51 foci and HR repair of a DSB is not defective in PARP-1 inhibited cells (Schultz *et al.,* 2003; Yang *et al.*, 2004). However, PARP-1 appears important in maintaining genetic stability, since cells lacking or with inhibited PARP-1 have an increase in HR, sister chromatid exchange (SCE) and micronuclei formation {Lindahl *et al*, 1995; Molinete *et al.*, 1993; de Murcia *et al*,, 1997; Wang *et al.,* 1997).

As PARP-1 is not required for HR, the reason for increased HR may be explained by an accumulation of recombinogenic substrates in PARP-1 deficient cells. Therefore, HR could have an important role in repairing lesions that occur in the absence of PARP-1.

1.4.4 The role of PARP-1 in BER

The BER complex repairs damage caused by x-rays, oxygen radicals, and alkylating agents. It does this by cutting out the damage, producing abasic sites that are recognised by APE1 (Dizdaroglu, 2003). This endonuclease cleaves the phosphodiester backbone to form a SSB in the DNA (Dianov *et al.*, 2003). PARP-1 can bind and recognise these SSBs (Satoh & Lindahl, 1994), and also binds to XRCC1, a scaffold protein that brings SSB repair proteins DNA polymerase β and DNA ligase III, to the site of damage (Kubota, *et* al., 1996; Masson *et al.*, 1998; Dantzer *et al.*, 1999). PARP has been shown

to poly(ADP-ribosyl)ate the proteins of the complex, and also has physical interaction with XRCC1 and DNA ligase III via their BRCT module (Masson *et al.,* 1998). The purpose of this interaction could be to recruit the repair proteins to the site of the DNA lesion. PARP-1 is not required for the repair of the SSB itself (Vodenicharov *et al.*, 2000), however it may be that the hypersensitivity of PARP depleted cells, or PARP inhibited cells reflects a reduced ability to attract the proteins required for complete BER. Therefore, PARP inhibitors may be used to enhance the cytotoxic effect of DNA damaging agents that cause lesions normally repaired by BER.

1.4.5 PARP-1 inhibitors

Almost all PARP inhibitors are competitive inhibitors of NAD^+. The first were analogues of nicotinamide, for example, 3-aminobenzamide (3-AB). These were useful for *in vitro* studies of PARP activity (Wedge *et al.,* 1996). However, there were of little clinical use as they had low potency, were difficult to dissolve, and lacked specificity.

The next generation of rationally designed inhibitors were much more potent. These included benzimidazole-carboxamides, quinazolin-4-[3H]-ones and isoquinoline derivatives, for example 2-(4-hydroxyphenyl)benzimidazole-4-carboxamide (NU1085), 8-hydroxy-2-methylquinazolin-4-(3H)one (NU1025) and dihydroisoquinalone (PD128763) and demonstrated an increased amount of chemosensatisation *in vitro* (Boulton *et al.*, 1995; Tentori *et al.*, 1997; Tentori *et al.*, 1998).

Figure 1.4.5.1 1,5-dihydroisoquinoline

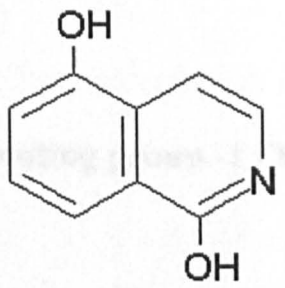

For example, NU1025 enhanced the cytotoxicity of the monofunctional DNA-alkylating agent temozolomide, the topoisomerase I inhibitor camptothecin and γ-irradiation in L1210 cells and in 12 human tumour cell lines (Bowman & White, 1998; Bowman *et al.*, 2001).

Figure 1.4.5.2 NU1025

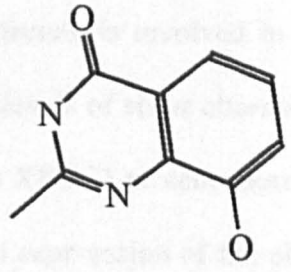

Unfortunately these were still not potent or specific enough for extensive pre-clinical trials. Recently a PARP inhibitor more than 1000 times more potent than 3-AB has been developed. AG14361 has been used *in vivo* at non-toxic doses to augment the effect of the DNA damaging agents irinotecan and temozolomide (Calabrese & Almassy, 2004). AG14361 treatment in conjunction with temozolomide caused complete remission of SW620 xenograft tumours (Wedge & Newlands, 1996; Tentori *et al.*, 2001; Curtin *et al.*, 2004). The suppression of PARP-1 activity increases the sensitivity of cells to DNA damaging agents. The understanding of how this happens may help us to understand

how this increased sensitivity occurs and design even more potent therapies in the future.

1.5 X-ray cross-complementing group -1 (XRCC1)

The first XRCC1 mutated cell line was the EM9 cell line that was isolated as clone sensitivity to ethyl methanesulphonate (EMS). It was found that this cell line was also sensitive to agents such as ionising radiation (Thompson, 1982). Several other X-ray sensitive cell lines were isolated and cross complementation was determined in cell fusion experiments (Thompson, 1991). The EM9 cell line belong to the first X-ray cross complementation group (XRCC1) and the gene was cloned (Thompson, 1990).

It was found that the XRCC1 protein is involved in DNA single-strand break (SSB) repair as well as in suppressing levels of sister chromatid exchange (SCE) (Thompson, 1990). Further evidence that the XRCC1 protein caused the defect in SSB repair and in abnormal SCE levels came from suppression of the phenotype through expression of a XRCC1 minigene (Caldecott, 1992). The XRCC1 protein was found to bind to the DNA ligase III protein (Caldecott, 1994) suggesting the protein had direct implication in repair of SSBs. It was early suggested that the XRCC1 protein also was involved in the base excision (BER) pathway as loss of XRCC1 protein resulted in sensitivity to EMS and other alkylating agents (Thompson, 1982).

The interaction between XRCC1 and other proteins such as DNA ligase III and DNA polymerase β have been further studied in detail. It was found that the XRCC1 binds

directly with DNA ligase III and DNA polymerase β. XRCC1 binds DNA ligase III through a breast cancer protein 1 carboxyl terminus (BRCT) motif (Taylor, 1998). These are folding units of about 90-100 amino acids, and so called because they were first identified in breast cancer cells. These BRCT motifs consist of four β-strands forming a core sheet structure and two α-helices, and are important in specific protein-protein interactions (Caldecott, 2003) (*Figure 1.5*). In fact, BRCT motifs have been found in DNA-damage responsive and cell cycle check-point proteins. DNA ligase III contains a BRCT motif in its C-terminal domain, amino acids 841 to 922, and XRCC1 contains two BRCT motifs, one at amino acids 314 to 402, and another in the C-terminal at amino acids 538 to 622. XRCC1 binds DNA ligase III through its C-terminal BRCT motif.

Figure 1.5. Crystal structure of a typical BRCT motif.

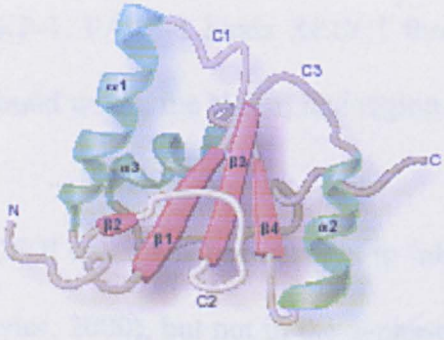

From Caldecott, 2003

XRCC1 binds DNA polymerase β through its N-terminal domain, amino acids 1 to183. This section of the XRCC1 protein also binds to SSBs in the DNA (Marintchev *et al.*, 2000). The three-dimensional structure of the N-terminal domain of XRCC1 has been

reported, and has been shown to be well-suited to the inside curvature of 90° bent DNA (Marintchev *et al.,* 1999). When PARP-1 binds to SSBs in the DNA, it induces a V-shape bend in the DNA. PARP-1 eventually moves away from the DNA, leaving room for the repair proteins to access the break. It may be that XRCC1 then binds the site recently vacated by PARP-1, bringing DNA polymerase β and DNA ligase III to the site. XRCC1 binds DNA polymerase β via its N-terminal region, but this domain has a much higher affinity for SSBs in the DNA, approximately 100 times greater. It could be that XRCC1 binds DNA polymerase β via the N-terminal, which is then possibly released upon binding to a SSB.

XRCC1 binds DNA ligase III through its C-terminal BRCT II motif and PARP-1 through its central BRCT I motif which binds directly with a BRCT motif within PARP-1's automodification domain (AMD) (Masson, 1998). This is the domain where PARP-1 automodifies itself by adding ADP-ribose polymers and XRCC1 preferentially binds to automodified PARP-1. PARP-1 binds XRCC1 through its BRCT motif, and also with the zinc-fingers found within the N-terminal region.

The disruption of the BRCT II motif has been shown to inhibit SSB repair in the G1-phase of the cell cycle (Taylor, 2000), but not in the S-phase. In contrast, a mutation in the BRCT I domain inhibits all SSB repair regardless of the cell cycle (Taylor, 2002). XRCC1 itself is not required for SSB repair, however, the presence of XRCC1 stimulates the poly nucleotide kinase which increases the speed of SSB repair (Whitehouse *et al*, 2001).

1.6 Camptothecin (CPT)

Camptothecin (CPT) is a chemotherapy drug, discovered by Dr. Monroe E Wall and Jonathon Hartwell in 1958. It is found in the bark of Camptotheca accuminta, or Xi Shu. This tree is also known in China as the 'happy tree' or 'cancer tree'.

Camptothecin inhibits topoisomerase I (Top1), an enzyme that relaxes DNA supercoiling ahead of replication and transcription complexes. Top1 induces a transient break in the DNA, so that the flanking segments of DNA can rotate freely around it. Camptothecin stabilises this break (Hsiang, 1985), by binding intercalating between upstream (-1) and downstream (+1) base pairs, displacing the downstream DNA and preventing relegation of the cleaved DNA, which in turn leaves Top1 covalently bound to the DNA (Pommier *et al.,* 2003). This leaves an unrepaired SSB in the DNA which must be repaired before it collides with oncoming replication machinery, and resulting in a DSB, through a run off mechanism leaving a free 5' phosphate DNA end (Strumberg, 2000) (*Figure 1.6.1*). It is well established replication is needed for CPT toxicity, which is explained by the collapse of replication forks (Avemann, 1988; Ryan, 1991; Tsao, 1993; Strumberg, 2000)

Figure 1.6.1 A SSB becomes a DSB after collision with an oncoming replication fork

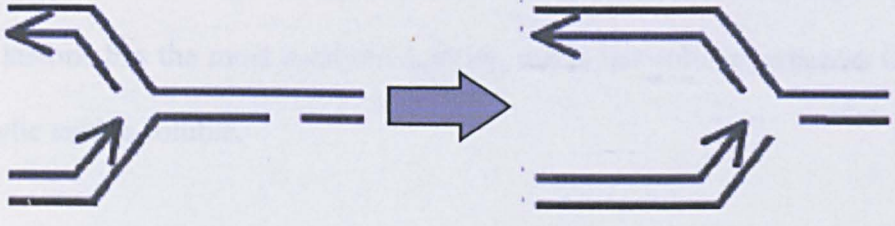

DSBs are lethal to the cell if left unrepaired. The repair pathways involved in repairing CPT lesions involve homologous recombination and non-homologous end joining (Arnaudeau *et al.*, 2001) or SSB repair involving the XRCC1 protein (Barrows et al., 1998). Therefore, drugs that inhibit the repair of CPT-induced DSBs can enhance the cytotoxicity of camptothecin. This has been shown, both in vitro and in vivo, by co-treatment with inhibitors of DNA-dependent protein kinase (DNA-PK) or with PARP-1 inhibitors (Shao *et al*, 1999), but the mechanism is still unknown.

CPT has a five ring structure, and exists naturally in equilibrium with a similar structure, with an 'open' ring. This equilibrium is governed by the pH of the surroundings.

Figure 1.6.2 Camptothecin ('closed' ring)

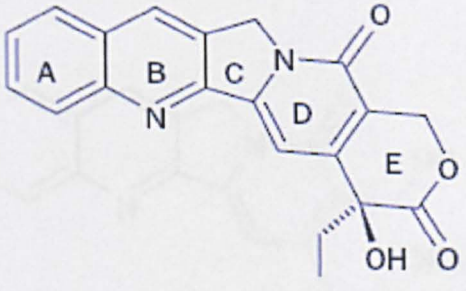

A high pH will favour the open ring, and a low pH will favour the closed ring. The closed ring lactone has the most catalytic activity, but is not soluble, whereas the open ring carboxylic acid is soluble.

Figure 1.6.3 Camptothecin ('open' ring)

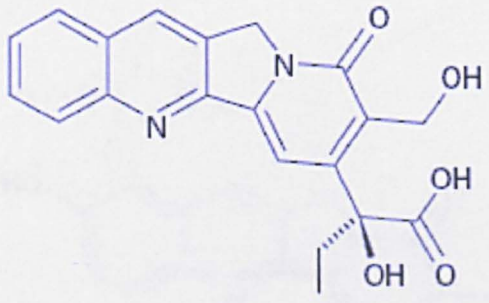

In the early 1970s, camptothecin sodium was used to treat gastro-intestinal cancer patients, but this was discontinued to severe side effects. Camptothecin sodium irreversibly opens the lactone ring, so a very high dose was needed to have any clinical effect. However, the low pH of the bladder, pushed the equilibrium in favour of the closed ring structure causing a huge toxic dose of the drug.

Figure 1.6.4 Camptothecin sodium

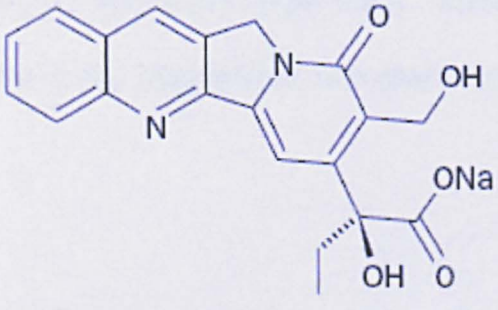

The toxic side effects of CPT are neutropenia (abnormally low levels of neutrophils), anaemia, vomiting, fever and pain (Verschraegen, et al, 2000). Since the 1970s, many analogues of CPT have been created, such as topotecan and irinotecan. These are less toxic and are used today in the treatment of several cancers.

Figure 1.5.5 Topotecan

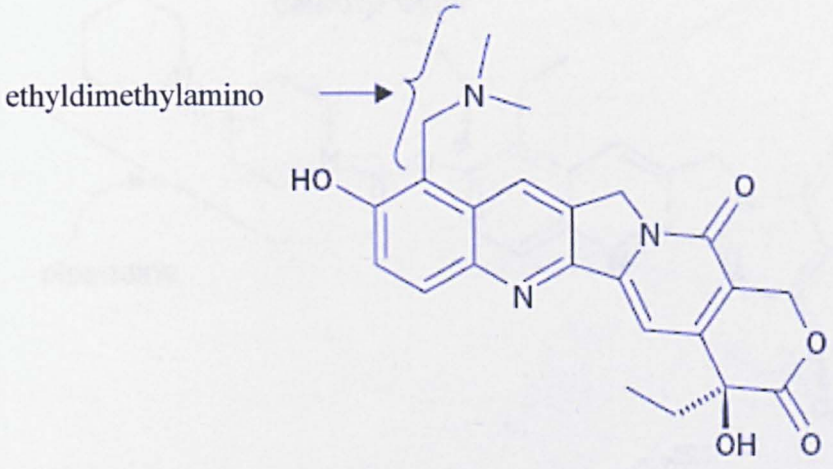

Topotecan (9-[(dimethylamino)methyl]-10-hydroxycamptothecin) is water-soluble due to the ethyldimethylamino side-chain at carbon nine of the A ring. This drug was approved for use in 1996, and is currently used to treat ovarian and small cell lung cancer.

Irinotecan (7-ethyl-10-[4-(1-piperidino-1-piperidino] carbonyloxycamptothecin) is water-soluble due to the bulky dipiperidino side-chain linked to the A ring via a carboxyl ester bond.

Figure 1.5.6 Irinotelan

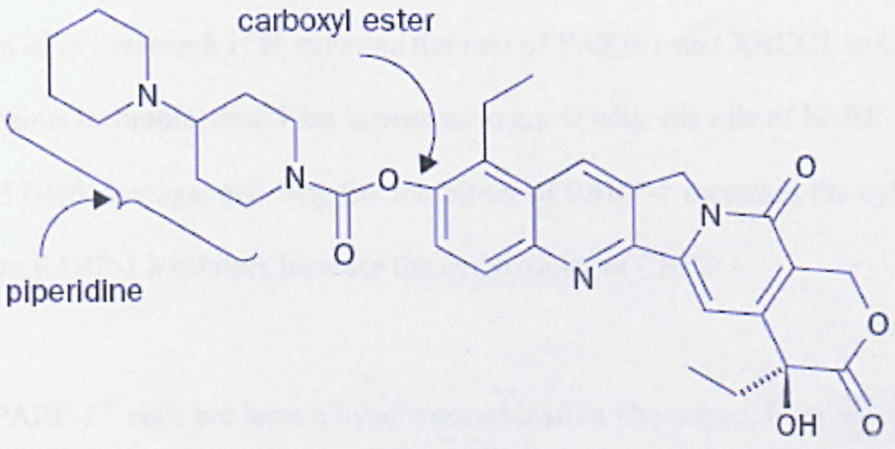

This side-chain decreases the anticancer activity of the drug, but is cleaved by carboxylesterases in the liver and gastro-intestinal tract to form SN-38 (7-ethyl-10-hydroxycamptothecin). This metabolite has 2-3-fold more activity than irinotecan. Currently, irinotecan is used to treat lung, cervical and ovarian cancers, but is mostly used to treat advanced colorectal cancers. Recently, it has been discovered that co-treatment of cancers with CPT and PARP-1 inhibitors increases the cytotoxicity of the CPT.

1.7 Aims of this thesis

The aim of my research is to examine the role of PARP-1 and XRCC1 in CPT-induced homologous recombination. I am interested to know what the role of PARP-1 is in CPT-induced DNA damage, and why the inhibition of PARP-1 increases the cytotoxicity of CPT. Do PARP-1 inhibitors increase the cytotoxicity of CPT?

Since PARP-$1^{-/-}$ cells are have a hyper-recombination phenotype, I am interested to find out the role of homologous recombination (HR) in the repair of CPT-induced damage and to know if there is more CPT-induced damage in PARP-$1^{-/-}$ cells. CPT stabilises the transient single-strand break (SSB) induced by Top1. Is PARP-1 involved in SSB repair? If so, how is it involved? HR repairs DNA double-strand breaks (DSBs). Are there more DSBs in $PARP^{-/-}$ cells after CPT treatment?

SSBs are usually repaired by DNA ligase III and DNA polymerase β. They are brought to the site of the SSB, by the scaffold protein, XRCC1. XRCC1 is thought to interact with PARP-1. In cells lacking XRCC1, is CPT more toxic? Is CPT more toxic to cells lacking a functional PARP-1 or XRCC1? Do these cells have an increase in DSBs?

This research is important because it will tell us why PARP-1 inhibitors increase the cytotoxicity of CPT and may provide insights for future clinical work. PARP-1 inhibitors may be developed for clinical use which will help in the treatment of cancers and decrease the amount of toxic side effects seen with CPT derivatives.

CHAPTER 2: MATERIALS & METHODS

CHAPTER 2: MATERIALS & METHODS

2.1 Materials

2.1.1 General lab equipment and reagents

2.1.1.1 Chemical reagents

Unless otherwise stated, all of the chemicals used in the preparation of solutions and buffers were of high purity.

Chemical	Supplier
2-mercapto-ethanol	Sigma
Acrylamide	BioRad
Ammonium persulphate	BDH
Ampicillin	Sigma
Aquaclean	ConTaFree liquids
Bovine serum albumin (BSA)	Sigma
Boric acid	BDH
Coomassie brilliant blue	BioRad
Dextran sulphate	Sigma
Dimethyl sulphoxide (DMSO)	Sigma-Aldrich
Ethylene diamine tetra acetic acid (EDTA)	BDH
Ethanol	BDH
Ethidium bromide	Sigma
Ficoll 400	BDH
Glycerol	BDH
Hydrex® HS disinfectant spray	Adams Healthcare
Hydrochloric acid	Fisher Scientific
Industrial methylated spirit	Adams Healthcare
Isopropanol	BDH
Low fat milk powder	Marvel
Methanol	BDH
Methylene blue	Sigma
N-laurylsarcosine	Sigma
Paraformaldehyde	Fisher Scientific
Phenol	BDH
Phenylmethyl sulphonyl fluoride (PMSF)	Sigma
Polyvinylpyrolidone	Sigma
Presept (sodium dichloroisocyanurate)	Johnson & Johnson Medical Limited
RBS detergent	Pierce
SeaKem agarose	FMC Bioproducts

Chemical	Supplier
Sodium acetate	BDH
Sodium chloride	BDH
Sodium citrate	BDH
Sodium hydroxide	BDH
Sodium hydroxide	BDH
Sodium lauryl sulphate (SDS)	Sigma
Sodium phosphate	BDH
Tris base	BDH
Triton-X 100	Sigma
Tween-20	BDH
Virusolve II	Amity U.K. Limited

2.1.1.2 Glassware

All glassware was washed with RBS detergent (Chemical concentrates), rinsed several times with tap water and washed with de-ionised water. Glassware was dried in a hot air oven and all items requiring sterilisation were autoclaved for 15 minutes at 15 p.s.i.

Item	Supplier
Bottle 100 ml	Schott Duran
Bottle 200 ml	Schott Duran
Bottle 500 ml	Schott Duran
Bottle 1 L	Schott Duran

2.1.1.2 Plastic and disposable equipment

Item	Supplier
25 ml vented Nunclon™ flasks	Nunc
75 ml vented Nunclon™ flasks	Nunc
175 ml vented Nunclon™ flasks	Nunc
100 mm cell culture plates	Greiner Bio-one
6-well cell culture plates	Greiner Bio-one
5 ml Stripette® disposable pipette	Corning Incorporated
10 ml Stripette® disposable pipette	Corning Incorporated
20 ml Stripette® disposable pipette	Corning Incorporated
Pasteur pipettes (glass)	Fisher Scientific
400 ml beaker	Azlon
1000 ml beaker	Azlon

Item	Supplier
2000 ml beaker	Azlon
Measuring cylinder 25 ml	Azlon
Measuring cylinder 100 ml	Azlon
Measuring cylinder 250 ml	Azlon
Measuring cylinder 500 ml	Azlon
Measuring cylinder 1000 ml	Plastibrand
Universals	Bibby Sterilin
15 ml centrifuge tubes	Sarstedt
50 ml centrifuge tubes	Corning Incorporated
Sterile needles	BD UK Ltd
Syringes	BD UK Ltd
UVette	Eppendorf
Cryovials	Sarstedt
Eppendorfs 0.5 ml	Sarstedt
Eppendorfs 1.5 ml	Sarstedt
Eppendorfs 2 ml	Sarstedt
Neptune barrier tips 10 µl	CLP
Neptune barrier tips 20 µl	CLP
Neptune barrier tips 100 µl	CLP
Neptune barrier tips 1000 µl	CLP
Plastic tips < 200 ml	Sarstedt
Plastic tips < 1000 ml	Sarstedt
Filtered tips p10	Starlab
Filtered tips p20	Starlab
Filtered tips p200	Starlab
Filtered tips p1000	Starlab
Super premium microscope slides	BDH
Coverslips	BDH

2.1.1.4 Miscellaneous disposable lab equipment

Item	Supplier
Parafilm	Pechiney Plastic Packaging
Comply™ Indicator tape	3M
Aluchef® Foil	Terinex
Clingfilm	Caterwrap
Surgical mask	Kimberley Clark
Disposable scalpel	Swann-Morton
Weigh boats 50 ml	Scientific Laboratory Supplies
Weigh boats 100 ml	Scientific Laboratory Supplies
Latex gloves (small)	Bodyguards®
Paper towels	Kimberley Clark
Tissues	Lotus Professional

2.1.1.5 General lab equipment

Item	Supplier
4°C fridge	Labcold
4°C fridge	Derby
4°C Medicool fridge	Sanyo
-20°C freezer	Labcold
-20°C freezer	Ezta
Ice machine	Scotsman
Microwave	Panasonic
Unitemp 37°C incubator	Harvard/LTE
Plus II oven	Gallenkamp
Unitemp drying cabinet	Harvard/LTE
MP24 control autoclave oven	Rodwell Scientific Instruments
Model G25 incubator shaker	New Brunswick Scientific Co. Inc.
CK2 microscope	Olympus
SM-LUX microscope	Leitz Wetzler
Mistral 2000R centrifuge	MSE
Microcentaur microcentrifuge	MSE
PM 4000 balance	Mettler
Fine balance	Gallenkamp
Biophotometer	Eppendorf
DPU-414 thermal printer	Seiko Instruments Inc
Min-spin plus	Eppendorf
Orbital shaker S0 3	Stuart Scientific
Vortex-Genie 2	Scientific Industries
Dryblock DB 2A	Techne
Heating block	Grant Boeial
[Zip] Color squid magnetic stirrer	IKA
SM-1 magnetic stirrer	Stuart Scientific
SS 3H Hotplate stirrer	Chemlab
Model 200/20 power supply	BioRad
Model 1000/500 power supply	BioRad
Power PAC 300	BioRad
pH meter	Denver Instruments
Water bath	Grant
Water bath	Laboratory Thermal Equipment Ltd
PipetAid	Drummond Scientific
p10 Pipetman	Gilson
p20 Pipetman	Gilson
p200 Pipetman	Gilson
p1000 Pipetman	Gilson
Pipetman stand	Gilson
Cell counter	Neubauer
Counter	ENM

2.1.1.6 De-ionised water

Tap water passed through a reverse osmosis unit (Fi-streem, Fisons) to produce de-ionised water with a resistance of 10 MΩ. The water was sterilised by autoclaving for 15 minutes at 15 p.s.i. All references to water within this thesis should be assumed to mean de-ionised water unless otherwise stated. Water of ultra-pure quality (>18 MΩ) was used for molecular experiments and was obtained from an installed Permulab de-ionising water system.

2.1.1.7 General buffers

All buffers were sterilised by autoclaving for 20 minutes at 15 p.s.i.

2.1.1.7.1 Phosphate-buffered saline (PBS) buffer

137 mM NaCl

2.7 mM KCl

10 mM Na_2HPO_4

2 mM KH_2PO_4

Adjusted pH to 7.4 with HCl

2.1.1.7.2 10 x Tris-Acetate-EDTA (TAE) buffer

0.4 M Tris-acetate

10 mM EDTA

pH 7.6

2.1.1.7.3 10 x Tris-Borate-EDTA (TBE) buffer

0.89 M Tris

0.89 M Boric acid

20 mM EDTA

pH 8.3

2.1.1.7.4 10 x Tris-EDTA (TE) buffer

0.1 M Tris

10 mM EDTA

pH 8.0

2.1.1.7.5 10 x Tris-Glycine-SDS (TGS) buffer

0.25 M Tris

2.5 M Glycine

0.1% w/v SDS

2.1.2 Materials for cell culture

2.1.2.1 Chemical reagents for cell culture

Chemical	Supplier
α-MEM	Cambrex
D-MEM	Gibco
HyClone® foetal bovine serum (FBS)	Perbio
L-glutamine	BDH
Non-essential amino acids (NEAA)	Cambrex
Penicillin	Sigma
Streptomycin sulphate	Sigma
Trypsin	Gibco
Carbon dioxide gas	BOC gases
Nitrogen refrigerated liquid	BOC gases

2.1.2.2 Specific equipment for cell culture

Item	Supplier
Class II microbiological safety cabinet	Walker Safety Cabinets Limited
CO_2 incubator	Gallenkamp
-135°C nitrogen freezer	Sanyo

2.1.2.3 Specific buffers for cell culture

2.1.2.3.1 Versene

0.02% EDTA in PBS.

2.1.3 Materials for pulsed-field gel electrophoresis

2.1.3.1 Chemical reagents for pulsed-field gel electrophoresis

Chemical	Supplier
Drugs	(See **2.2 DRUGS**)
Pulsed-field certified agarose	Fisher Biotech
Agarose for PFGE: sample preparation	Sigma
Proteinase-K	Fisher Biotech
CHEF DNA size standards, *S. cerevisiae*	BioRad

2.1.3.2 Specific equipment for pulsed-field gel electrophoresis

Item	Supplier
CHEF-DR III power module	BioRad
CHEF-DR III electrophoresis cell	BioRad
Cooling module	BioRad
Variable speed pump	BioRad
Screened caps	BioRad
Plug molds	BioRad
Standard casting stand	BioRad
Wide/long combination casting stand	BioRad
10 well comb (14 cm x 0.75 mm)	BioRad
30 well comb (21 cm x 0.75 mm)	BioRad
Combination comb holder	BioRad
Tygon tubing	BioRad
UV transilluminator	UVP Inc.
DC 290 200M digital camera	Kodak
Power Mac G3 series	Apple
17/200 monitor	Pronitron
Safety mat	Kodak

2.1.4 Materials for Southern blot

2.1.4.1 Chemicals for Southern blot

2.1.4.1.1 Chemical reagents for DNA extraction

Chemical	Supplier
Proteinase K	Fisher Biotech

2.1.4.1.2 Chemical reagents for DNA digestion

Chemical	Supplier
XhoI restriction enzyme	New England Biolabs
HindIII	New England Biolabs
NcoI	New England Biolabs
NEB buffer 2	New England Biolabs

2.1.4.1.3 Chemical reagents for preparation of the probe

Chemical	Supplier
LB-broth	Fisher Scientific
LB-agar	Fisher Scientific
XhoI restriction enzyme	New England Biolabs
BamHI restriction enzyme	New England Biolabs
NEB buffer 2	New England Biolabs
Hyperladder I	Bioline
QIAquick® gel extraction kit	Qiagen
QIA prep spin mini-prep kit	Qiagen

2.1.4.1.4 Chemical reagents for radiolabelling

Chemical	Supplier
Prime-it® II random primer labelling kit	Stratagene
9-mer primer	
5 x dCTP buffer	
Exo(-) Klenow enzyme	
$^{32\text{-}\alpha p}$dCTP	MD Biosciences
DyEx kit	Qiagen
Decon 90	Decon Laboratories Limited

2.1.4.2 Specific equipment for Southern blot

Item	Supplier
Hybridisation oven/shaker	Stuart Scientific
DNA thermal cycler 400	Perkin Elmer
FLA-300 phospho-imager	Fujifilm
Power Mac G4	Apple
Visionmaster™ Pro 511	Iiyama
H5 horizontal gel electrophoresis cell	Gibco
Hybond-N$^+$	Amersham Biosciences
Whatman paper	Scientific Lab Supplies
Safety glass	Nalgene
Series 900 Geiger counter	Mini-monitor
Glass tubes with screw lid	Stuart Scientific

2.1.4.2 Computer software for analysis of Southern blot

Item	Supplier
Image gauge V3.3	Fujifilm
Image reader V1.8E	Fujifilm
L Process V1.8	Fujifilm

2.1.4.4 Specific buffers for Southern blot

2.1.4.2.1 20 x SSPE

3 M NaCl

0.2 M NaH_2PO_4.H20

20 mM EDTA

pH 7.4

2.1.4.2.2 20 x SSE

3 M NaCl

0.3 M $Na_3C_6H_5O_7$.5.5H_20

pH 7.0

2.1.4.2.3 Denhardt's solution

1% w/v Ficoll 400

1% w/v Polyvinylpyrolidone

1% w/v BSA

2.1.5 Materials for immunofluorescence

2.1.5.1 Chemical reagents for immunofluorescence

Chemical	Supplier
Primary antibody	(see **2.3.1 Primary antibodies**)
Secondary antibody	(see **2.3.2 Secondary antibodies**)
Slowfade® Antifade kit	Molecular Probes
Nail varnish	Boots

2.1.5.2 Specific equipment for immunofluorescence

Item	Supplier
TE 300 Eclipse microscope	Nikon
Pentium III computer	Maple
Trinitron Multiscan 500 PS	Sony
Microscope (MBB)	

2.1.5.3 Computer software for analysis of immunofluorescence

Item	Supplier
softWoRx	Delta Vision

2.1.6 Materials for recombination assays

2.1.6.1 Chemical reagents for recombination assays

Chemical	Supplier
Drugs	(see **2.2 DRUGS**)
Hypoxanthine	Sigma
Azaserine	Sigma
Thymidine	Sigma
6-thioguanine (6-tG)	Sigma
Geneticin (G418)	Gibco

2.1.6.2 Specific buffers for recombination assays

2.1.6.2.1 Dialysed serum

Foetal bovine serum (Perbio) was poured into dialysis tubing and left to soak in 1 x PBS with agitation at 4°C. The buffer was changed every 4 hours for 16 hours. Removed serum from the dialysis tubing and vacuum filtered, before autoclaving at 15 p.s.i.

2.1.6.2.2 HAsT medium

Added hypoxanthine (6.865 mg/ml), azaserine (1.731 mg/ml) and thymidine (12.12 mg/ml) to DMEM and inverted to mix.

2.1.7 Materials for survival assays

2.1.7.1 Chemical reagents for survival assays

Chemical	Suppliers
Drugs	(see **2.2 DRUGS**)

2.1.7.2 Specific equipment for survival assays

Item	Supplier
Colony counter	Stuart Scientific

2.1.8 Materials for fluctuation assays

2.1.8.1 Chemical reagents for fluctuation assays

Chemical	Supplier
Geneticin (G418	Gibco

2.1.8.2 Specific equipment for fluctuation assays

Item	Supplier
Colony counter	Stuart Scientific

2.1.9 Materials for flow cytometry

2.1.9.1 Chemical reagents for flow cytometry

Chemical	Supplier
Drugs	(see **2.2 DRUGS**)
Bromodeoxyuridine (BrdU)	Sigma
Primary antibody	(see **2.3.1 Primary antibodies**)
Secondary antibody	(see **2.3.2 Secondary antibodies**)
Propidium iodine	Sigma

2.1.9.2 Specific equipment for flow cytometry

Item	Supplier
FACSorter	Becton Dickenson
Computer	Mac OS 9.1
Monitor	Formac

2.1.9.3 Computer software for analysis of flow cytometry

Item	Supplier
Cellquest	Becton Dickenson

2.1.10 Materials for Western blot

2.1.10.1 Chemical reagents for Western blot

Chemical	Supplier
Protease inhibitor cocktail	Roche
TEMED	Sigma
ECL Western blotting detection reagents	Amersham Biosciences
BioRad protein assay	BioRad
Precision Plus: Dual color standard	BioRad

2.1.10.2 Specific equipment for Western blot

Item	Supplier
Hoefer mighty small dual cell caster	Amersham Biosciences
Hoefer SE 250	Amersham Biosciences
Hoefer SE 260	Amersham Biosciences
Lid with cables	Amersham Biosciences
Lower buffer chamber for SE250	Amersham Biosciences
Deep lower buffer chamber for SE260	Amersham Biosciences
Hoefer glass plates 8 x 10 cm (SE250)	Amersham Biosciences
Hoefer glass plates 10 x 10.5 cm (SE260)	Amersham Biosciences
Notched alumina plates	Amersham Biosciences
Clamps	Amersham Biosciences
Spacers 8 cm x 1 mm	Amersham Biosciences
Spaces 10.5 cm x 1 mm	Amersham Biosciences
Trans-blot® SD semi-dry transfer	BioRad
Extra thick blot paper (mini-blot size)	Amersham Biosciences
Hybond-C extra	Amersham Biosciences
Hyperfilm™	Amersham Biosciences
Super RX Fuji medical x-ray film	Fujifilm

2.1.10.3 Specific buffers for Western blot

2.1.10.3.1 5 X RIPA buffer

5 M NaCl

1 M Tris

5% NP-40

10% DOC

10% SDS

2.1.10.3.2 2 x Protein loading buffer

1 M Tris

Glycerol

10% SDS

β-mercaptoethanol

Bromophenol blue

2.1.10.4 Acrylamide gels for Western blot

30% acrylamide

1.5 M Tris (pH 8.8)

10% SDS

10% APS

TEMED

2.1.10.5 Computer software for analysis of Southern blot

Item	Supplier
Kodak ID 3.5.4 USB	Kodak Scientific Imaging Systems

2.1.11 Materials for transfection

2.1.11.1 Chemical reagents for transfection

Chemical	Supplier
Lipofectamine^{2000}	Invitrogen

2.1.11.5 Specific equipment for transfection

Item	Supplier
EasyjecT Plus	Equibio
ADP-400 printer	Equibio
Electroporation cuvettes	Equibio

2.1.12 Materials for reverse-transcription PCR (RT-PCR)

2.1.12.1 Chemical reagents for RT-PCR

Chemical	Supplier
RNeasy® mini-kit	Qiagen
Reverse-it one step kit	Abgene
Sense primer	(see **7.2 Primers**)
Anti-sense primer	(see **7.2 Primers**)
RT-ase	Abgene

2.1.12.2 Specific equipment for RT-PCR

Item	Supplier
PTC-100™ programmable thermal cycler	MJ Research Inc

2.2 Drugs

2.2.1 PARP inhibitors

2.1.1.1 1,5-dihydroxyisoquinoline (ISQ)

ISQ, (also known as 1,5-dihydroxyisoquinolinediol), is a nicotinamide adenine dinucleotide (NAD) analogue and is a potent inhibitor of poly (ADP-ribose) polymerase (PARP) (IC_{50} = 0.39 μM) (Banasik *et al*, 1992). It is an aromatic nitrogen compound characterised by a double-ring structure, containing a benzene ring and a pyridine ring. ISQ (Sigma) is a yellow-brown powder that is made to a stock solution of 100 mM in DMSO, and stored at -20°C. ISQ was added to the cell culture medium to a final concentration of 0.6 mM (Semionov *et al*, 1999).

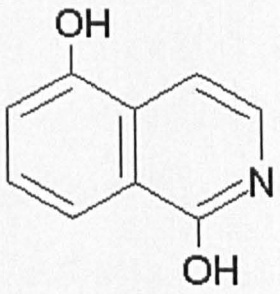

2.1.1.2 NU1025

NU1025, or 8-hydroxy-2-methylquinazoline-4-one, is also a potent PARP inhibitor (IC_{50} = 0.4 μM) (Boulton *et al*, 1995).

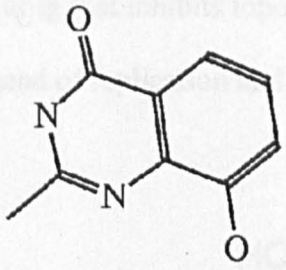

It potentiates the cytotoxicity of various DNA-active agents, including the DNA strand break-inducing drug, temozolomide, topotecan, bleomycin, and ionising radiation in murine L1210 leukaemia cells, Chinese hamster ovary cells, and a variety of human tumour cell lines. NU1025 is an off-white solid (Mw = 176.2) that is made to a stock solution of 10 mM in DMSO and is stored at -20°C.

2.2.2 Chemotherapy drugs

2.2.2.1 Camptothecin (CPT)

Camptothecin is a chemotherapy drug that inhibits topoisomerase I (Top1), an enzyme that relaxes DNA supercoiling ahead of replication and transcription complexes.

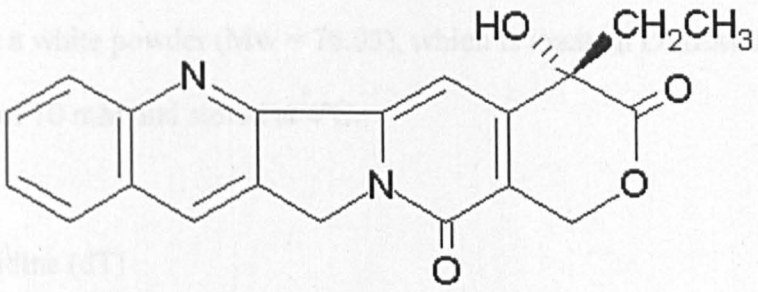

Top1 induces a transient break in the DNA, so that the flanking segments of DNA can rotate freely around it. This break is stabilised by camptothecin, and as replication forks move towards it, they collide and cause the formation of a double strand break, which eventually leads to cell death. Camptothecin (Sigma) is a yellow powder (Mw = 348.35) that is made up in DMSO as a 100 mM stock solution, and stored at -20°C.

2.2.2.2 Hydroxyurea (HU)

HU is a replication fork inhibitor that inhibits DNA synthesis by destroying the catalytically essential free tyrosyl radical of ribonucleoside diphosphate reductase (RNR), blocking the *de novo* synthesis of deoxyribonucleotides.

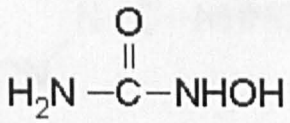

HU (Sigma) is a white powder (Mw = 76.05), which is made in DMEM to a stock concentration of 10 mM and stored at 4°C.

2.2.2.3 Thymidine (dT)

Thymidine is a nucleoside component of DNA and slows replication forks by limiting the dCTP supply.

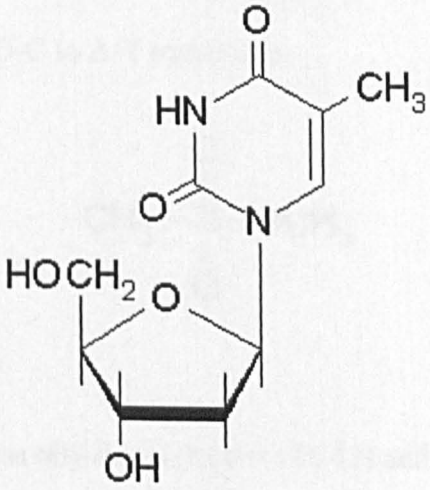

Thymidine (Sigma) is a white powder (Mw = 242.23) that is made up in DMEM at a stock concentration of 40 mM, and stored at 4°C.

2.2.2.4 N-methyl-N-nitro-nitrosoguanidine (MNNG)

MNNG is an alkylating agent and a very potent mutagen. MNNG forms covalent bonds with DNA and forms O^6-methyguanine, causing G-C to A-T transitions.

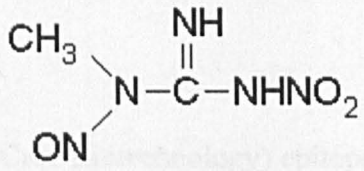

MNNG (Sigma) is a yellow powder (Mw = 147.09) and is made up in DMSO to a stock concentration of 5 mM.

2.2.2.5 Methylmethanesulfonate (MMS)

MMS, or methanesulphonic acid methyl ester, is an alkylating agent and is highly carcinogenic. This chemical also forms covalent bonds with DNA to form O^6-methyguanine, and causes G-C to A-T transitions.

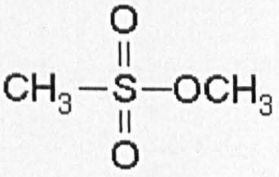

MMS (Sigma) is a colourless oily liquid (Mw = 110.13) and arrived at a concentration of 11.8 moles. Made up a stock solution of 5 mM in DMSO.

2.3 Antibodies

2.3.1 Primary antibodies

2.3.1.1 Anti-Rad51

Rabbit polyclonal IgG (Santa Cruz Biotechnology) epitope corresponds to amino acids 1-92 of human Rad51, but also has cross-reactivity with mouse, rat and hamster Rad51. The antibody was used at a concentration of 1:1000 in PBS, with 3% BSA. Storage was at 4°C.

2.3.1.2 Anti-hXRCC1

Polyclonal anti-hXRCC1 antibody (SeroTec) was raised in rabbit against human XRCC1, and is not cross-reactive with any other species. The antibody was used at a concentration of 1:1000 in PBS, with 3% BSA. Storage was at 4°C.

2.3.1.3 Anti-BrdU

Monoclonal mouse anti-BrdU antibody (Dako) binds to cells that have incorporated bromodeoxyuridine (BrdU) into their DNA during the S-phase of the cell cycle. Anti-BrdU was used at a concentration of 1:1000, in PBS-T. Storage was at 4°C.

2.3.2 Secondary antibodies

2.3.2.1 Anti-rabbit Cy-3-conjugate

Cy™3 Goat anti-Rabbit IgG (H+L) antibody (Zymed) was used at a concentration of 1:500 in PBS with 3% BSA, and because of the light-sensitive nature of the Cy-3 conjugate, was used and stored in the dark. Storage was at 4°C.

2.3.2.2 Anti-rabbit FITC-conjugate

Anti-Rabbit IgG (whole molecule)-FITC antibody (Sigma) was raised in goat, and used at a concentration of 1:1000 in PBS, with 3% BSA. Storage was at 4°C.

2.3.2.3 Anti-mouse FITC-conjugate

Polyclonal goat anti-mouse FITC-conjugated antibody (Dako) was used at a concentration of 1:50,000 in PBS-T. Storage was at 4°C.

2.4 Methods

2.4.1 Cell culture

PARP-1 $^{+/+}$ (A19) and PARP$^{-/-}$ (A11) cells lines are mouse embryonic fibroblasts which have been immortalised (Wang *et al*, 1997). SPD8 are a Chinese hamster lung cell line containing a partial duplication in the *hprt* gene (Helleday *et al*, 1998). These cell lines were grown in Dulbecco's modified Eagle's medium (DMEM) with 10% foetal bovine serum, penicillin (100 U/ml) and streptomycin sulphate (100 μg/ml) under an atmosphere containing 5% CO_2.

The EM9-pcD2EXH, EM9-pcD2EXH5, EM9-pcD2E, EM9-pcXH1-528, EM9-pcXHW385D, EM9-pcXHLI360/361DD were a kind gift from Keith Caldecott, and were grown in α-MEM, with 10% foetal bovine serum, 2% glutamine, penicillin (100 U/ml) and streptomycin sulphate (100 μg/ml) at 37°C under an atmosphere containing 5% CO_2. These cell lines are all XRCC1-/- cell lines that have been complimented with a vector. T he EM9-pcD2EXH and EM9-pcD2EXH5 have been complimented with human XRCC1 (hXRCC1). The EM9-pcD2E cell line has been complimented with an empty vector. The EM9-pcXH1-528 cell line has been complimented with a short version of hXRCC1, it is missing the BRCT II domain. The EM9-pcXHW385D and EM9-pcXHLI360/361DD cell lines have been complimented with hXRCC1 proteins that have a mutated BRCT I domain. The BRCT I domain in EM9-pcXHW385D has the tryptophan residue at position 385 exchanged for an aspartic acid residue. The

BRCT I domain in EM9-pcXHLI360/361DD has the leucine residue at position 360 and the isoleucine residue at position 361 exchanged for aspartic acid residues.

2.4.2 Pulsed-field gel electrophoresis

2.4.2.1 Method for pulsed-field gel electrophoresis

2 x 10^6 cells were plated onto 100 mm cell culture plates in 10 ml DMEM, and allowed to settle overnight at 37°C. Treatment (*Table 1*) was for 24 hours. After treatment, cells were washed x 1 in phosphate-buffered saline (PBS), trypsinised and resuspended into 10 ml DMEM in a 15 ml Falcon tube. Cells were then counted and media containing 1 x 10^6 cells was centrifuged at 2000 rpm for 5 min to form a pellet. The pellets were resuspended in 40 µl PBS, to which 40 µl 1.5% pulsed-field grade agarose (Sigma) in PBS was added, and pipetted into a plug mould (BioRad) The agarose was boiled to 100°C beforehand to prepare and then kept molten at 40°C while the pellet was prepared. The plugs were left to set at 4°C for 5 min. Set plugs were added to 50 ml Falcon tubes containing 1 ml 0.5M EDTA, with 1% N-laurylsarcosine and 1 mg/ml proteinase K (Fisher Scientific), and incubated for 48 hrs at 50°C. After 48 hrs, plugs were washed 4 x 1 hr in cold 1 x TE buffer, and then embedded into a 0.8% agarose gel. Agarose was pulsed-field certified (BioRad) and made in 1 x TBE buffer. The gel was placed into a CHEF-DR® III pulsed-field electrophoresis chamber with 3 L 0.5 x TBE buffer. Buffer was pumped constantly through the chamber by x and kept at 14°C by a cooling module (BioRad). Pulsed-field electrophoresis was carried out for 24 hrs at

4V/cm. Reorientation angle was 120° and switch times were 60-240s. DNA size standard was *S. cerevisiae* (BioRad).

Chapter 2 Table 2.4.2.1: Drugs and concentrations added to each cell line

Cell line	Drug	Concentration
A19 (PARP-1 +/+) A11 (PARP-1 -/-)	Camptothecin Hydroxyurea Thymidine Isoquinoline NU1025	100 nM 0.5 mM 10 mM 0.6 mM 1 mM
AA8 (XRCC1 +/+) EM9 (XRCC1 -/-)	Camptothecin Thymidine MNNG Isoquinoline NU1025	30 nM 10 mM 2 μM 0.6 mM 1 mM

2.4.2.2 Theory of pulsed-field gel electrophoresis

Techniques for measuring double strand breaks (DSBs) in mammalian cells are used to study a number of physiological processes, such as recombination and replication, and pathological processes, such as chemotherapeutic drugs and chemical toxicants.

DSBs are formed as a result of exposure to ionising radiation, clastogenic chemicals, recombination, replication and certain types of repair. The definition of DSBs are closely or oppositely placed lesions, in each of the two phospho-diester backbones of the duplex DNA, that under denaturing conditions will cause one double helical molecule of DNA to become two shorter ones. DSBs are the most deleterious lesion for the cell in terms of lethality, aberration induction and generation of the transformed phenotype. The measurement of DSBs is crucial to the development of understanding

the mechanisms underlying these processes, and pulsed-field gel electrophoresis (PFGE) is one of the most popular techniques.

PFGE is a technique for resolving chromosome-sized DNA (Schwartz and Cantor, 1984), which can be used to measure the amount of DSB formation. By alternating the electric current between spatially distinct pairs of electrodes, mega-base (mb) sized DNA is able to reorient and move at different speeds through the pores in an agarose gel. Here, the CHEF-DR III system has been used, which uses clamped homogeneous electric fields (CHEF) (Chu, 1986, 1990) and programmable autonomously controlled electrodes (PACE) to provide homogenous electric fields within the gel (Clark, 1988; Birren, 1989), using an array of 24 electrodes, which are clamped to intermediate potentials to eliminate lane distortion.

DSBs appear at the top of the gel as large chromosomal fragments and the amount of DSBs induced is shown as a comparison to control lanes, using Kodak 1D3.5.4 USB software (Kodak Scientific Imaging Systems).

2.4.3 Southern blotting

2.4.3.1 Methods for Southern blotting

2.4.3.1.1 Method for DNA extraction

Extracted DNA from 10 x 10^6 cells using 1 ml DNA lysis buffer, with 100 µg/ml proteinase K, and incubated overnight at 37C. Added one volume of isoproponol, mixed by inversion, and transferred the precipitated DNA into 1 ml water. Dissolved the DNA by pipetting and incubating at 37°C. Purified the DNA by phenol-chloroform extraction.

2.4.3.1.2 Method for DNA digestion

Digested DNA in appropriate enzymes and buffers (table 2) for 3 hrs at 37°C, and then ran on a 1% agarose gel to check digestion.

Chapter 3 Table 2.4.3.1.2: Enzymes and buffers added to each digestion mix

Enzyme	Buffer
XhoI	NEB2
HindIII	NEB2
XhoI /HindIII	NEB2
XhoI/HindIII/NcoI	NEB2

2.4.3.1.3 Method for DNA transfer

Ran 35 µl of each digestion, with 5 µl of loading dye, on a 1% gel and ran for 12 hours at 32V. On a light box, cut the gel to size to prevent excess binding of labelled probe to DNA ladder (which was also removed). Soaked gel in 500 ml of 0.25M HCl, with shaking, for 30 min at room temperature (RT). Removed HCL, and rinsed once in sterile water. Poured 1 L 0.4M NaOH into a large tray and set up transfer equipment (see *figure 2.4.3.1.3*)

Figure 2.4.3.1.3: Set-up for Southern blot DNA transfer

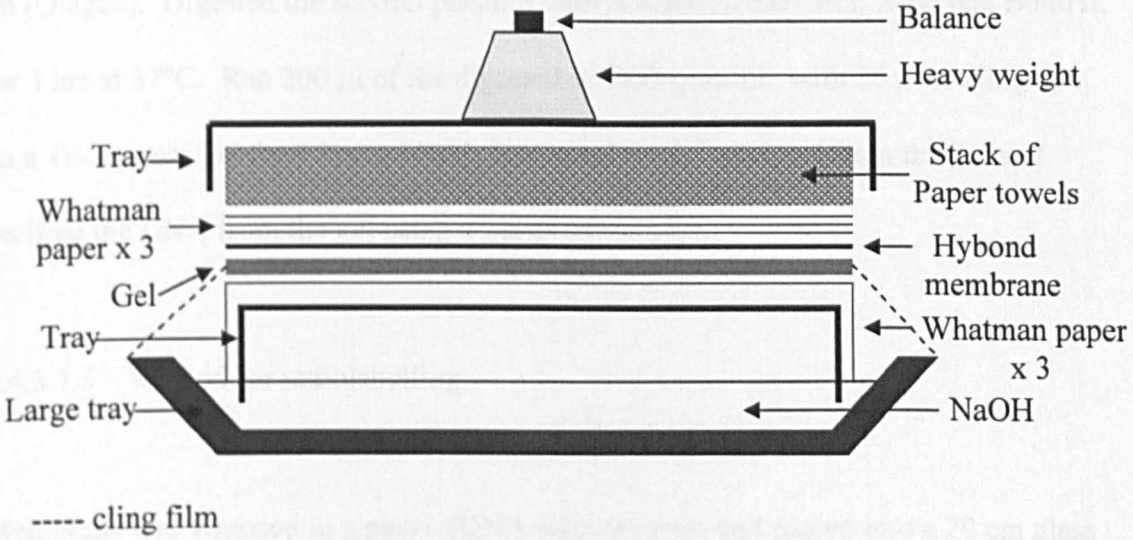

Placed an upturned, wetted, tray into the large tray and placed on top of this, three sheets of wetted (in NaOH) Whatman paper. The gel was arranged on top of the paper and sealed in using Clingfilm, from the edges of the gel to the edge of the large tray. A piece of Hybond nucleotide transfer membrane was cut to the size of the gel and placed on top. Onto this was placed, three sheets of Whatman paper, also cut to size, a stack of paper towels, an upturned tray, and a weight. A balance was placed on top of

the weight in order to ensure equal pressure. Allowed DNA to transfer to the membrane at RT over 16 hrs. Apparatus was dismantled, and membrane was incubated in 2 x SSC for 2 min, before allowing to dry on Whatman paper for 30 min.

2.4.3.1.4 Method for the preparation of the scNEO probe

Took a small sample of bacteria containing a plasmid with the scNEO vector, from a glycerol stock and spread on a LB-ampicillin plate. Incubated the plate overnight at 37°C, and then selected one of the colonies, and grew up overnight in 5 ml of LB-broth, with ampicillin, at 37°C. The plasmid was extracted using the QIAprep spin mini-prep kit (Qiagen). Digested the scNEO plasmid with restriction enzymes, XhoI and BamHI, for 3 hrs at 37°C. Ran 200 µl of the digested scNEO plasmid, with 20 µl loading dye, on a 1% agarose gel for 3 hrs at 100V. Extracted the 1.2 kb band from the gel and purified the DNA from the gel using a gel extraction kit.

2.4.3.1.5 Method for radiolabelling

Membrane was wrapped in a gauze (DNA side inwards) and placed into a 20 cm glass tube, with a screw lid. Into this tube was poured 25.5 ml pre-hybridisation buffer:

10 x SSPE	12.5 ml
100 x Denhardt's solution	1.25 ml
10% SDS	1.25 ml
Water	10 ml
Denatured sonicated DNA	0.5 ml

Sonicated DNA was heated to 100°C, and then chilled, before adding to buffer. Tube was placed into a revolving heated at 65°C overnight. Radiolabelled the scNEO probe by adding 100 ng of the 1.2 kb DNA to 18 µl water and 10 µl of 9-mer primer (Invitrogen). Heated this mix for 5 min at 100°C and then centrifuged briefly at RT. Added 5 x dCTP buffer (Invitrogen) and 7 µl labelled $^{32\text{-}\alpha}$P dCTP, and mixed well with a pipette tip. Added 1 µl exo(-) Klenow enzyme (Invitrogen) and mixed thoroughly with a pipette tip, before incubating at 40°C for 10 min.

The probe was purified using the Qiagen DyeEx kit and then added to 0.5 ml of sonicated DNA and heated to 100°C for 5 min, and put on ice. Mix was added to 25 ml of pre-hybridisation buffer, containing 0.1 g/ml dextran sulphate, to make hybridisation buffer. Poured off the pre-hybridisation buffer from the glass tube, and replaced with the hybridisation buffer. Placed into rotating oven at 65°C overnight. Membrane was then washed x 2 in 2 x SSPE (with 0.1% SDS), with shaking, for 10 min, followed by a washing x 1 in 1 x SSPE (with 0.1% SDS), with shaking, at 65°C. The membrane was then further washed x 1 in 1 x 0.1 x SSPE (with 0.1% SDS) at 65°C. The membrane was then wrapped in Clingfilm and the image was taken using a Fuji phospho-imager.

2.4.4 Immunofluorescence

2.4.4.1 Method for immunofluorescence

1×10^5 cells were plated onto a glass coverslip in 60 mm culture plates in 2 ml DMEM, and allowed to settle for 4 hrs at 37°C. Treatment was for 24 hours. After treatment, cells were washed x 1 in PBS, and fixed for 20 min at RT in 3% paraformaldehyde in PBS-T (with 0.1% triton-X 100 and 0.15% BSA). Coverslips were rinsed for 15 min x 4 in PBS-T and then incubated in primary antibody for 16 hrs at 4°C. After rinsing coverslips for 15 min x 4 in PBS-T, coverslips were incubated in secondary antibody for 1 hr at RT (in dark). Rinsed coverslips for 15 min x 2 in PBS-T, and then for 5 min x 1 in PBS before mounting with SlowFade® Antifade kit (Molecular probes). 2-3 drops of component B (antifade reagent in PBS) were added to each coverslip and blotted before mounting onto microscope slides with component C (equilibrium buffer). Coverslips were sealed with clear varnish and stored at 4°C in a hydrated atmosphere. Images were obtained with a confocal microscope and manipulated using SoftWorx.

2.4.4.2 Theory of immunofluorescence

When exposed to excitation light, all fluorescent dyes fade, or photo-bleach. Photo-bleaching depends on the intensity and duration of illumination. The photon output of a dye represents the average number of cycles of excitation, followed by the emission that the dye goes through before it is reversibly photo-bleached. The average photon output is defined by the ratio of the probability that the dye will fluoresce and the probability that it will photoreact irreversibly to become a non-fluorescent species. These can be

significantly altered by the dye's environment. The main environmental influence on photo-bleaching is oxygen, or a free radical species. Antifade reagents sustain the dye's fluorescence by inhibiting the diffusion of radical oxygen species, therefore decreasing the amount of photo-bleaching, using a compound called 1,4,diazabicyclo[2.2.2]octane, or DABCO, which is a free radical scavenger that extends useful fluorescence emission.

2.4.5 Recombination assays

2.4.5.1 Recombination assays using the HPRT system

Recombination assays using the HPRT system were performed using SPD8 cells, which are a Chinese hamster lung cell line containing a partial duplication in the *hprt* gene.

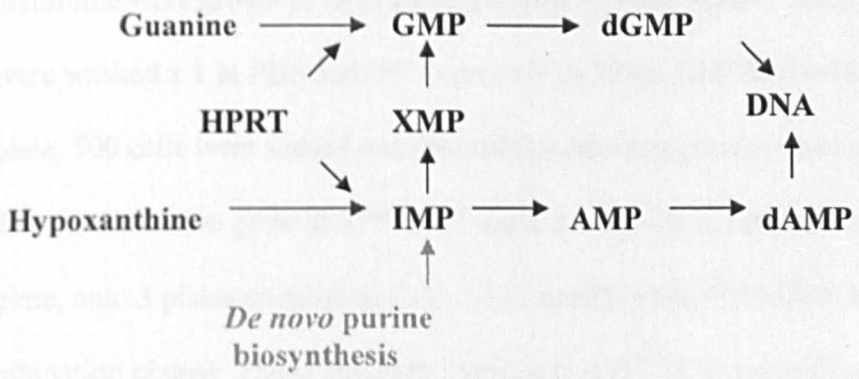

The *hprt* gene codes for the hypoxanthine phosphoribosyltransferase (HPRT) protein, which is involved in the biosynthesis of nucleotides via the salvage pathway (→). The partial duplication in SPD8 leads to inactivation of this gene, and the cells can synthesise nucleotides through the *de novo* pathway (→).

Loss of HPRT activity gives rise to 6-thioguanine (6-tG) resistance. 6-tG is a purine analogue that can be processed by the cell via the salvage pathway, but is toxic if incorporated into the DNA. Therefore only cells lacking the HPRT protein will survive in the presence of this drug. In order to keep SPD8 cells in the HPRT - phenotype they were grown in the presence of 6tG (5 μg/ml).

2.4.5.1.1. Method for recombination assays using the HPRT system

Plated 1 x 10^3 cells into each well of 6-well plates in 2 ml DMEM and grew for 4 days at 37°C. From each well, plated 1 x 10^6 cells onto a 100 mm cell culture plate and left overnight to settle at 37°C. Treatment (*Table 2.4.5.1.1*) was for 24 hours. Cells treated with thymidine were grown in DMEM containing dialysed serum. After treatment, cells were washed x 1 in PBS and left to recover in 10 ml DMEM for 48 hours. From each plate, 500 cells were seeded onto two plates (cloning plates), covered with 10 ml DMEM and allowed to grow at 37°C for 7 days. 3 x 10^5 cells were also seeded from each plate, onto 3 plates containing 1 ml HAsT medium and 9 ml DMEM (recombination plates). HAsT medium contains 5 x 10^{-5} M hypoxanthine, 1 x 10^{-5} M azaserine and 5 x 10^{-6} M thymidine. Hypoxanthine can be converted by HPRT to IMP. Azaserine inhibits the *de novo* pathway.

These plates were grown at 37°C for 10 days. After the specified length of time, the media was poured off each plate, rinsed x 1 with PBS, and stained with methylene blue (0.4% in methanol). Colonies were counted and these data were used to calculate the cloning efficiency and the recombination frequency.

Table 2.4.5.1.1 Drugs and concentrations

Drug	Concentration
Camptothecin	100 Nm
Hydroxyurea	0.5 mM
Thymidine	10 mM
ISQ	0.6 Mm
NU1025	10 μM

2.4.5.1.2 Theory of recombination assays using the HPRT system

SPD8 cells contain a partial duplication of the *hprt* gene, which gives rise to HPRT- phenotype in the presence of 6tG. When the cells are grown in the presence of HAsT media, this blocks the *de novo* synthesis pathway, forcing the cells to synthesise nucleotides via the salvage pathway, and therefore undergoes recombination in order to restore a functional *hprt* gene.

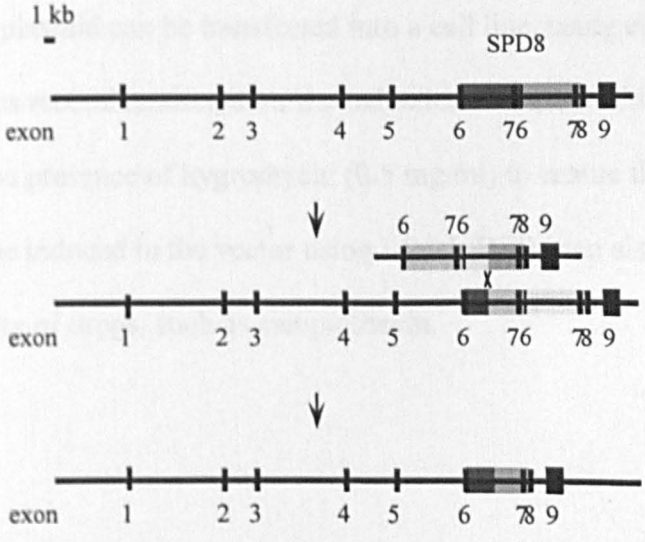

This mechanism can be used as a tool to examine the amount of recombination occurring inside of a cell.

2.4.5.2 Recombination assays using the scNEO system

The scNEO vector contains two defective neomycin phosphotransferase genes, 3′ *neo*, which is a 5′ truncation of the *neo* gene, and *S2neo*, which is mutated by a small internal deletion. The *S2neo* deletion destroys an *Nco*I site and is accompanied by the insertion of the 18 bp I-*Sce*I endonuclease site (Colleaux *et al.*, 1988). Homologous recombination between the two defective *neo* genes can result in a neo^+ gene, which is scored by resistance of cells to the drug G418. Expression of I-*Sce*I allows DSB-promoted recombination events to be scored specifically.

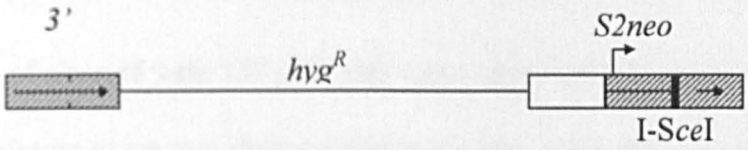

The vector inside a plasmid can be transfected into a cell line, using electroporation, to measure homologous recombination, after the induction of a DSB. Transfected cells must be grown in the presence of hygromycin (0.5 mg/ml) to ensure the plasmid is kept. A single DSB can be induced in the vector using I-SceI. DSBs can also be formed in the vector using a variety of drugs, such as camptothecin.

2.4.5.2.1 Method for transfection

Cell lines used for this assay were SPD8 Chinese hamster cells and EM9 ($XRCC1^{-/-}$) cells. SPD8 cells containing the scNEO vector were then labelled S8SN.11. The EM9 cells containing the scNEO vector were labelled EM9SN.2, EM9SN.7, EM9SN.11, EM9SN.12 and EM9SN.13.

Trypsinised cells, and washed in PBS before resuspending in PBS according to the formula:

$$\frac{\text{Number of cells x volume of media}}{15 \times 10^6} = \text{X ml of PBS}$$

Mixed 15 µg of plasmid with 750 µl of cell suspension and left on ice for 10 minutes. Added this mixture to a 4 mm electroporation cuvette, and electroporated the cells using the EasyjecT electroporator (Equibio) at 1 Kv/cm 50. Left on ice for a further 10-minutes, and then seeded onto 100 mm culture plates at three different volumes, in order to get an even spread of colonies. Incubated the plates at 37°C for several days and added the selective agent, G418 after two days. When colonies could be clearly seen, picked several colonies from each plate and transferred them to separate 25 ml flasks. Grew colonies in alpha-MEM with 100mg/ml G418.

2.4.5.2.2 Method for recombination assays using the scNEO system

1×10^3 cells were plated into each well of 6-well plates in 2 ml DMEM and grew for 4 days at 37°C. After 24 hours, hygromycin (0.5 mg/ml) was added to the medium. From each well, plated 1×10^6 cells onto a 100 mm cell culture plate and left overnight to settle at 37°C. Treatment (*Table 2.4.5.2.1*) was for 24 hours. Cells treated with thymidine were grown in DMEM containing dialysed serum. After treatment, cells were washed x 1 in PBS and left to recover in 10 ml DMEM for 48 hours.

From each plate, 500 cells were seeded onto two plates (cloning plates), covered with 10 ml DMEM and allowed to grow at 37°C for 7 days. 2×10^5 cells were also seeded from each plate, onto five plates containing 10 ml DMEM (recombination plates) and left at 37°C overnight. 100 mg/ml (adjusted) geneticin (G418) was then added to each recombination plate, before returning the plates to the incubator for a further 9 days. After the specified length of time, the media was poured off each plate, rinsed x 1 with PBS, and stained with methylene blue (0.4% in methanol). Colonies were counted and these data were used to calculate the cloning efficiency and the recombination frequency.

Drug	Concentration
Camptothecin	100 nM
Hydroxyurea	0.5 mM
Thymine	10 mM
MMS	3 mM
MNNG	10 μM
I-Sce-I	2 μM (see below)

I-Sce-I was prepared by adding 2 μM of I-Sce-I to 200 μl serum-free DMEM, and mixing this in a 1.5 ml Eppendorf tube with 10 μl lipofectamine^{2000} in 200 μl serum-free DMEM. Mixture was left to stand for 30 minutes at room temperature before

adding to the cell culture plates. The plates were prepared by washing the cells in 3 ml serum free media prior to treatment. Added the mixture to each plate with a further 1600 µl serum-free media and left at 37°C for five hours. As a control, added 10 µl lipofectamine^{2000} in 400 µl serum-free media. After five hours, removed treatment and added 10 ml complete DMEM. The plates were left overnight at 37°C before seeding cloning and recombination plates. Continued as above.

2.4.5.2.2 Theory of recombination assays using the scNEO system

After a DSB has been induced in the scNEO vector, recombination can occur in one of two ways. The vector can either use a homologous section of the *3' neo* gene to remove the I-SceI site in the *S2neo* gene to create a functional *neo* gene, or a homologous site on another vector.

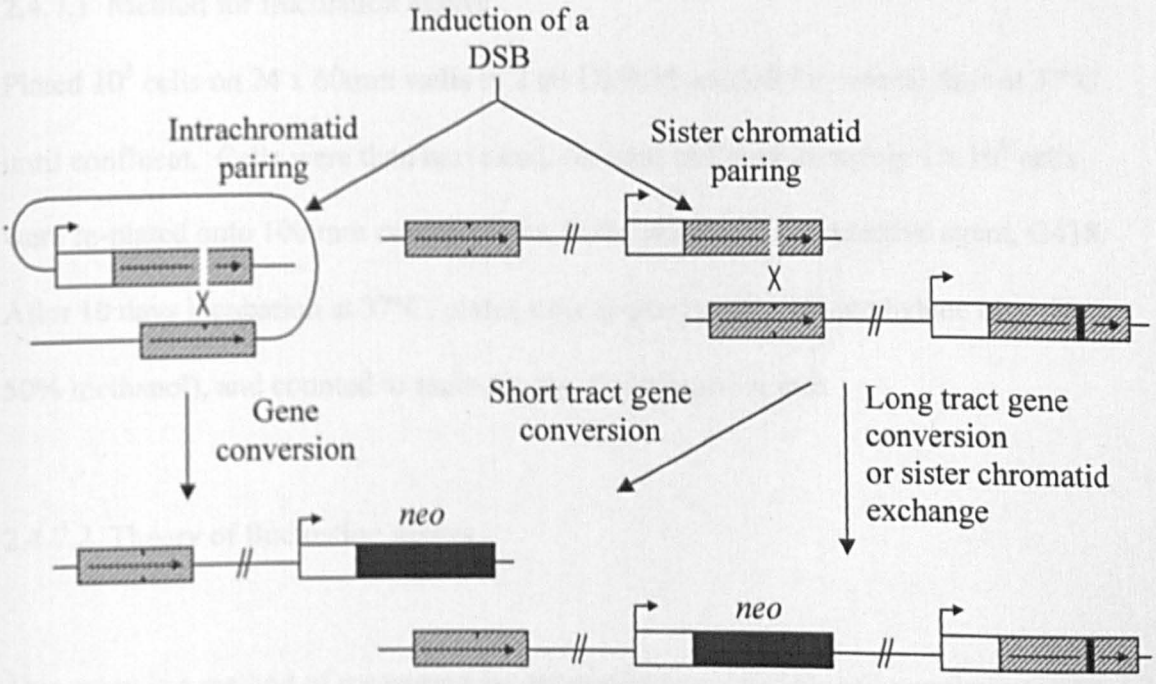

Cells containing the functional gene are selected for by treating with neomycin (G418).

2.4.6 Survival assays

2.4.6.1 Method for survival assays

500 cells were plated onto 100 mm cell culture plates in 10 ml of appropriate media (see **2.4.1**) and allowed to settle for 4 hours at 37°C. Treatments were for continuous for 7 days. After 7 days, the media was removed and plates were rinsed x1 in PBS, before staining with 0.4% methylene blue (in 50% methanol). Colonies bigger than 30 cells were counted and survival was scored as the percentage of colonies per treatment plate compared to an untreated control.

2.4.7 Fluctuation assays

2.4.7.1 Method for fluctuation assays

Plated 10^3 cells on 24 x 60mm wells in 2 ml DMEM and left for several days at 37°C until confluent. Cells were then harvested, counted and approximately 1 x 10^6 cells were re-plated onto 100 mm culture plates, in the presence of a selective agent, G418. After 10 days incubation at 37°C, plates were stained with 0.4% methylene blue (in 50% methanol), and counted to ascertain the recombination rate.

2.4.7.2 Theory of fluctuation assays

This assay is a method of measuring the recombination rate in a cell population. The recombination frequency is the number of recombinants per total number of cells in the

population, but the recombination rate is the number of recombination events per cell division. Depending upon when the first mutation appeared in the population, the recombination rate may show large fluctuations. However, if the cell population is large, the number of cell divisions is approximately equal to the number of cells in the population (N). Fluctuation assays can determine the recombination rate using these formulas:

P_0	=	fraction of total cultures with no reversion
NI	=	initial number of cells/culture
NF	=	final number of cells/culture
N	=	number of cell generations /cell culture = NF-NI / ln2
		or where NF >NI, N = NF/ln2
M	=	average number of revertants per plate = - ln P_0

$$\text{Recombination rate (RR)} = \frac{M}{N} = \frac{-\ln P_0}{NF/\ln 2}$$

Table 2.4.7.2: Example of the calculation of the recombination rate

NI	NF	Without Colonies	Few colonies	P_0	M	N	RR
10^3	10^6	13	11	0.542	-0.613	1442695.04	-1.18327E-09

If the reversion arises spontaneously, there will be a wide fluctuation in revertants from cells grown on different plates. This means that there will be great variation in the number of revertants on each individual plate relative to the mean number of revertants calculated from the sum of all of the plates. In contrast, if the reversions arise by induction there will be relatively little fluctuation in revertants from cells grown on

different plates. In this case, the number of revertants on each plate is approximately equal to the mean number of revertants.

2.4.8 T-test

The t-test assesses whether the data from two groups are statistically different from each other. The formula to work out t is:

$$t = \frac{\text{mean}^1 \text{ (of data set 1)} - \text{mean}^2 \text{ (of data set 2)}}{\sqrt{\frac{\text{variance}^1}{\text{sample size}} + \frac{\text{variance}^2}{\text{sample size}}}}$$

Once you compute the t-value you have to look it up in a table of significance to test whether the ratio is large enough to say that the difference between the groups is not likely to have been a chance finding. Usually the significance level is 0.05. This means that five times out of a hundred you would find a statistically significant difference between the means even if there was none (i.e., by "chance"). You also need to determine the degrees of freedom (df) for the test. In the t-test, the degrees of freedom is the sample size of both groups minus 2. If the level of significance of the t value is $\leq$ 0.05, then the data is significant.

CHAPTER 3: THE ROLE OF PARP-1 IN CAMPTOTHECIN-INDUCED HOMOLOGOUS RECOMBINATION

CHAPTER 3: THE ROLE OF PARP-1 IN CAMPTOTHECIN-INDUCED HOMOLOGOUS RECOMBINATION

3.1 Introduction

Camptothecin is a topoisomerase I (Top1) inhibitor, and stabilises the transient single-strand break (SSB) induced in the DNA by Top1 (Hsiang, 1985). When this SSB encounters an oncoming replication fork, or transcription machinery, a DSB is formed. DSBs are repaired through homologous recombination (HR) (Chadwick & Leenhouts, 1978) and this mechanism appears to be the major repair pathway for CPT-induced DSBs, although non-homologous end joining (NHEJ) also plays an important role (Arnaudeau *et al.*, 2001).

Figure 3.1.1 Top I induces a transient SSB in the DNA.

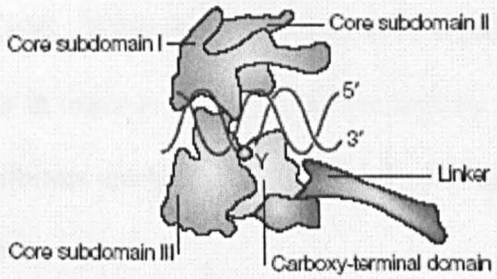

Top1 is organised into multiple subdomains that 'clamp' around the DNA and induce a transient SSB in the DNA in order to relax supercoiled DNA. The 3' end of the broken DNA strand is covalently linked to the active site tyrosyl group of Top1 (red circle). This allows the DNA downstream of the break to rotate, and relaxes the DNA. Top1 then religates the broken DNA strand.

From Wang, 2002

CPT can stabilise the transient SSB created by Top1 by intercalating between upstream (-1) and downstream (+1) base pairs, displacing the downstream DNA and preventing relegation of the cleaved DNA. This means that the SSB will still be intact when a replication fork advances onto it, and cause a DSB to form (**CHAPTER 1**, *Figure 1.6.1*).

DSBs are lethal to the cell if left unrepaired. Therefore, drugs that inhibit the repair of CPT-induced DSBs can enhance the cytotoxicity of camptothecin. This has been shown, both *in vitro* and *in vivo*, by co-treatment with inhibitors of DNA-dependent protein kinase (DNA-PK) or with PARP-1 inhibitors (Bowman *et al.*, 2001), but the mechanism is still unknown.

DNA-PK is involved in the early stages of NHEJ, and is made up of three sub-units, DNA-PKcs, Ku70 and Ku80. These three subunits work together to bind the DNA ends and recruit other proteins in order to repair the DNA ends by re-alignment, joining and re-ligation. DNA-PK inhibitors are likely to enhance the killing of CPT via inhibition of NHEJ mediated DSB repair.

PARP-1 is a nuclear enzyme that detects single-strand and double-strand breaks in the DNA (Neame *et al.*, 1990). Inhibition of PARP-1 affects DNA-PK activity and inhibits repair of ionising-radiation (IR) induced DSBs (Veuger *et al.*, 2004). Thus it is possible that PARP inhibitors affect the NHEJ mediated repair of CPT-induced DSBs. However, double knockout mice deficient in both PARP-1 and DNA-PKcs display enhanced NHEJ and restored V(D)J recombination, compared to DNA-PKcs knockout mice

(Morrison *et al.*, 1997), so this is unlikely. However, inhibition and loss of the protein might have different effects.

PARP-1 has been shown to bind to Top1 directly (Yung *et al*, 2004), and add poly(ADP-ribose) polymers to the Top1 whilst it is bound to the DNA (Malanga & Althaus, 2004). This modifies Top1 so that it removes itself from the DNA and religates the gap. When the Top1-DNA complex is stabilised by CPT, PARP-1 destabilises the complex and enhances religation (Park & Cheng, 2005). However, $PARP^{+/+}$ cells show high sensitivity to CPT, so not all of the complexes can be repaired in this way, leaving a lot of SSBs in the DNA. This could explain the increased sensitivity of PARP-/- or inhibited cells to CPT. If the Top1-DNA-CPT complex cannot be destabilised by PARP-1, this would lead to increased SSBs. Also, tyrosyl-DNA phosphodiesterase 1 (Tdp1) can remove the Top1-DNA-CPT complex from the DNA. However, this leaves a SSB, as Tdp1 does not enhance religation. In the absence of PARP-1, Tdp1 may try to compensate for the lack of PARP-1, but increase the number of SSBs.

Another possibility is that PARP inhibitors affect HR mediated repair of CPT-induced DSBs. Cell lines deficient in PARP-1 have been shown to have an increase in sister-chromatid exchange (SCE), which suggests a hyper-recombination phenotype (de Murcia *et al.*, 1997; Simbulan-Rosenthal *et al.*, 1999; Wang *et al.*, 1997). Since PARP-1 can detect DSBs and DSBs are repaired by HR, we were interested to discover the exact role of PARP-1 in HR. Here, there are two possibilities; either HR is upregulated by loss or inhibition of PARP-1, or that more DSBs are formed following a defect in SSB

repair caused by PARP-1 inhibition. However, if HR is upregulated by PARP-1 inhibition, one would expect resistance to CPT when inhibiting PARP-1.

3.2 Camptothecin has increased cytotoxicity in PARP-1$^{-/-}$ cells

It has been shown that cells co-treated with CPT and PARP-1 inhibitors have increased sensitivity to CPT. When PARP is inhibited it is suggested that it is irreversibly stuck onto DNA strand breaks. Expression of the PARP-1 DNA-binding domain (DBD) acts as a dominant negative and results in increased SCE and reduced DNA repair (Masson *et al.*, 1995; Molinete *et al.*, 1993).

PARP-1 is a 113 kDa protein that is made up of three domains; the N-terminal DBD (46 kDa), an automodification domain (22 kDa), and the C-terminal catalytic domain (54 kDa) (Neame et al., 1990). The DBD contains two zinc fingers, which bind with high affinity to breaks in the DNA. Upon binding, the catalytic domain is stimulated 500-fold to produce long polymers of ADP-ribose. These poly(ADP-ribose) polymers can modify downstream proteins in the DNA repair pathway, but also bind to PARP-1, in the automodification domain (AMD). Once enough of these ADP-ribose polymers have bound to the AMD, PARP-1 leaves the site of the DNA break. This may be because of an electrostatic effect; the ADP-ribose polymers are negatively charged, as is the DNA. This mechanism is believed to clear a space next to the break for repair enzymes to access the break and carry out repair (Lindahl *et al.*, 1995). If only the DBD domain of PARP-1 binds to the DNA break, the catalytic domain cannot be activated, and no poly(ADP-ribose) polymers can form. Therefore, the AMD of PARP-1 cannot be

automodified, and PARP-1 will not move away from the site of the break, in order for repair enzymes to access the break and carry out repair.

The ability of PARP to enhance the cytotoxicity of CPT may therefore be because PARP-1 is bound irreversibly onto CPT-induced SSBs. This prevents the DNA repair enzymes from accessing the site of damage, and prevents repair. This unrepaired SSB could become a DSB if it collides with an oncoming replication fork, and be lethal to the cell. Alternatively, a loss of PARP-1 protein, and therefore its activity, could increase sensitivity to CPT. To test this, we treated the PARP-$1^{-/-}$ (A11) and PARP-$1^{+/+}$ (A19) mouse embryonic fibroblast cell lines continuously with increasing doses of CPT for 7 days.

Figure 3.2 Camptothecin has increased cytotoxicity in PARP-$1^{-/-}$ cells

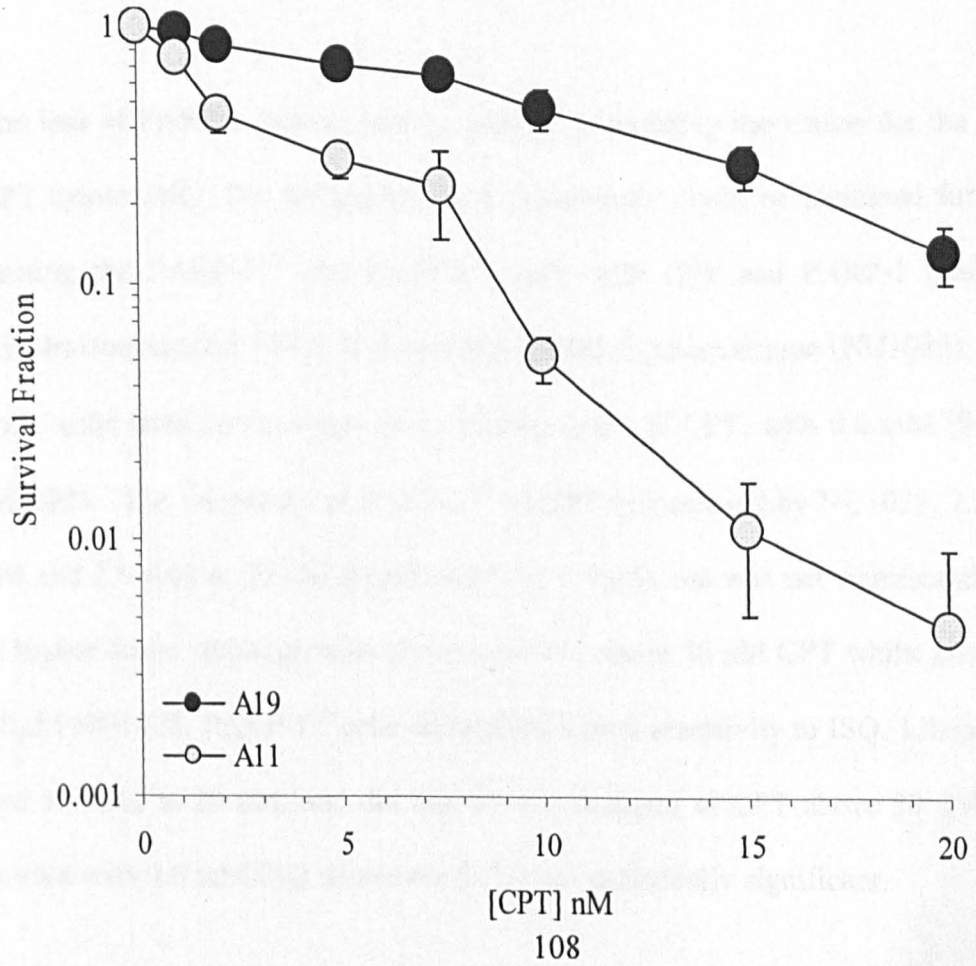

PARP-$1^{+/+}$ (A19) and PARP-$1^{-/-}$ (A11) cells were treated in increasing doses of CPT for 7 days at 37°C, under an atmosphere containing 5% CO2. The effect of CPT on cells is expressed as a percentage of controls and the values are the mean ± S.E. of three independent experiments.

We observed that PARP-$1^{-/-}$ cells were more sensitive to CPT than the PARP-$1^{+/+}$ cell line, and showed a 28.7-fold increase in cytotoxicity at a 20 nM dose (*figure 3.2*), which is significant to $p < 0.01$. This suggests that it is the loss of PARP-1 protein or its activity rather than an inability for PARP-1 to be displaced from DNA that is causing enhanced CPT sensitivity.

3.3 Co-treatment of PARP-$1^{+/+}$ and PARP$^{-/-}$ cells with camptothecin and PARP-1 inhibitors increases the killing effect of camptothecin

The loss of PARP-1 protein and its activity is probably the reason for the increase in CPT cytotoxicity. We wondered if the cytotoxicity could be increased further by co-treating the PARP-$1^{+/+}$ and PARP-$1^{-/-}$ cells with CPT and PARP-1 inhibitors, 1,5-dihydroisoquinoline (ISQ) or 8-hydroxy-2-methylquinazolinone (NU1025). We treated both cells lines continuously in increasing doses of CPT, with 0.6 mM ISQ or 10μM NU1025. The sensitivity of PARP-$1^{+/+}$ to CPT is increased by NU1025, 2.2-fold at 10 nM and 2.9-fold at 20 nM (significant to $p < 0.05$), but was not significantly increased at higher doses, although cells did not survive above 50 nM CPT whilst co-treated with 10μM NU1025. PARP-$1^{+/+}$cells showed increased sensitivity to ISQ, 1.4-fold at 10 nM and 1.5-fold at 20 nM, and did not survive at doses of CPT above 50 nM, whilst co-treated with 0.6 mM ISQ. However this is not statistically significant.

Figure 3.3 Co-treatment of PARP-1$^{+/+}$ and PARP-1$^{-/-}$ cells with camptothecin and PARP-1 inhibitors increases the killing effect of camptothecin

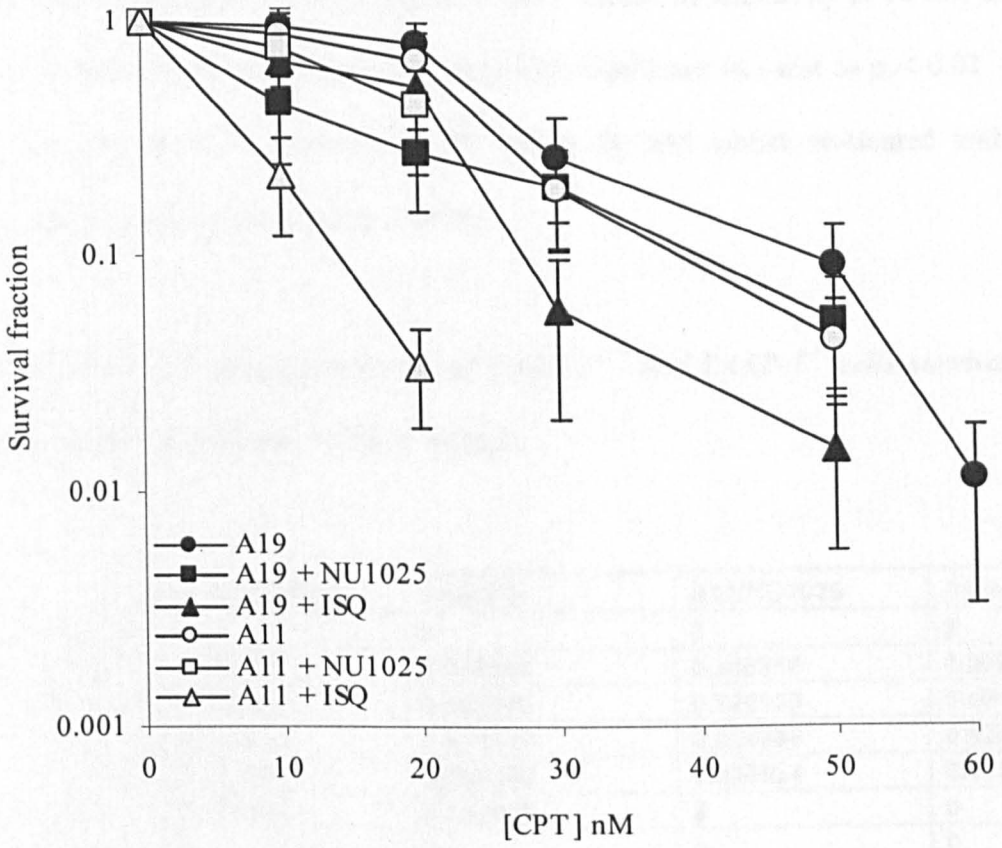

PARP-1+/+ (A19) and PARP-1-/- (A11) cells were treated in increasing doses of CPT for 7 days at 37°C, with or without PARP-1 inhibitors, 1,5-dihydroisoquinoline (0.6 mM) or NU1025 (10 μM), under an atmosphere containing 5% CO2. The effect of CPT and inhibitors on cells is expressed as a percentage of controls and the values are the mean ± S.E. of six independent experiments.

PARP-1$^{-/-}$ cells did not show a significant increase in sensitivity to CPT whilst co-treated with NU1025, 1.1-fold at 10 nM and 1.5-fold at 20 nM, and did not survive at

doses above 20 nM CPT when co-treated with 10 μM NU1025. This lack of survival above 20 nM is significant to $p < 0.05$. Co-treatment with 0.6 mM ISQ had a much greater effect on PARP-$1^{-/-}$ cells, with a 4-fold increase in sensitivity at 10 nM and 20-fold at 20 nM (*Figure 3.3*). This is statistically significant in t-test to $p < 0.01$. These cells did not survive at doses of CPT above 20 nM whilst co-treated with ISQ (statistically significant in t-test, $p < 0.05$).

Table 3.3 T-test showing significance of PARP-$1^{+/+}$ and PARP-$1^{-/-}$ cells survival after co-treatment with CPT and NU1025 or ISQ.

		A19/NU1025	A19/ISQ	A11/NU1025	A11/ISQ
CPT nM	0	0	0	0	0
	10	0.049255	0.125528	0.386318	0.007428
	20	0.02105	0.162976	0.226132	0.004762
	30	0.326214	0.071714	0.024896	0.024896
	50	0.24318	0.063262	0.029524	0.029524
	60	0.092639	0.092639	0	0
	80	0	0	0	0
	100	0	0	0	0

These results suggest that the inhibition of PARP-1 by ISQ or NU1025 increases the cytotoxicity of CPT in PARP-$1^{+/+}$ cells, but that cells deficient in PARP-1 show a much greater sensitivity to ISQ. PARP-$1^{-/-}$ cells do not show increased sensitivity when co-treated with CPT and NU1025.

There are several proteins in the PARP family, however PARP-1, PARP-2 and PARP-3 are thought to have slightly overlapping roles. PARP-1 is the most abundant of these three as PARP-2 and PARP-3 are present in the cell at comparatively low levels.

Therefore, PARP-1 has the most activity and could be the most important in CPT toxicity. However, it could be hypothesised that PARP-2 and PARP-3 could compensate for the lack of PARP-1 in some way. This increase in cytotoxicity with co-treatment of CPT and ISQ could be because NU1025 is inhibiting only PARP-1 and ISQ is inhibiting PARP-2 and PARP-3, as well as PARP-1, and therefore removing any compensatory effect.

The cytotoxicity of CPT is not increased in PARP-$1^{-/-}$ cells when co-treated with CPT and NU1025. This is probably because the PARP-1 protein is not present in this cell line, so cannot be inhibited. However, an increase in cytotoxicity was observed when PARP-$1^{-/-}$ cells were co-treated with CPT and ISQ. This could be because ISQ is inhibiting PARP-2 and PARP-3, which of course are present in this cell line, and could have a small compensatory effect. This could explain why the cytotoxicity of CPT is increased still further in PARP-$1^{-/-}$ cells.

3.4 Camptothecin increases the formation of DNA double-stranded breaks in PARP-$1^{-/-}$ cells

Camptothecin is a topoisomerase I inhibitor (Top1), which stabilises the transient single-strand break (SSB) that Top1 causes in order to relax the DNA. When this stabilised SSB collides with an oncoming replication fork this causes the formation of DSBs. It is possible that increased levels of SSBs following inhibition of PARP-1 cause more replication forks to collapse, which may result in an increased amount of toxic DSBs.

Figure 3.4: Camptothecin increases the formation of DNA double strand breaks in PARP-1$^{-/-}$ cells.

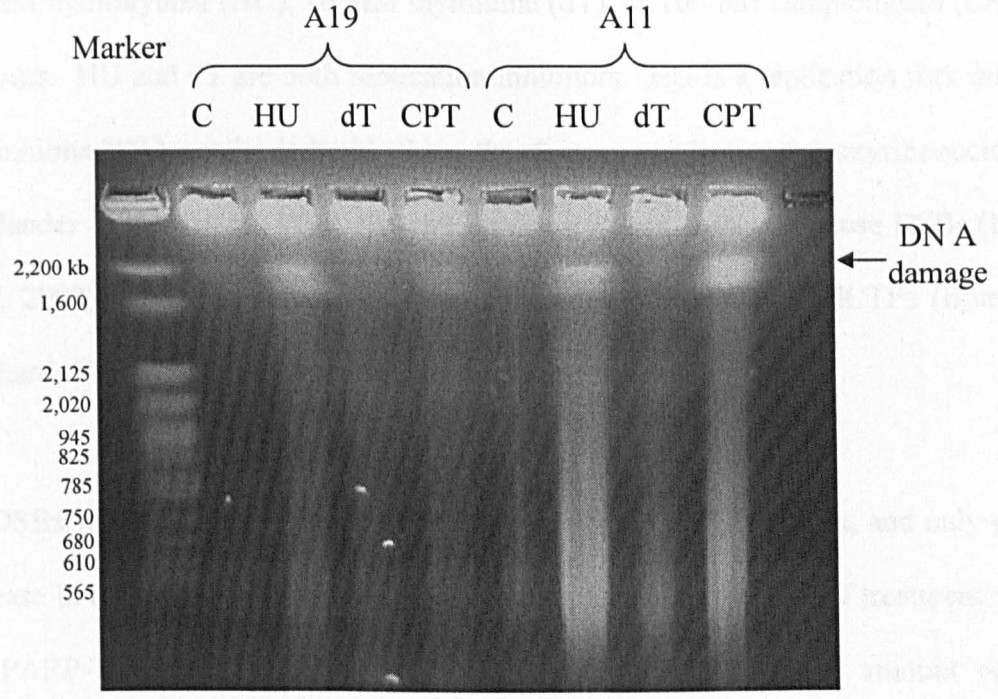

C - control	HU – hydroxyurea 0.5 mM
dT – thymidine 10 mM	CPT – camptothecin 100 nM

PARP-1$^{+/+}$ (A19) and PARP-1$^{-/-}$ (A11) cells were treated with HU (0.5 mM), dT (10 mM) or CPT (100 nM) for 24 hours at 37°C, under an atmosphere containing 5% CO2. Cells were then embedded in 0.75% agarose plugs and treated with N-laurylsarcosine (1% v/v) and proteinase K (1 mg/ml) for 48 hours at 50°C, to remove cell membranes and proteins so that only DNA remains in the plug. Plugs were then embedded in a 0.8% agarose gel and ran at 4V/cm for 24 hours in a CHEF-DR III pulsed-field gel electrophoresis chamber. Switch times were 60-120s and the reorientation angle was 120°. Double-strand breaks are indicated by the chromosome fragments at 2,200 kb. The smears on the PFGE are the result of nucleosomal fragments from apoptosis.

To test this we determined the amount of DSBs in PARP-$1^{+/+}$ and PARP-$1^{-/-}$ cell lines using a pulsed-field gel electrophoresis (PFGE). Both cell lines were treated with 0.5 mM hydroxyurea (HU), 10 mM thymidine (dT), or 100 nM camptothecin (CPT) for 24 hours. HU and dT are both replication inhibitors. HU is a replication fork inhibitor that inhibits DNA synthesis by blocking the *de novo* synthesis of deoxyribonucleotides (Thelander & Reichard, 1979), and has previously been shown to cause DSBs (Lundin *et al*, 2002). dT stalls replication forks by depleting the pool of dCTPs (Bjursell & Reichard, 1973), but is not thought to cause DSBs.

No DSBs were detected in the control or following the dT treatment, and only a small increase in the amount of DSB formation was detected following HU treatment of both the PARP-$1^{+/+}$ and PARP-$1^{-/-}$ cell lines. However, an increased amount of DSB formation was seen in the CPT-treated plug from the PARP-$1^{-/-}$ cell line, compared to the PARP-$1^{+/+}$ cell line (*Figure 3.4*).

When CPT stabilises the transient SSBs caused by Top1, these SSBs are left unrepaired, and can form DSBs if they collide with an oncoming replication fork (**CHAPTER 1**, *Figure 1.6.1*). These results show that DSBs are formed in both the PARP-$1^{+/+}$ and the PARP-$1^{-/-}$ cell lines, after treatment with 100 nM CPT, probably due to stabilised SSBs colliding with an oncoming replication fork to cause DSBs. There is an increase in DSBs caused by CPT in PARP-$1^{-/-}$ cells. This is probably because there are increased levels of SSBs in these cells, because of the lack of PARP-1. Once stabilised, Top1 cannot relegate the SSB, leaving an unrepaired SSB in the DNA. In PARP-$1^{+/+}$ cells,

these breaks are detected by PARP-1 and repaired by repair proteins, although this repair does not appear to be efficient, as a lot of DSBs are still formed.

In PARP-$1^{-/-}$ cells, these SSBs are left undetected and are able to form DSBs when in collision with an oncoming replication fork. It seems that any repair of these SSBs, after detection by PARP-1, offers some protection to the cell, and makes sure at least some of the SSBs are repaired and do not form DSBs. In the absence of PARP-1, it could be that these SSBs are undetected and that none of the SSBs are detected and therefore lead to more DSBs.

3.5 DNA double-strand breaks are increased in PARP-$1^{+/+}$ cells co-treated with camptothecin and PARP-1 inhibitors

CPT causes DSBs in PARP-$1^{+/+}$ cells, and this is increased in PARP-$1^{-/-}$ cells, where the PARP-1 protein is absent. We were interested to see if the same effect could be seen if PARP-1+/+ cells were co-treated with CPT and ISQ or NU1025. PARP-$1^{+/+}$ and PARP-$1^{-/-}$ cell lines were treated for 24 hours with 100 nM CPT. PARP-$1^{+/+}$ cells were also co-treated with 100 nM CPT and 0.6 mM ISQ or 10 μM NU1025 for 24 hours. Cells were embedded into plugs and investigated by PFGE.

CPT-treated plugs from the PARP-$1^{-/-}$ cells showed an increase in DSBs compared to CPT-treated plugs from the PARP-$1^{+/+}$ cells (*Figure 3.5*). However, plugs from the PARP-$1^{+/+}$ cells co-treated with CPT and ISQ, or CPT and NU1025 showed an increase in DSB formation, to the same level as the breaks detected in plugs from the PARP-$1^{-/-}$ cell line.

Figure 3.5: DNA double-strand breaks are increased in PARP-1$^{+/+}$ co-treated with camptothecin and PARP-1 inhibitors.

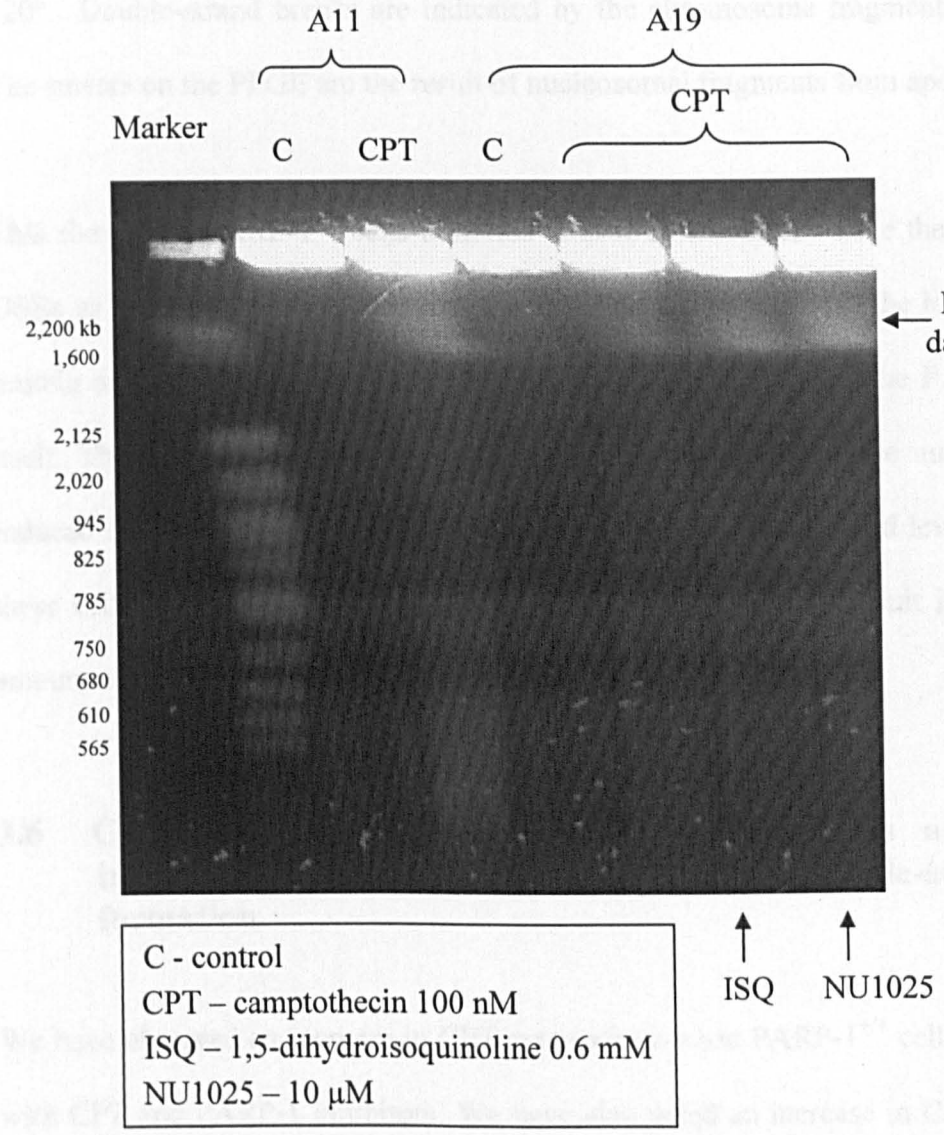

PARP-1$^{-/-}$ (A11) cells were treated with CPT (100 nM) and PARP-1$^{+/+}$ (A19) were treated with CPT (100 nM) with or without 1,5-dihydroisoquinoline (ISQ, 0.6 mM) or NU1025 (10 µM) for 24 hours at 37°C, under an atmosphere containing 5% CO2. Cells were then embedded in 0.75% agarose plugs and treated with N-laurylsarcosine (1% v/v) and proteinase K (1 mg/ml) for 48 hours at 50°C, to remove cell membranes and proteins so that only DNA remains in the plug. Plugs were then embedded in a 0.8%

agarose gel and ran at 4V/cm for 24 hours in a CHEF-DR III pulsed-field gel electrophoresis chamber. Switch times were 60-120s and the reorientation angle was 120°. Double-strand breaks are indicated by the chromosome fragments at 2,200 kb. The smears on the PFGE are the result of nucleosomal fragments from apoptosis.

This shows that PARP-$1^{+/+}$ cells inhibited with ISQ or NU1025 have the same level of DSBs as PARP-$1^{-/-}$ cells when treated with CPT. Therefore, it is the lack of PARP-1 protein activity that increases the level of SSBs, not the lack of the PARP-1 protein itself. This also shows that the inhibition of PARP-1 increases the number of CPT-induced DSBs formed in PARP-$1^{+/+}$ cells, probably due to increased levels of SSBs in these cells which cause more replication forks to collapse and result in an increased amount of toxic DSBs.

3.6 Co-treating PARP-$1^{-/-}$ cells with camptothecin and PARP-1 inhibitors increases the amount of DNA double-strand break formation

We have observed an increase in CPT cytotoxicity when PARP-$1^{+/+}$ cells are co-treated with CPT and PARP-1 inhibitors. We have also noted an increase in CPT cytotoxicity in PARP-$1^{-/-}$ cells as compared with PARP-$1^{+/+}$ cells. We have noticed a further increase in CPT cytotoxicity when PARP-$1^{-/-}$ cells are co-treated with CPT and ISQ. ISQ is known to inhibit several PARP proteins, unlike NU1025, which is specific for PARP-1. Therefore it is possible that an increased amount of cytotoxicity could be seen due to removal of some compensatory effect from PARP-2 and PARP-3. If this is the case, you would expect to see a further increase in DSB formation in PARP-$1^{-/-}$ cells when co-treated with CPT and ISQ.

Figure 3.6: Co-treating PARP-1$^{-/-}$ cells with camptothecin and PARP-1 inhibitors increases the amount of DNA double-strand break formation.

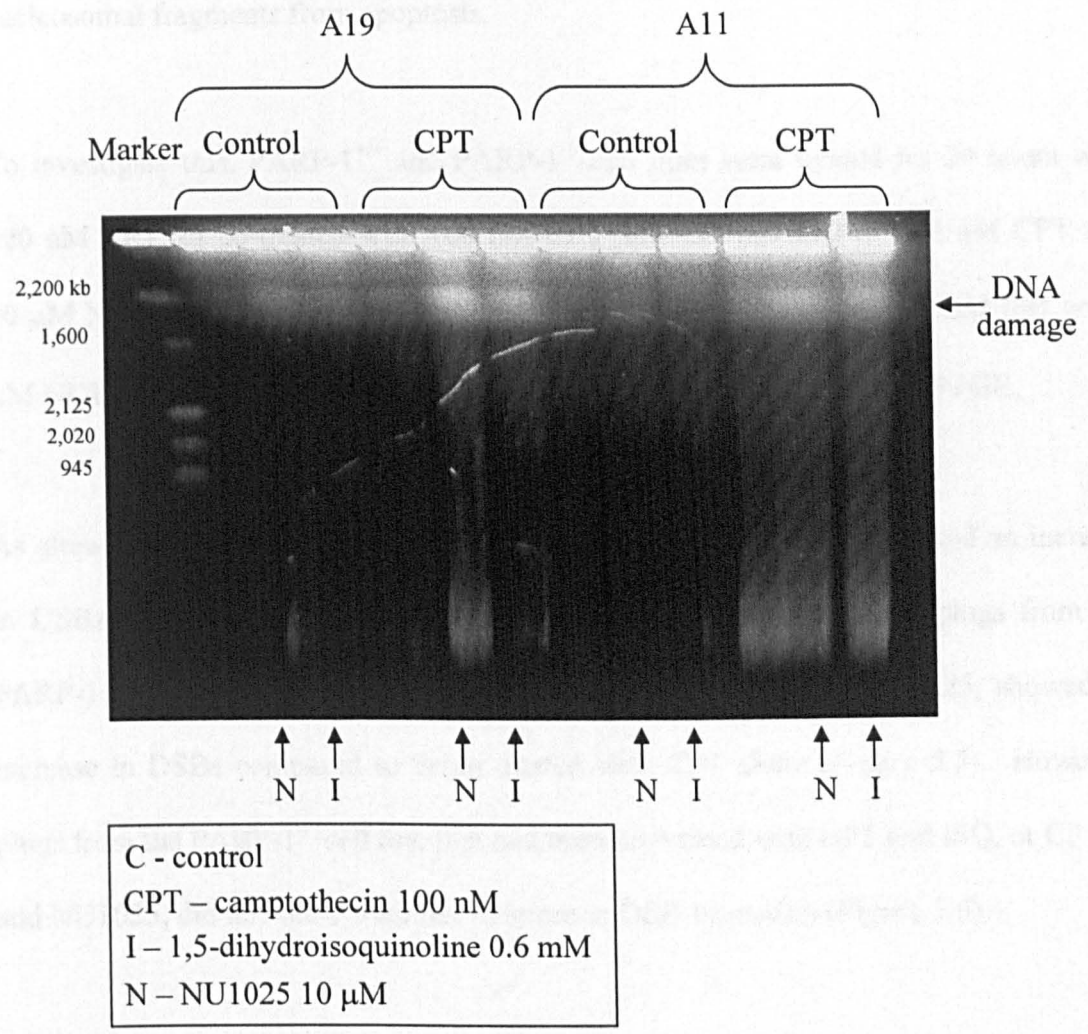

PARP-1$^{+/+}$ (A19) and PARP-1$^{-/-}$ (A11) were treated with 1,5-dihydroisoquinoline (ISQ, 0.6 mM) or NU1025 (10 μM) with or without CPT (100 nM) for 24 hours at 37°C, under an atmosphere containing 5% CO2. Cells were then embedded in 0.75% agarose plugs and treated with N-laurylsarcosine (1% v/v) and proteinase K (1 mg/ml) for 48 hours at 50°C, to remove cell membranes and proteins so that only DNA remains in the plug. Plugs were then embedded in a 0.8% agarose gel and ran at 4V/cm for 24 hours in a CHEF-DR III pulsed-field gel electrophoresis chamber. Switch times were 60-120s

and the reorientation angle was 120°. Double-strand breaks are indicated by the chromosome fragments at 2,200 kb. The smears on the PFGE are the result of nucleosomal fragments from apoptosis.

To investigate this, PARP-$1^{+/+}$ and PARP-$1^{-/-}$ cell lines were treated for 24 hours with 100 nM CPT, or co-treated with 100 nM CPT and 0.6 mM ISQ or 100 nM CPT and 10 μM NU1025. Both cell lines were also treated for 24 hours with 0.6 mM ISQ or 10 μM NU1025 alone. Cells were embedded into plugs and analysed using PFGE.

As already seen, the CPT-treated plug from the PARP-$1^{-/-}$ cell line showed an increase in DSBs, compared to the PARP-$1^{+/+}$ cell line (*Figure 3.4*), and the plugs from the PARP-1+/+ cell line co-treated with CPT and ISQ, or CPT and NU1025, showed an increase in DSBs compared to being treated with CPT alone (*Figure 3.5*). However, plugs from the PARP-$1^{-/-}$ cell line that had been co-treated with CPT and ISQ, or CPT and NU1025, did not show a further increase in DSB formation (*Figure 3.6*).

These results show an increase in DSBs in PARP-$1^{+/+}$ cells when co-treated with CPT and PARP-1 inhibitors, NU1025 or ISQ, compared to PARP-$1^{+/+}$ cells treated with CPT alone. The results also show that there is no increase in DSB formation in PARP$^{-/-}$ cells when co-treated with CPT and PARP-1 inhibitors, NU1025 or ISQ. This would suggest that PARP-2 and PARP-3 do not cause an increase in DSBs and so any increase in CPT cytotoxicity caused by co-treatment of cells with CPT and ISQ is not due to an increase in DSB formation.

3.7 Camptothecin-induced RAD51 foci formation is increased in PARP-1$^{-/-}$ cells

RAD51 foci are small nuclear foci containing all of the proteins involved in homologous recombination (HR). These foci form whenever the cell undergoes HR, and a measurement of these can be used as an indication of the amount of HR that is taking place within a cell.

Homologous recombination (HR) appears to be the major repair pathway for CPT-induced DSBs, so to determine if HR is increased in PARP-1$^{+/+}$ and PARP-1$^{-/-}$ cells when treated with CPT, we measured the amount of RAD51 foci formed in cells from both cell lines when treated with CPT and when no treatment was given. The PARP-1$^{+/+}$ and PARP-1$^{-/-}$ cell lines were treated with 100 nM CPT for 24 hours and fixed onto coverslips.

The level of RAD51 foci was examined using immunofluorescence. PARP-1$^{-/-}$ cells have an increased amount of spontaneous RAD51 foci compared to PARP-1$^{+/+}$ cells (*Figure 3.7.1*), 10.4% of PARP-1$^{-/-}$ cells have > 10 RAD51 foci per cell compared to 3.2% of PARP-1$^{+/+}$ cells. This is a 3.3-fold significant difference ($p < 0.05$). Both PARP-1$^{+/+}$ and PARP-1$^{-/-}$ cells have an increased amount of RAD51 foci formation after a 24 hour treatment with CPT, 21-fold and 8.8-fold respectively, above their spontaneous levels. PARP-1$^{-/-}$ cells, however, have a much higher level of RAD51 foci formation, 92% of PARP-1-/- cells compared to 67% of PARP-1$^{+/+}$ cells. This is a 1.4-fold significant difference ($p < 0.001$) (*figure 3.7.2*).

Figure 3.7.1: Rad51 foci in untreated PARP$^{+/+}$ and PARP$^{-/-}$ cells.

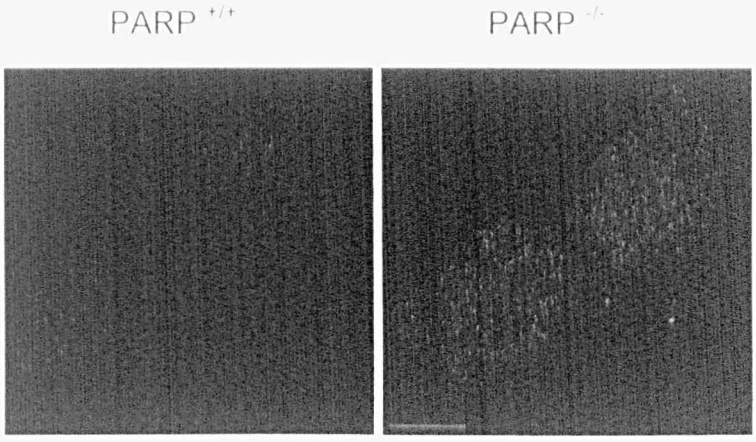

PARP-1$^{+/+}$ (A19) and PARP-1$^{-/-}$ (A11) cells were fixed in 3% paraformaldehyde, and incubated with anti-Rad51 primary antibody, and then a Cy3-conjugated antibody. Images were obtained with a confocal microscope and manipulated using SoftWorx.

These results suggest that HR is increased spontaneously in PARP$^{-/-}$ cells, probably because of an increase in SSBs leading to DSB formation when encountered by replication machinery, and that HR is the preferred mechanism for the repair of these DSB. HR is also shown to be increased in PARP-1$^{-/-}$ cells when treated with CPT. This suggests that HR is the major pathway for the repair of CPT-induced damage.

In this assay, it was noted that there was an increase in RAD51 foci in PARP$^{-/-}$ cells treated with CPT. This suggests that HR is increased in this cell line when treated with CPT. It was also noted that this increase in HR was above the level observed for CPT-treated PARP-1$^{+/+}$ cells. It has already been noted that there is an increased amount of RAD51 foci in untreated PARP$^{-/-}$ cells. This could be accounted for because of the hyper recombination phenotype of this cell line. This further increase in HR when

Figure 3.7.1: Rad51 foci in untreated PARP $^{+/+}$ and PARP $^{-/-}$ cells.

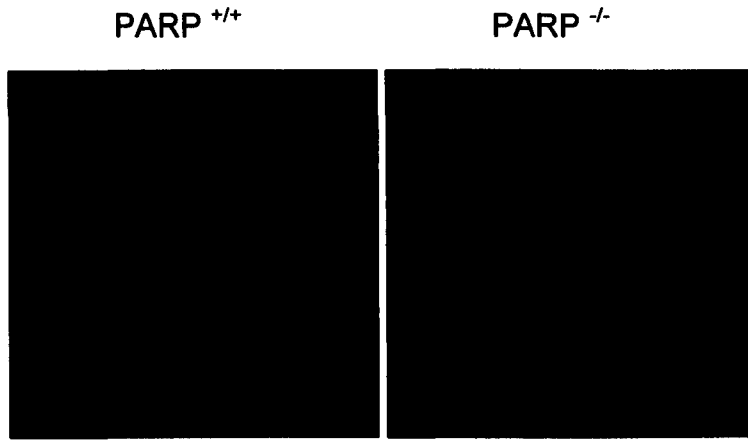

PARP-1$^{+/+}$ (A19) and PARP-1$^{-/-}$ (A11) cells were fixed in 3% paraformaldehyde, and incubated with anti-Rad51 primary antibody, and then a Cy3-conjugated antibody. Images were obtained with a confocal microscope and manipulated using SoftWorx.

These results suggest that HR is increased spontaneously in PARP$^{-/-}$ cells, probably because of an increase in SSBs leading to DSB formation when encountered by replication machinery, and that HR is the preferred mechanism for the repair of these DSB. HR is also shown to be increased in PARP-1$^{+/+}$ cells when treated with CPT. This suggests that HR is the major pathway for the repair of CPT-induced damage.

In this assay, it was noted that there was an increase in RAD51 foci in PARP$^{-/-}$ cells treated with CPT. This suggests that HR is increased in this cell line when treated with CPT. It was also noted that this increase in HR was above the level observed for CPT-treated PARP-1$^{+/+}$ cells. It has already been noted that there is an increased amount of RAD51 foci in untreated PARP$^{-/-}$ cells. This could be accounted for because of the hyper-recombination phenotype of this cell line. This further increase in HR when

treated with CPT could be due to a synergistic effect. There is already increased HR in these cells, but HR is increased further in order to repair an increased number of DSB lesions caused by CPT.

Figure 3.7.2: Camptothecin-induced Rad51 foci formation is increased in PARP-1$^{-/-}$ cells.

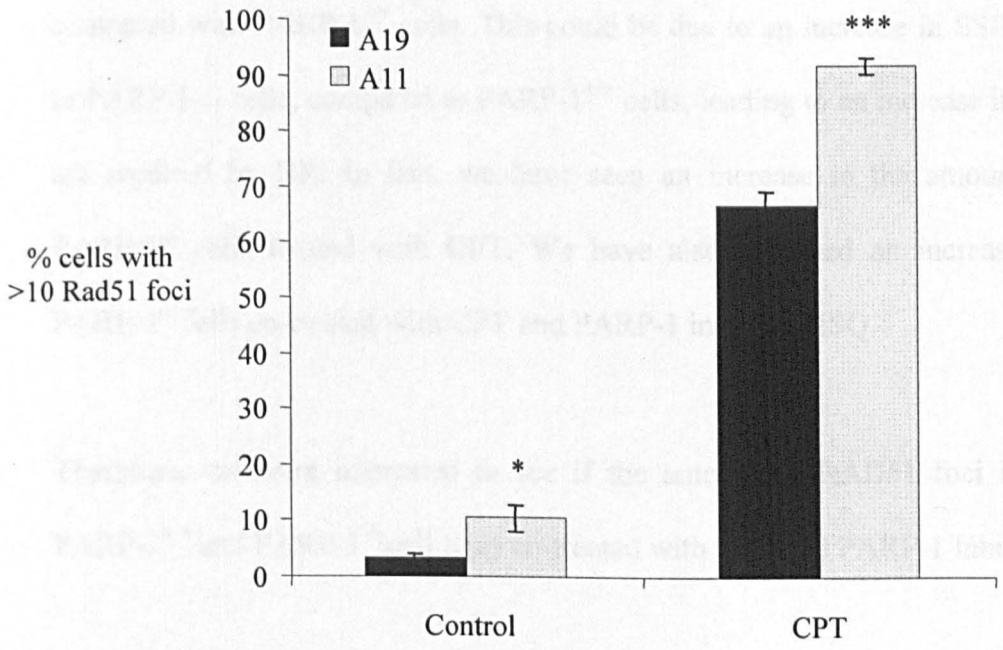

PARP-1$^{+/+}$ (A19) and PARP-1$^{-/-}$ (A11) cells were treated with 100 nM CPT for 24 hours at 37°C, under an atmosphere containing 5% CO2. Cells were then fixed in 3% paraformaldehyde, and incubated with anti-Rad51 primary antibody, and then a Cy3-conjugated antibody. The effect of CPT on cells is expressed as a percentage of cells containing more than 10 Rad51 foci and the values are the mean ± S.E. of three independent experiments.

3.8 Co-treatment of PARP-$1^{+/+}$ and $PARP^{-/-}$ cells with camptothecin and 1,5-dihydroisoquinoline significantly increases the amount of RAD51 foci formation in PARP-$1^{-/-}$ cells but not in PARP-$1^{+/+}$ cells

We have observed an increased amount of RAD51 foci formation in PARP-$1^{-/-}$ cells, and in PARP-$1^{+/+}$ and PARP-$1^{-/-}$ cells treated with CPT. We have also noticed an increased amount of RAD51 foci formation in PARP-$1^{-/-}$ cells treated with CPT, compared with PARP-$1^{+/+}$ cells. This could be due to an increase in SSB accumulation in PARP-1-/- cells, compared to PARP-$1^{+/+}$ cells, leading to an increase in DSBs, which are repaired by HR. In fact, we have seen an increase in the amount of DSBs in PARP-$1^{-/-}$ cells treated with CPT. We have also observed an increase in DSBs in PARP-$1^{-/-}$ cells co-treated with CPT and PARP-1 inhibitor, ISQ.

Therefore, we were interested to see if the amount of RAD51 foci is increased in PARP-$1^{+/+}$ and PARP-$1^{-/-}$ cell lines co-treated with CPT and PARP-1 inhibitor, ISQ.

Figure 3.8: Co-treatment of PARP-1$^{+/+}$ and PARP-1$^{-/-}$ cells with camptothecin and 1,5-dihydroisoquinline does not significantly increase the amount of Rad51 foci formation.

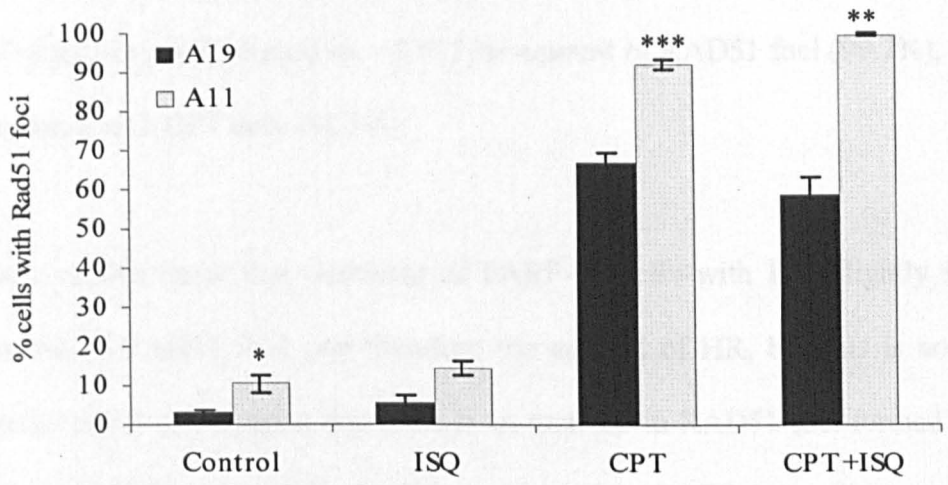

PARP-1$^{+/+}$ (A19) and PARP-1$^{-/-}$ (A11) cells were treated with 100 nM camptothecin (CPT), 1,5-dihydroisoquinoline (ISQ) (0.6 mM) or a co-treatment of both, for 24 hours at 37°C under an atmosphere containing 5% CO2. Cells were then fixed in 3% paraformaldehyde, and incubated with anti-Rad51 primary antibody, and then a Cy3-conjugated antibody. The effect of CPT on cells is expressed as a percentage of cells containing more than 10 Rad51 foci and the values are the mean ± S.E. of three independent experiments.

As already seen, PARP-1-/- cells have an increased amount of spontaneous RAD51 foci (*Figure 3.7*), and RAD51 foci formation is greatly increased in both cell lines after treatment with CPT, but significantly higher in PARP-1$^{-/-}$ cells. Treatment with ISQ alone slightly increases the amount of RAD51 foci formation (*Figure 3.8*), 5.8% of PARP-1$^{+/+}$ cells have > 10 RAD51 foci per cell, and 14.5% of PARP-1$^{-/-}$ cells, but this is not significant.

The amount of RAD51 foci formation in PARP-$1^{+/+}$ cells after co-treatment with CPT and ISQ was slightly decreased (58.8%), compared to treatment with CPT only (66.7%), but not significantly. In contrast, in PARP-$1^{-/-}$ cells, co-treatment with CPT and ISQ significantly increased ($p < 0.01$) the amount of RAD51 foci (99.7%), compared to treatment with CPT only (91.8%).

These results show that treatment of PARP-$1^{-/-}$ cells with ISQ slightly increases the amount of RAD51 foci, and therefore the amount of HR, but this is not significant. These results also suggest that there is an increase in RAD51 foci formed in PARP-$1^{-/-}$ cells co-treated with CPT and ISQ, compared to PARP-1-/- cells treated with CPT alone. This is not seen in the PARP-$1^{+/+}$ cell line, which actually shows a slight decrease in the amount of RAD51 foci formation when co-treated with CPT and ISQ, compared to PARP-$1^{+/+}$ cells treated with CPT alone.

3.9 Discussion

PARP-1$^{-/-}$ cell lines are hypersensitive to CPT, which suggests that PARP-1 has a role in the repair of the damage caused by this drug. We have shown that CPT induces the formation of DSBs in both wildtype and PARP-1-/- cell lines, but that there are a greater number of DSBs in the deficient cell line. One hypothesis is that that the repair of the DSBs in the PARP-1$^{-/-}$ cell line is decreased, leading to an increase in this particular lesion. Alternatively, the number of DSB lesions is increased due to loss of some other repair pathway that may result in an increased number of DSBs.

HR is an important pathway in repair of CPT-induced DSBs (Arnaudeau *et al* ., 2001). Although HR deficient cell lines (irs1SF) and NHEJ deficient cell lines (V3-3) are more sensitive to CPT than wildtype cells, the HR deficient cell line was more senstitive than the NHEJ deficient cell line. We see an increase in the amount of RAD51 foci formation in cells that lack PARP-1, indicating that the level of HR repair has increased. . Thus, it appears that there is no general loss of DSB repair by HR in PARP-1$^{-/-}$ cells, which is also supported from the literature. Previously, it was found that the level of DSB repair by HR is not altered in cells with inhibited or lost PARP activity (Schultz *et al*., 2003; Yang *et al*., 2004). Alternatively, the increased amount of DSBs may reflect that PARP-1 inhibits the NHEJ pathway. However, this pathway appears less important in repairing CPT-induced DSBs than HR (Arnaudeau *et al.,* 2001). In conclusion, our data supports the second hypothesis, that loss of PARP-1 may affect some other repair pathway that may result in an increased number of DSBs.

We know that CPT stabilises the transient SSB induced by Top1, and that SSBs are repaired by base excision repair (BER). PARP-1 has been shown to interact with proteins involved in the SSB repair pathway, and binds directly to the SSB repair scaffold protein, XRCC1 (Masson *et al.*, 1998). We also know that PARP-1 can recognise SSBs and does this with a very high affinity. Thus, the role of PARP-1 in SSB repair may be relevant to explain the increased number of DSBs found when inhibiting or losing PARP-1.

PARP-1 has been shown to bind to Top1 directly (Yung *et al*, 2004), and add poly(ADP-ribose) polymers to the Top1 whilst it is bound to the DNA (Malanga & Althaus, 2004). This modifies Top1 so that it removes itself from the DNA and religates the gap. When the Top1-DNA complex is stabilised by CPT, PARP-1 destabilises the complex and enhances religation (Park & Cheng, 2005). However, $PARP^{+/+}$ cells show high sensitivity to CPT, so not all of the complexes can be repaired in this way, leaving a lot of SSBs in the DNA.

We hypothesise that when PARP-1 binds to a SSB, it attracts XRCC1 via PARP-1's poly(ADP-ribosyl)ation of itself (Caldecott, 2003), to carry out efficient SSB repair. In $PARP\text{-}1^{-/-}$ cells, the Top1-DNA-CPT complex is not destabilised by PARP-1. However, the Top1 can be removed from the DNA by tyrosyl-DNA phosphodiesterase 1 (Tdp1), leaving a SSB in the DNA (Vance & Wilson, 2001). Because of the absence of PARP-1, SSB repair proteins are not brought to the site of the break and SSB repair is reduced, which results in an increased amount of open SSBs. This may lead to more SSBs collapsing at replication forks and thus more DSBs. An increase in collapsed forks will

in turn leads to an increase in HR to repair the DSBs. This model would explain the increase in RAD51 foci observed in PARP$^{-/-}$ or inhibited cells (*Figure 3.1.7* and *Figure 3.1.8*). Also, this model explains how PARP-1 inhibitors, for example, ISQ and NU1025, increase the cytotoxicity of wildtype cells to CPT, and increase the number of DSBs in these cells when co-treated with these drugs.

One important issue is whether PARP-1 itself or PARP activity is important for the increased toxicity with PARP inhibitors. One idea is that inhibited PARP-1 may act as a negative regulator of DNA-PK-dependent NHEJ, while the absence of PARP-1 does not show the same inhibitory effect (Veuger, 2004). Here, we find an increased number of DSBs and hypersensitivity to CPT in PARP-1-/- cells as well as when inhibiting PARP-1. These data suggest that the activity of PARP-1 is important for survival and to avoid forming DSBs at replication forks.

We did see that inhibition with ISQ has greater effect than NU1025 on production of CPT-induced DSBs and cytotoxicity. One reason might be that ISQ is more efficient than NU1025 in inhibiting PARP-1. However, the PARP-1 enzyme is fully inhibited at the doses used here. Rather, we believe that ISQ is less specific for PARP-1 and may inhibit other PARP-1's more efficiently that NU1025. In support for this view is that PARP-1$^{-/-}$ cells are further sensitised to CPT with ISQ, while NU1025 does not sensitise PARP-1$^{-/-}$ cells to CPT.

This can be explained by the presence of other PARP family proteins in mammalian cells. There are a number of PARP proteins in the PARP family, two of which can be

found in the mammalian nucleus, PARP-1 and PARP-2. PARP-1 is the most abundant, but these other PARP proteins may also be affected by the PARP inhibitors and contribute to the increased amount of DSBs. Thus, the additional killing effect with ISQ could be related to that both PARP-1 and PARP-2 are inhibited, which may be additionally lethal since PARP-1 and PARP-2 double knockout mice die *in utero* (deMurcia, 2000). Alternatively, ISQ may have additional effects, such as being a topoisomerase inhibitor. If this is the case one may expect additional killing with ISQ that is unrelated to PARP inhibition. PARP-$1^{-/-}$ cells also show an increase in RAD51 foci after co-treatment with CPT and the PARP-1 inhibitor, ISQ, probably as a result of the increased number of DSBs, possibly due to additional effects with ISQ.

This rise in RAD51 foci after co-treatment of CPT and ISQ, is not seen in PARP-$1^{+/+}$ cells, in fact the percentage of cells displaying RAD51 foci is slightly decreased, but not to a significant level. This may be because PARP-1 inhibitors do not completely deplete the cell of PARP activity, whereas the activity of this protein is completely diminished in the PARP-$1^{-/-}$ cells. Therefore, there is still some background activity in PARP-1 after treatment with the PARP inhibitors, but in the PARP-$1^{-/-}$ cells, there is none. Therefore there is more of an effect if the other two proteins are inhibited.

If, as we predict from the hyper-recombination phenotype, HR repair is increased following inhibition of PARP, and CPT causes DSBs that can be repaired by HR then one would imagine that inhibition of PARP would in fact decrease sensitivity to CPT rather than enhance it. However, we have seen that this is not the case. The inhibition of PARP-1 increases the sensitivity of CPT.

In conclusion, we suggest that the role of PARP-1 in SSB repair of CPT lesions most likely explains the results found. The inhibition of PARP-1 may slow the repair of CPT-induced SSBs, which in turn would lead to more SSBs collapsing at replication forks and thus more DSBs. This is a plausible mechanism although it is not clear whether PARP-1 binds the SSB within the CPT stabilised Topo I cleavage complex.

CHAPTER 4: THE ROLE OF XRCC1 IN CPT-INDUCED HOMOLOGOUS RECOMBINATION

CHAPTER 4: THE ROLE OF XRCC1 IN CPT-INDUCED HOMOLOGOUS RECOMBINATION

4.1 Introduction

In the previous chapter, we showed that camptothecin (CPT) has increased cytotoxicity in PARP-1$^{-/-}$ cells due to an increased amount of DNA double strand breaks (DSBs) formed. We also showed that RAD51 foci formation is increased in camptothecin (CPT) treated PARP-1$^{-/-}$ cells, indicating that homologous recombination (HR) is increased in these cells. We saw an increase in DSBs whether PARP-1 was absent or inhibited, demonstrating that it is the activity of the enzyme that is important for protection against CPT toxicity.

CPT stabilises the transient single strand break (SSB) induced by topoisomerase I (Top1) (Hsiang, 1985), which increases the number of unrepaired SSBs in the cell. PARP-1 binds to Top1 (Yung *et al*, 2004) and adds poly(ADP-ribose) polymers to the protein, which allows it to destabilise from the Top1-DNA-CPT complex (Malanga & Althaus, 2004; Park & Chung, 2004). PARP-1 also recognises SSBs with a very high affinity and is required for efficient repair of SSBs (Trucco *et al*, 1998). When PARP-1 is absent or inhibited, it cannot destabilise the Top1-DNA-CPT complex. This leads to Top1 being removed from the DNA by Tdp1, leaving a SSB. If SSBs are not repaired they collapse into replication forks which leads to DSB formation. Thus, the role of PARP-1 in SSB repair may explain the increased number of DSBs found when inhibiting or losing PARP-1. Further, an increase in collapsed forks would in turn lead

to an increase in HR to repair the DSBs, which would explain the increase in RAD51 foci observed in PARP deficient or inhibited cells.

PARP-1's role in SSB repair may be due to its interaction with the BER scaffold protein, x-ray repair cross-complementing 1 (XRCC1) (Masson *et al.*, 1998). Following oxidative damage in the absence of PARP-1, XRCC1 does not form foci at the sites of damage and it is thought that following SSB formation, PARP-1 binds to the break, is activated, and autoribosylates itself, as XRCC1 preferentially interacts with modified PARP-1 it is then attracted to the site of damage. Therefore we hypothesis that in PARP-$1^{-/-}$ cells, it is this inability or reduced ability for XRCC1 to sense CPT-induced SSBs which is responsible for reduced SSB repair and hence increase DSB formation and HR we observe.

4.2 Increased cytotoxicity to camptothecin in XRCC1^{defective} cells

CPT stabilises the transient SSB created by Top1 by binding and intercalating between upstream (-1) and downstream (+1) base pairs, displacing the downstream DNA and preventing relegation of the cleaved DNA, which in turn leaves Top1 covalently bound to the DNA (Beidler & Cheng, 1995). This leaves an unrepaired SSB in the DNA which must be repaired before it collides with the oncoming replication machinery, and results in a DSB.

PARP-1 is a 113 kDa protein that is made up of three domains; the N-terminal DNA-binding domain (DBD) (46 kDa), an automodification domain (AMD) (22 kDa), and

the C-terminal catalytic domain (CTD) (54 kDa) (Neame *et al.*, 1990). The DBD contains two zinc fingers, which binds with high affinity to breaks in the DNA. Upon binding, the CTD is stimulated 500-fold to produce long polymers of ADP-ribose. These polymers are added to several downstream proteins, but are predominantly added to the auto-modification domain of PARP-1.

Figure 4.2.1 XRCC1 binds PARP-1 and DNA ligase III through BRCT motifs.

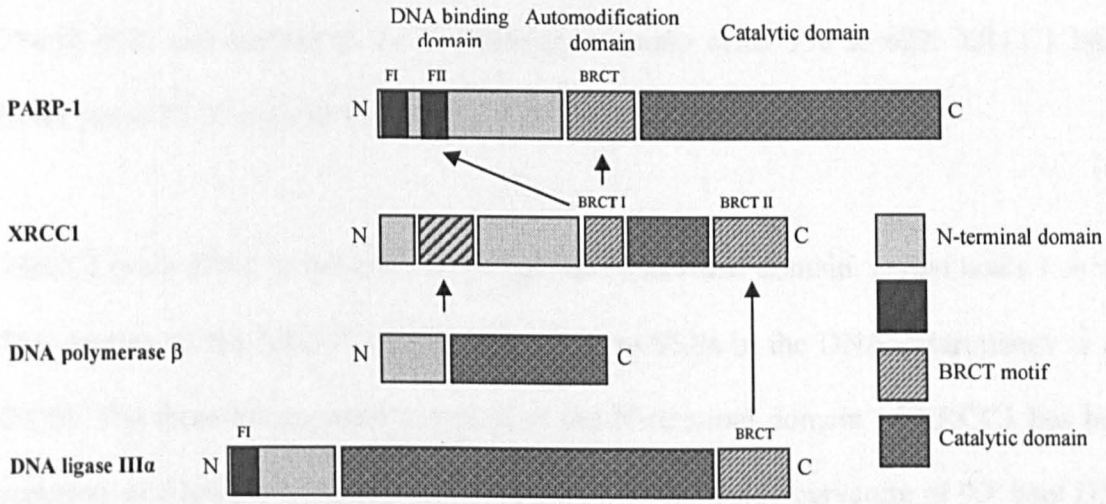

Adapted from Masson *et al.*, 1998

XRCC1 has been shown to bind preferentially to automodified PARP-1, indicating that PARP-1 may function to recruit SSB repair proteins to the site of damage (Masson *et al.*, 1998). When PARP-1 detects a SSB, it binds to it, triggering automodification. XRCC1 binds to the automodified PARP-1, bringing with it proteins involved in SSB repair. XRCC1 has no demonstrated catalytic activity, and is thought to be a scaffold protein interacting directly with DNA ligase III and DNA polymerase β (Caldecott,

2003) (*Figure 4.2.1*). XRCC1 binds DNA ligase III through a breast cancer protein 1 carboxyl terminus (BRCT) motif. These are folding units of about 90-100 amino acids, and so called because they were first identified in breast cancer cells. These BRCT motifs consist of four β-strands forming a core sheet structure and two α-helices, and are important in specific protein-protein interactions (**CHAPTER 1**, *Figure 1.5*). In fact, BRCT motifs have been found in many DNA-damage responsive and cell cycle check-point proteins. DNA ligase III contains a BRCT motif in its C-terminal domain, amino acids 841 to 922, and XRCC1 contains two BRCT motifs, one at amino acids 314 to 402, and another in the C-terminal at amino acids 538 to 622. XRCC1 binds DNA ligase III through its C-terminal BRCT motif.

XRCC1 binds DNA polymerase β through its N-terminal domain, amino acids 1 to183. This section of the XRCC1 protein also binds to SSBs in the DNA (Marintchev *et al.,* 2000). The three-dimensional structure of the N-terminal domain of XRCC1 has been reported, and has been shown to be well-suited to the inside curvature of 90° bent DNA (Marintchev *et al.,* 1999). When PARP-1 binds to SSBs in the DNA, it induces a V-shape bend in the DNA. PARP-1 eventually moves away from the DNA, leaving room for the repair proteins to access the break. It may be that XRCC1 then binds the site recently vacated by PARP-1, bringing DNA polymerase β and DNA ligase III to the site. XRCC1 binds DNA polymerase β via its N-terminal region, but this domain has a much higher affinity for SSBs in the DNA, approximately 100 times greater. It could be that XRCC1 binds DNA polymerase β via the N-terminal, which is then possibly released upon binding to a SSB.

XRCC1 binds PARP-1 through its central BRCT motif which binds directly with a BRCT motif within PARP-1's automodification domain (AMD). This is the domain where PARP-1 automodifies itself by adding ADP-ribose polymers and XRCC1 preferentially binds to automodified PARP-1. PARP-1 binds XRCC1 through its BRCT motif, and also with the zinc-fingers found within the N-terminal region. The XRCC1^{defective} cell line (EM9) contains XRCC1 that has a frameshift mutation at codon 221. This results in a truncated protein (*Figure 4.2.2*) that is missing two thirds of the normal sequence (Shen *et al.,* 1998). Therefore EM9 is effectively a null mutant, whose properties can be compared to cell lines carrying a knock-out mutation (Tebbs *et al.,* 1999).

Figure 4.2.2 Structure of XRCC1 in EM9 cells compared to full length XRCC1.

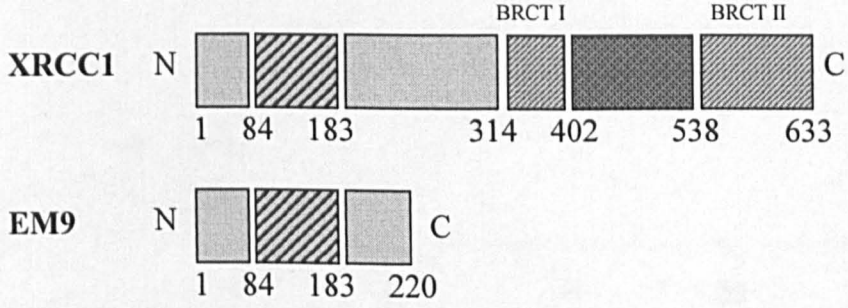

We observed that XRCC1^{defective} EM9 cells were more sensitive to CPT than the wildtype cell line (AA8), and showed a 1.7-fold increase in cytotoxicity at a 40 nM dose (*figure 4.2.4*), which is statistically significant to $p < 0.05$ in t-test. The sensitivity of EM9 cells to CPT increased to 2.5-fold at 50 nM, 4.4-fold at 75 nM ($p < 0.01$), and 8.2-

fold at 100 nM (p 0.001). This suggests that in the absence of XRCC1, SSBs cannot be repaired, or are repaired more slowly, because the SSB repair proteins cannot reach the site of damage. Whether there is no repair, or whether it is slower repair is unclear.

Figure 4.2.3: Camptothecin has increased cytotoxicity in XRCC1^{defective} cells

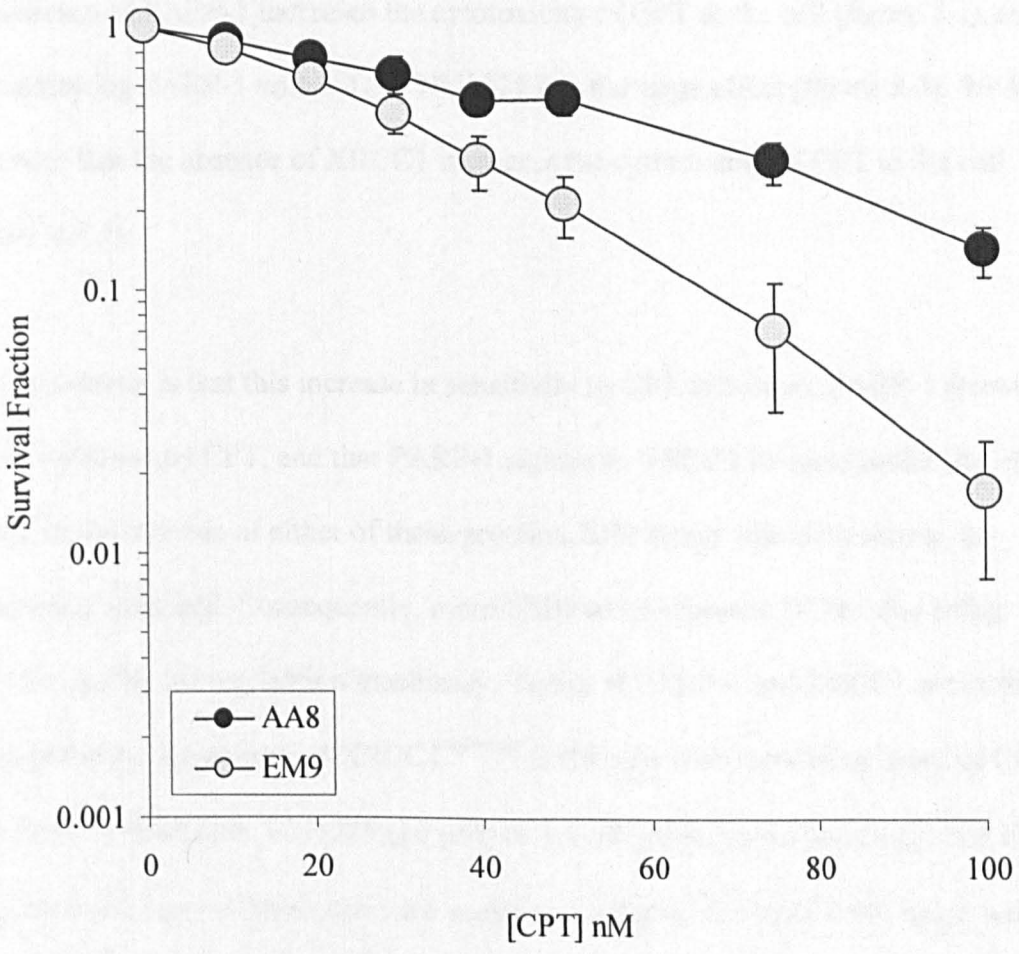

XRCC1^{wt} (AA8) and XRCC1^{defective} (EM9) cells were treated in increasing doses of CPT for 7 days at 37°C, under an atmosphere containing 5% CO2. The effect of CPT on cells is expressed as a percentage of controls and the values are the mean ± S.E. of three independent experiments.

4.3 Co-treatment of XRCC1^{wt} and XRCC1^{defective} cells with camptothecin and PARP-1 inhibitors increases the killing effect of camptothecin

We know that XRCC1 binds to automodified PARP-1, and brings the SSB repair proteins, DNA ligase III and DNA polymerase β to the site of SSBs. We have seen that the absence of PARP-1 increases the cytotoxicity of CPT to the cell (*figure 3.2*), and that inhibiting PARP-1 with ISQ or NU1025 has the same effect (*figure 3.3*). We have also seen that the absence of XRCC1 increases the cytotoxicity of CPT to the cell (*figure 4.2.3*).

Our hypothesis is that this increase in sensitivity to CPT is because PARP-1 detects the SSBs stabilised by CPT, and that PARP-1 signals to XRCC1 to come to the site of the break. In the absence of either of these proteins, SSB repair would be slower, or completely impaired. Consequently, more SSBs would become DSBs after being encountered by the replication machinery. To test if PARP-1 and XRCC1 act in the same pathway, we co-treated XRCC1^{defective} EM9 cells with increasing doses of CPT and PARP-1 inhibitors, NU1025 (10 μM) or 1,5-dihydroisoquinoline (ISQ) (0.6 mM). We observed that wildtype cells are sensitive to higher doses of CPT; there was 35% survival at 80 nM CPT, and 17% survival at 100 nM CPT (*figures 4..3.2* and *4.3*).

When this cell line was co-treated with NU1025, survival decreased 1.7-fold at 80 nM CPT, and 2-fold at 100 nM CPT (statistically significant in t-test, $p < 0.01$). When XRCC1^{wt} cells were co-treated with CPT and 0.6 mM ISQ, survival was decreased still

further. Survival was decreased 4-fold at 50 nM CPT, 7-fold at 60 nM CPT, 44-fold at 80 nM CPT and 66-fold at 100 nM CPT (statistically significant to $p < 0.001$).

Figure 4.3: Co-treatment of XRCC1^{wt} and XRCC1^{defective} cells with camptothecin and PARP-1 inhibitors increases the killing effect of camptothecin.

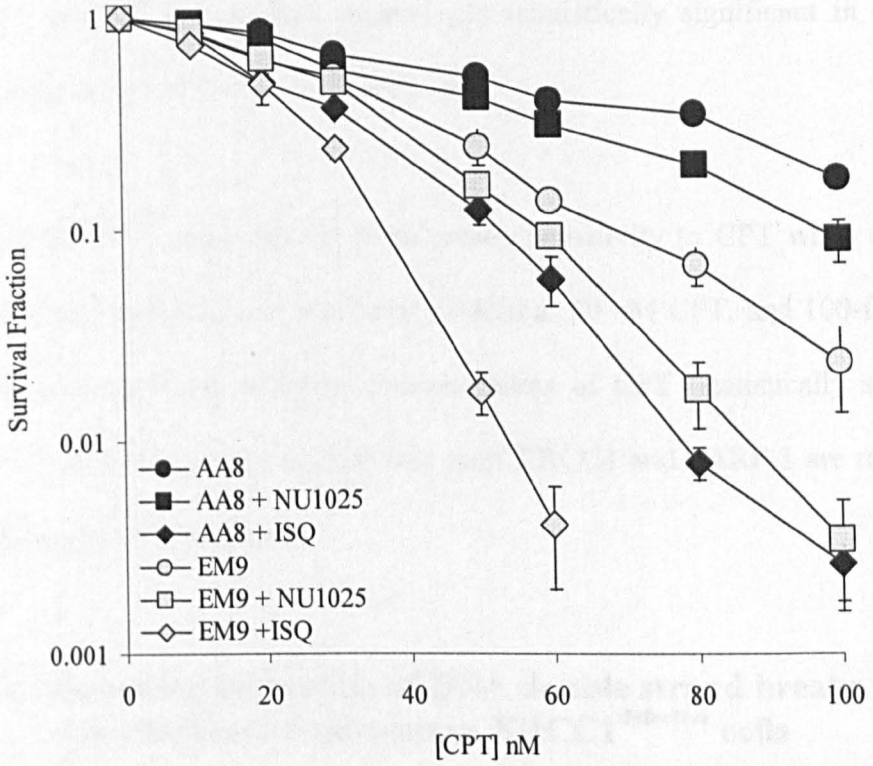

XRCC1^{wt} (AA8) and XRCC1^{defective} (EM9) cells were treated in increasing doses of CPT for 7 days at 37°C, under an atmosphere containing 5% CO2. Some cells were co-treated with 10 μm NU1025 or 0.6 mM ISQ. The effect of CPT on cells is expressed as a percentage of controls and the values are the mean ± S.E. of three independent experiments.

In addition, we observed that XRCC1^{defective} EM9 cells are even more sensitive to CPT, as shown in *figure 4.2.3*, and that this sensitivity is also increased when co-treated with

CPT and 10μM NU1025 or 0.6 mM ISQ (*figure 4.3*). Survival was decreased 2-fold at 50 nM CPT when treated with CPT alone (statistically significant in t-test, $p < 0.01$), and decreased further by 3-fold at 60 nM CPT, 6-fold at 80 nM CPT, and 12-fold at 100 nM CPT (statistically significant in t-test, $p < 0.001$). When co-treated with CPT and 10 μM NU1025, survival at 50 nM, 60 nM, 80 nM, and 100 nM CPT, was 3-fold, 4-fold, 20-fold and 50 fold respectively (statistically significant in t-test, $p < 0.001$), compared to survival of wildtype cells.

XRCC1^{defective} cells showed even greater sensitivity to CPT when co-treated with 0.6 mM ISQ. Survival was decreased 31-fold at 50 nM CPT, and 100-fold at 60 nM CPT. No cells survived at higher concentrations of CPT (statistically significant in t-test, $p < 0.001$). This data suggests that both XRCC1 and PARP-1 are required for survival following CPT treatment.

4.4 Increased formation of DNA double strand breaks following camptothecin treatment in XRCC1^{defective} cells

Our hypothesis is that the absence of XRCC1 in the cell increases the amount of unrepaired SSBs, as DNA ligase III and DNA polymerase β are not brought to the site of the SSB. These two proteins are usually bound to the scaffold protein, XRCC1, and carried to the site of damage. In the absence of XRCC1, this is not likely to happen, and this would explain slower SSB repair, as the proteins need to find SSBs independently of XRCC1. If this is indeed the case, you would expect to find an increased amount of DSBs in the cell, as the SSBs are encountered by oncoming replication forks.

Figure 4.4: Camptothecin increases the formation of DNA double strand breaks in XRCC1^{defective} cells.

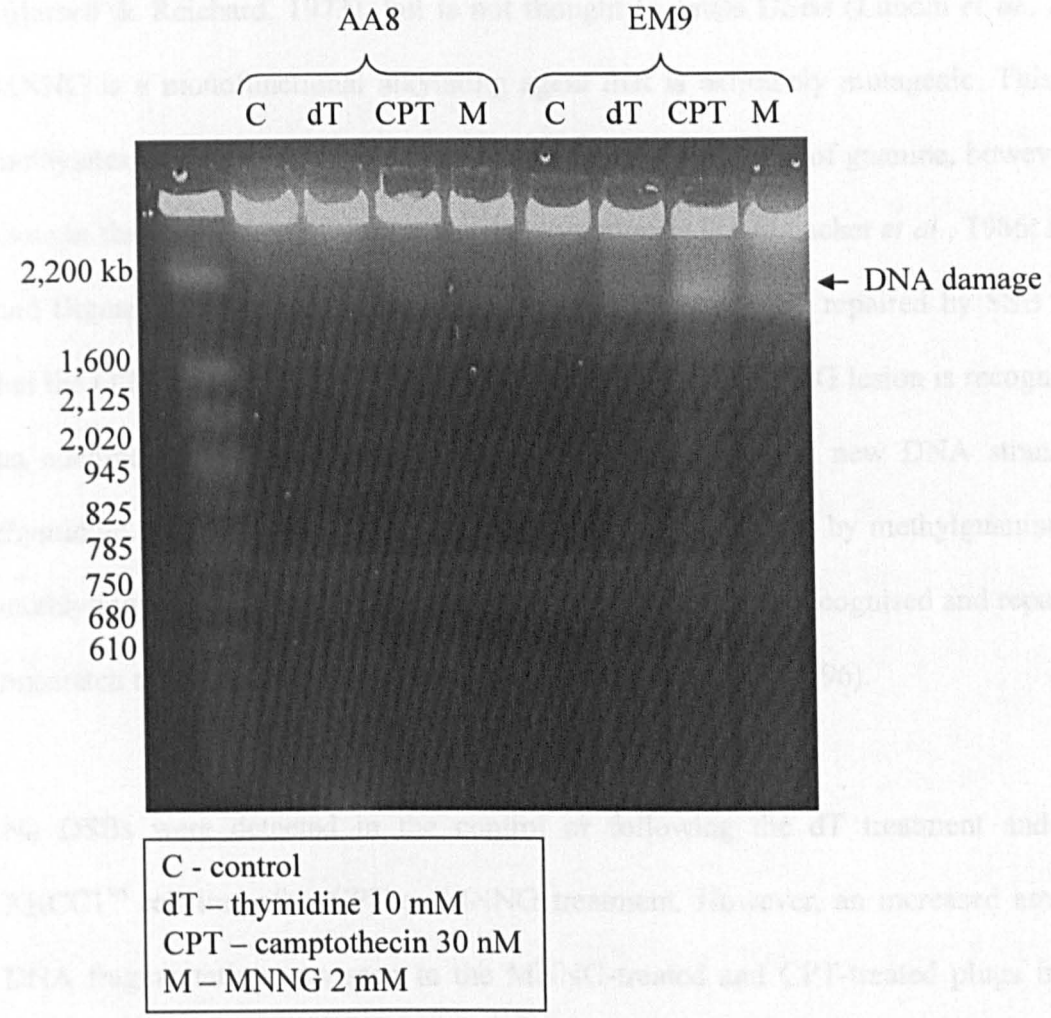

XRCC1^{wt} (AA8) and XRCC1^{defective} (EM9) cells were treated with HU (0.5 mM), dT (10 mM) or CPT (100 nM) for 24 hours at 37°C, under an atmosphere containing 5% CO2. Cells were then embedded in 0.75% agarose plugs and treated with N-laurylsarcosine (1% v/v) and proteinase K (1 mg/ml) for 48 hours at 50°C, to remove cell membranes and proteins so that only DNA remains in the plug. Plugs were then embedded in a 0.8% agarose gel and ran at 4V/cm for 24 hours in a CHEF-DR III pulsed-field gel electrophoresis chamber. Switch times were 60-120s and the reorientation angle was 120°. Double-strand breaks are indicated by the chromosome fragments at 2,200 kb.

dT is a replication inhibitor that stalls replication forks by depleting the pool of dCTPs (Bjursell & Reichard, 1973), but is not thought to cause DSBs (Lundin *et al.,* 2002). MNNG is a monofunctional alkylating agent that is extremely mutagenic. This agent methylates the N^3 position of adenine and N^7 and O^6 position of guanine, however it is thought that the O^6MeG lesion is the most mutagenic (Goldmacher *et al.*, 1986; Karran and Bignami, 1992). The N^3MeA and N^7MeG are efficiently repaired by SSB repair, but the O^6MeG lesion is not. After DNA replication, the O^6MeG lesion is recognised as an adenine instead of a guanine and is mismatched in the new DNA strand with thymidine. This is primarily repaired via direct demethylation by methylguanine-DNA methlytransferase (MGMT) (Lindahl *et al.*, 1982) but is also recognised and repaired by mismatch repair (MMR) (Griffin *et al.*, 1994; Duckett *et al.*, 1996).

No DSBs were detected in the control or following the dT treatment and in the XRCC1^{wt} cell line after CPT or MNNG treatment. However, an increased amount of DNA fragmentation was seen in the MNNG-treated and CPT-treated plugs from the XRCC1^{defective} cell line, compared to the XRCC1^{wt} cell line (*Figure 4.4*). It is unlikely that the DNA fragmentation following MNNG treatment represents real DSBs as methylated DNA is heat-labile and converts to SSBs, which when close to another SSB will resulting a DSB (Lundin *et al.*, 2005). The increase in DSBs seen supports our hypothesis that lack of XRCC1 decreases SSB repair following CPT induced DNA damage.

4.5 Camptothecin-induced RAD51 foci formation is increased in XRCC1^{defective} cells

RAD51 foci are small nuclear foci containing all of the proteins involved in homologous recombination (HR). These foci form whenever the cell undergoes HR, and a measurement of these can be used as an indication of the amount of HR that is taking place within a cell.

HR appears to be the major repair pathway for CPT-induced DSBs, so to determine if HR is increased in XRCC1^{wt} and XRCC1^{defective} cells when treated with CPT, we measured the amount of RAD51 foci formed in cells from both cell lines when treated with or without 100 nM CPT for 24 hours.

The level of RAD51 foci in XRCC1^{wt} and XRCC1^{defective} cells was examined using immunofluorescence. XRCC1^{defective} cells have an increased amount of spontaneous RAD51 foci compared to XRCC1^{wt} cells (*Figure 4.5*), 42% of XRCC1^{defective} cells have >10 RAD51 foci per cell compared to 2.4% of XRCC1^{wt} cells. This is a 17-fold significant difference (statistically significant in t-test, $p < 0.001$). Both XRCC1^{wt} and XRCC1^{defective} cells have an increased amount of RAD51 foci formation after a 24 hour treatment with CPT, 14-fold ($p < 0.05$) and 3-fold ($p < 0.001$) above their spontaneous levels) respectively. XRCC1^{defective} cells however, have a much higher level of RAD51 foci formation, 95% of XRCC1^{defective} cells compared to 33% of XRCC1^{wt} cells. This is a 2.9-fold significant difference ($p < 0.01$).

Figure 4.5: Camptothecin-induced RAD51 foci formation is increased in XRCC1^{defective} cells.

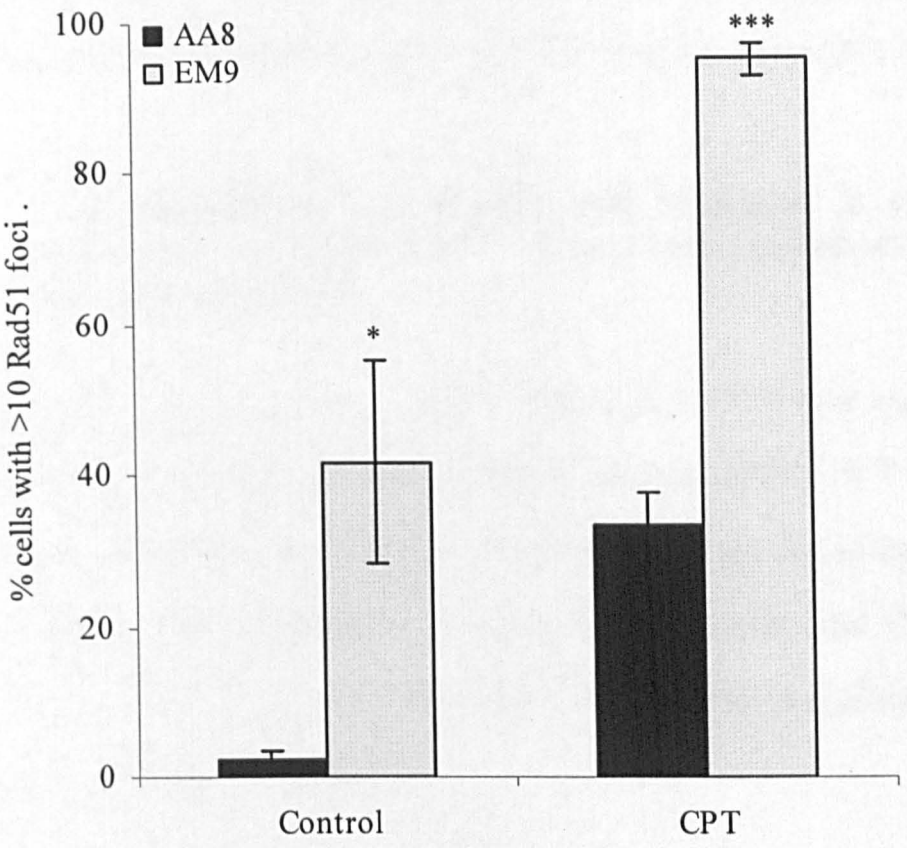

XRCC1^{wt} (AA8) and XRCC1^{defective} (EM9) cells were treated with 100 nM CPT for 24 hours at 37°C, under an atmosphere containing 5% CO2. Cells were then fixed in 3% paraformaldehyde, and incubated with anti-Rad51 primary antibody, and then a Cy3-conjugated antibody. The effect of CPT on cells is expressed as a percentage of cells containing more than 10 Rad51 foci and the values are the mean ± S.E. of three independent experiments.

In this assay, it was noted that there was an increase in RAD51 foci in XRCC1^{defective} cells treated with CPT. This suggests that HR is increased in this cell line when treated with CPT. It was also noted that this increase in HR was above the level observed for CPT-treated XRCC1^{wt} cells. It has already been noted that there is an increased amount

of RAD51 foci in untreated XRCC1^{defective} cells (*Figure 4.5*) i.e. there is already increased spontaneous HR in these cells, but these data suggest that HR is increased further in order to repair an increased number of DSB lesions caused by CPT.

4.6 Camptothecin-induced RAD51 foci formation is significantly increased in XRCC1^{defective} cells, when co-treated with 1,5-dihydroisoquinoline.

To determine if HR is increased in XRCC1^{wt} and XRCC1^{defective} cells when PARP-1 is inhibited, we co-treated both cell lines with CPT and ISQ. XRCC1^{defective} and XRCC1^{wt} cells were treated with either 100 nM CPT or 0.6 mM ISQ, or co-treated them with both. We also examined the level of RAD51 foci in untreated cells. These cell lines were treated for 24 hours and then fixed onto coverslips. The level of RAD51 foci was examined using immunofluorescence.

As we have already noted, XRCC1^{defective} cells have an increased amount of spontaneous RAD51 foci compared to XRCC1^{wt} cells (*Figure 4.5*), and both XRCC1^{wt} and XRCC1^{defective} cells have an increased amount of RAD51 foci formation after a 24 hour treatment with CPT. XRCC1^{defective} cells however, have a much higher level of CPT-induced RAD51 foci formation that XRCC1^{wt} cells.

Figure 4.6: Camptothecin-induced RAD51 foci formation is significantly increased in XRCC1^{defective} cells, when co-treated with 1,5-dihydroisoquinoline.

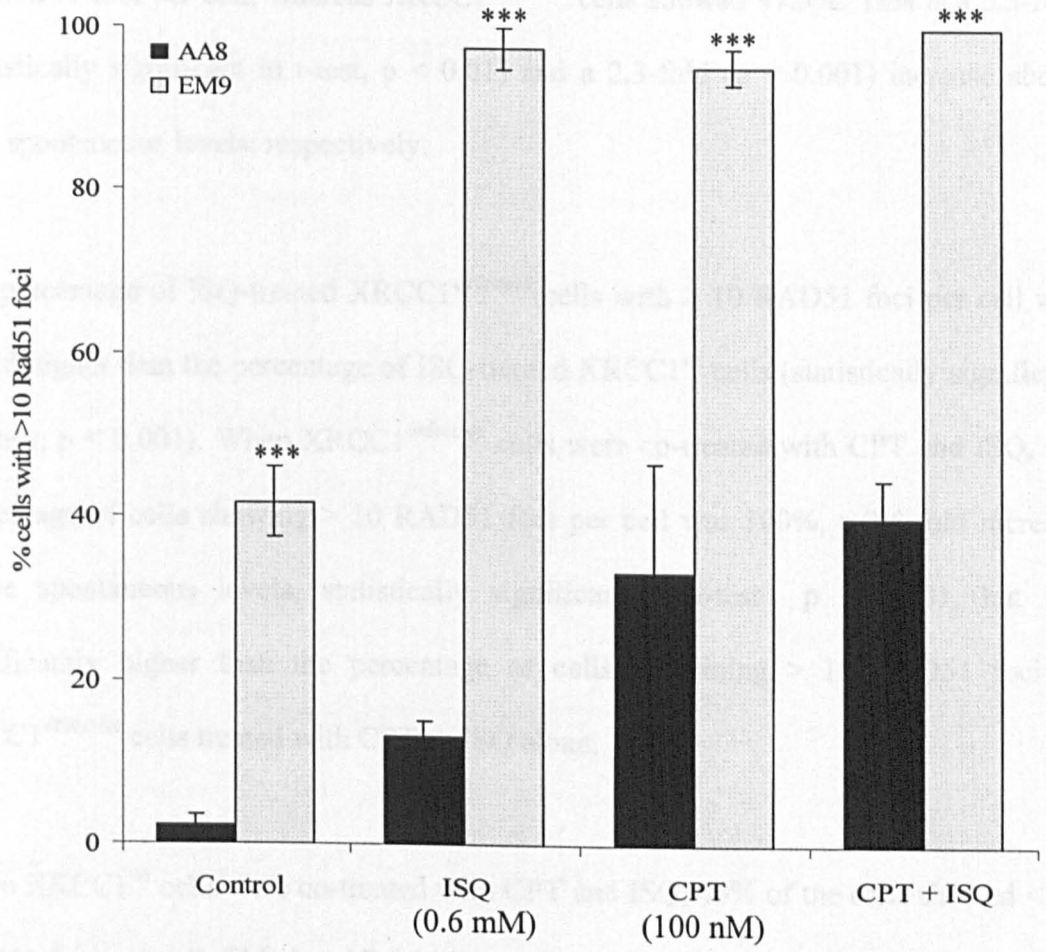

XRCC1^{wt} (AA8) and XRCC1^{defective} (EM9) cells were treated with 100 nM CPT or 0.6 mM ISQ for 24 hours at 37°C, under an atmosphere containing 5% CO2. Some cells were co-treated with 100 nM CPT and 0.6 mM ISQ. Cells were then fixed in 3% paraformaldehyde, and incubated with anti-Rad51 primary antibody, and then a Cy3-conjugated antibody. The effect of CPT on cells is expressed as a percentage of cells containing more than 10 Rad51 foci and the values are the mean ± S.E. of three independent experiments.

Here we observed that the amount of RAD51 foci formation is also increased in both cell lines when treated with ISQ alone (*Figure 4.6*). 13% of XRCC1^{wt} cells showed > 10 RAD51 foci per cell, whereas XRCC1^{defective} cells showed 97.5%. This is a 5.5-fold (statistically significant in t-test, $p < 0.01$) and a 2.3-fold ($p < 0.001$) increase above their spontaneous levels, respectively.

The percentage of ISQ-treated XRCC1^{defective} cells with > 10 RAD51 foci per cell was 7-fold higher than the percentage of ISQ-treated XRCC1^{wt} cells (statistically significant in t-test, $p < 0.001$). When XRCC1^{defective} cells were co-treated with CPT and ISQ, the percentage of cells showing > 10 RAD51 foci per cell was 100%, a 2.4-fold increase above spontaneous levels, statistically significant in t-test $p < 0.001$, but not significantly higher than the percentage of cells containing > 10 RAD51 foci in XRCC1^{defective} cells treated with CPT or ISQ alone.

When XRCC1^{wt} cells were co-treated with CPT and ISQ, 40% of the cells showed < 10 RAD51 foci per cell. This is a 17-fold increase above spontaneous levels ($p < 0.001$), a 3-fold increase above the level (13%) when treated only with ISQ ($p < 0.01$), but not significantly more than when XRCC1^{wt} cells are treated with CPT alone. As with the survival data this data suggests that both XRCC1 and PARP-1 are important for repair of both spontaneous and CPT induced SSBs, as we propose that a failure of SSB repair will result in increased HR to repair the resultant DSBs which form at replication forks.

4.7 Expression of a mutated BRCT I motif increases sensitivity to camptothecin in XRCC1 ^{defective} cells.

The XRCC1 protein has been implicated to be involved in a DNA ligase III dependent and independent SSB repair (Taylor, 2002). The DNA ligase III dependent SSB repair appears to be active throughout the cell cycle and involves the BRCT I motif of the XRCC1 protein, whilst DNA ligase III independent XRCC1 repair appears to be active at replication forks and involves the BRCT II motif of the XRCC1 protein. Here, we wanted to test which repair pathway was implicated in the repair of CPT-induced DNA damage. To do this we used XRCC1 mutant cell lines that had one or both of the BRCT motifs removed.

XRCC1 is thought to be a scaffold protein in SSB repair that transports DNA ligase III and DNA polymerase β to the site of SSBs in the DNA. It is also known to bind to automodified PARP-1. XRCC1 binds DNA ligase III by the BRCT II motif. To test whether it is lack of XRCC1 or the inability to bring DNA ligase III to the site of damage which is responsible for the increase in HR, we used an XRCC1^{defective} cell line, EM9, which had been complemented with a short XRCC1 (XH-ST). This protein was missing the last 95 amino acids, the part that comprises the BRCT II motif, and therefore could not bind DNA ligase III.

XRCC1 binds PARP-1 by the BRCT I motif. If XRCC1 cannot bind PARP-1, it cannot bring DNA ligase III and DNA polymerase β to the SSB. To see if it is XRCC1's ability to interact with PARP-1 that s responsible for the increase in HR, we used the XRCC1^{defective} EM9 cell line, which had been complemented with one of two different

mutated XRCC1 proteins. The EM9-pcD2EXH and EM9-pcD2EXH5 have been complimented with human XRCC1 (hXRCC1). The EM9-pcD2E cell line has been complimented with an empty vector. The EM9-pcXH1-528 cell line has been complimented with a short version of hXRCC1, it is missing the BRCT II domain. The EM9-pcXHW385D and EM9-pcXHLI360/361DD cell lines have been complimented with hXRCC1 proteins that have a mutated BRCT I domain. The BRCT I domain in EM9-pcXHW385D has the tryptophan residue at position 385 exchanged for an aspartic acid residue. The BRCT I domain in EM9-pcXHLI360/361DD has the leucine residue at position 360 and the isoleucine residue at position 361 exchanged for aspartic acid residues. This disrupted the folding of β-sheet three of the BRCT I motif and so could not bind PARP-1 (Caldecott, 1992).

We treated all of these cell lines, as well as the $XRCC1^{wt}$ cell line and the uncomplemented EM9 cell line, with increasing concentrations of CPT. To be sure any effects were due to the mutated XRCC1 proteins, and not due to the vector containing the XRCC1 mutants, we also tested the $XRCC1^{defective}$ EM9 cell line, which had been complemented with the full XRCC1 protein (XH and XH5), and the same cell line complemented with an empty vector (EM9-V). In line with our previous results, we found that $XRCC1^{defective}$ cells were more sensitive to CPT than $XRCC1^{wt}$ cells, showing a 1.7-fold increase in sensitivity at 10 nM CPT (statistically significant in t-test, $p > 0.01$), increasing to a 59-fold increase at 40 nM CPT (statistically significant in t-test, $p > 0.001$). $XRCC1^{defective}$ cells complemented with an empty vector (EM9-V) were similarly sensitive, showing a 1.9-fold increase in sensitivity at 10 nM CPT, increasing to 33-fold at 40 nM CPT (statistically significant in t-test, $p > 0.001$). This

sensitivity was reversed when EM9 cells were complemented with human XRCC1 (XH and XH5) (*Figure 4.7*). Both XH and XH5 showed similar levels of sensitivity to CPT as the XRCC1^{wt} cell line.

Figure 4.7: Camptothecin has increased cytotoxicity in XRCC1defective cells complemented with XRCC1 that is missing the BRCT I motif.

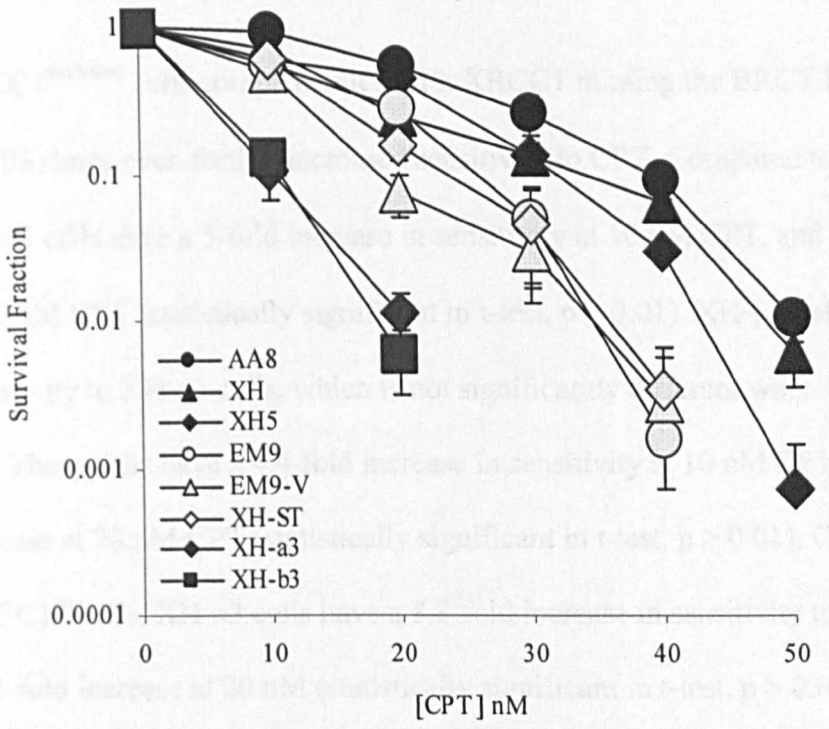

AA8 - wildtype
EM9 – XRCC1$^{-/-}$
XH/XH5 – EM9 complemented with hXRCC1
EM9-V – EM9 complemented with empty vector
XH-ST – EM9 complemented with short (ST) hXRCC1 (missing BRCT II)
XH-a3/b3 – EM9 complemented with hXRCC1 missing BRCT I

All cell lines were treated in increasing doses of CPT for 7 days at 37°C, under an atmosphere containing 5% CO2. The effect of CPT on cells is expressed as a percentage of controls and the values are the mean ± S.E. of three independent experiments.

XRCC1^{defective} cells complemented with short XRCC1 (XH-ST) had a similar level of sensitivity to CPT as EM9 and EM9-V. Compared to XRCC1^{wt} cells, XH-ST cells showed a 1.6-fold increase in sensitivity at 10 nM CPT (statistically significant in t-test, $p > 0.01$), which increased to a 27.7-fold increase at 40 nM CPT (statistically significant in t-test, $p > 0.001$), suggesting that it was the lack of DNA ligase III which was responsible for the increased cytotoxicity seen in EM9 cells.

XRCC1^{defective} cells complemented with XRCC1 missing the BRCT I motif (XH-α3 or XH-β3) have even further increased sensitivity to CPT. Compared to the EM9 cell line, XH-α3 cells have a 5-fold increase in sensitivity at 10 nM CPT, and a 24-fold increase at 20 nM CPT (statistically significant in t-test, $p > 0.01$). XH-β3 cells show a similar sensitivity to XH-α3 cells, which is not significantly different when subjected to the t-test. These cells have a 4.4-fold increase in sensitivity at 10 nM CPT, and a 46.2-fold increase at 20 nM CPT (statistically significant in t-test, $p > 0.01$). Compared to the XRCC1^{wt} cells, XH-α3 cells have a 8.8-fold increase in sensitivity to 10 nM CPT, and a 47.5-fold increase at 20 nM (statistically significant in t-test, $p > 0.001$ and $p > 0.01$ respectively). XH-β3 cells showed a 7.4-fold increase in sensitivity at 10 nM CPT, compared to XRCC1^{wt} cells, and a 90.7-fold increase at 20 nM CPT (statistically significant in t-test, $p > 0.001$ and $p > 0.01$ respectively). Both XH-α3 and XH-β3 cells did not survive above 20 nM CPT. These data suggest that mutation of the PARP-1 interaction domain of XRCC1 has a dominant negative effect on CPT sensitivity but the way in which this occurs is unknown.

4.8 Camptothecin-induced RAD51 foci formation is increased in XRCC1^{defective} cells complemented with XRCC1 that is missing the BRCT I motif

To examine if HR was also increased in these cell lines, we examined the level of RAD51 foci formation in each cell line after treatment for 24 hours with or without 100 nM CPT. We have already seen that XRCC1^{defective} cells have an increased amount of spontaneous RAD51 foci compared to XRCC1^{wt} cells (*Figure 4.5*), and both XRCC1^{wt} and XRCC1^{defective} cells have an increased amount of RAD51 foci formation after a 24 hour treatment with CPT. We have also observed that the amount of RAD51 foci formation is increased in both cell lines when treated with ISQ alone.

We found that spontaneous and CPT-induced RAD51 foci formation was similar in XRCC1^{defective} cell lines complemented with XRCC1, XH and XH5, as in the XRCC1^{wt} cell line (*Figure 4.8*). 2.6% of XH and XH5 cells showed spontaneous RAD51 foci, compared to XRCC1^{wt} cells, and 41% of XH cells had >10 RAD51 foci per cell in response to treatment with 100 nM CPT, compared to 39% of XH5 cells and 33% of XRCC1^{wt} cells (*Figure 4.8*). These results were not significantly different from each other when subjected to the t-test.

The percentage of cells with spontaneous and CPT-induced RAD51 foci in XRCC1^{defective} cells complemented with an empty vector (EM9-V) was similar to XRCC1^{defective} EM9 cells. 50% of untreated EM9-V cells showed > 10 RAD51 foci, compared to 42% of EM9 cells, and 98.5% of EM9-V cells showed > 10 RAD51 foci after treatment with CPT, compared to 95% of EM9 cells. The amount of RAD51 foci formation in XRCC1^{defective} cells complemented with short XRCC1 (XH-ST) was

slightly increased compared to EM9 cells, but not significantly. 51% of untreated XH-ST cells had > 10 RAD51 foci, compared to 42% of EM9 cells, and 96% of XH-ST cells showed > 10 RAD51 foci after CPT treatment, compared to 95% of EM9 cells.

Figure 4.8: Camptothecin-induced RAD51 foci formation is increased in XRCC1defective cells complemented with XRCC1 that is missing the BRCT I motif.

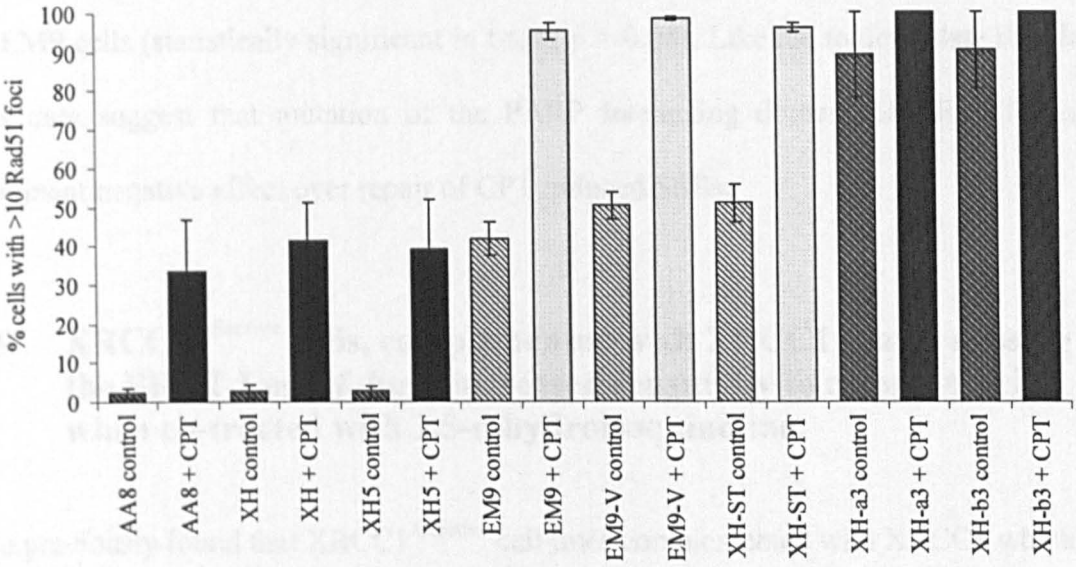

AA8 - wildtype
EM9 – XRCC1$^{-/-}$
XH/XH5 – EM9 complemented with hXRCC1
EM9-V – EM9 complemented with empty vector
XH-ST – EM9 complemented with short (ST) hXRCC1 (missing BRCT II domain)
XH-a3/b3 – EM9 complemented with hXRCC1 missing BRCT I domain

All cell lines were treated with 100 nM CPT for 24 hours at 37°C, under an atmosphere containing 5% CO2. Cells were then fixed in 3% paraformaldehyde, and incubated with anti-Rad51 primary antibody, and then a Cy3-conjugated antibody. The effect of CPT on cells is expressed as a percentage of cells containing more than 10 Rad51 foci and the values are the mean ± S.E. of three independent experiments.

XRCC1^{defective} cells complemented with XRCC1 which had the BRCT I motif removed (XH-α3 and XH-β3), had a dramatically increased amount of both spontaneous and CPT-induced RAD51 foci. 89% of untreated XH-α3 cells and 90% of XH-β3 cells showed >10 RAD51 foci, compared to 2.4% of XRCC1^{wt} cells (statistically significant in t-test, $p > 0.001$) and 42% of EM9 cells (statistically significant in t-test, $p > 0.01$). 100% of XH-α3 and XHβ3 cells had >10 RAD51 foci when treated with CPT, compared to 33% of XRCC1^{wt} cells (statistically significant in t-test, $p>0.01$) and 95% of EM9 cells (statistically significant in t-test, $p > 0.05$). Like the toxicity data this data this data suggest that mutation of the PARP interacting domain of XRCC1 has a dominant negative effect over repair of CPT induced SSBs.

4.9 XRCC1^{defective} cells, complemented with XRCC1 that is missing the BRCT I motif, have increased sensitivity to camptothecin when co-treated with 1,5-dihydroisoquinoline.

We previously found that XRCC1^{defective} cell lines complemented with XRCC1 which had the BRCT I motif removed, XH-α3 and XH-β3, had increased sensitivity to CPT, compared to the XRCC1^{wt} cell line, the XRCC1^{defective} EM9 cell line, the XRCC1^{defective} cell line complemented with an empty vector, and the XRCC1^{defective} cell line complemented with human XRCC1. They were also more sensitive to CPT than XRCC1^{defective} cell lines complemented with short XRCC1(XH-ST), which had the BRCT II motif missing (*figure 4.7*).We also found that the XH-α3 and XH-β3 cell lines had increased spontaneous and CPT-induced RAD51 foci formation, compared to those other cell lines (*figure 4.8*). We next examined the sensitivity of these cell lines to CPT

when co-treated with PARP-1 inhibitors, NU1025 or ISQ. We treated XH-α3 and XH-β3 with increasing doses of CPT and 10 μM NU1025 or 0.6 mM ISQ.

Figure 4.1.9: XRCC1defective cells, complemented with XRCC1 that is missing the BRCT I motif, have increased sensitivity to camptothecin when co-treated with 1,5-dihydroisoquinoline.

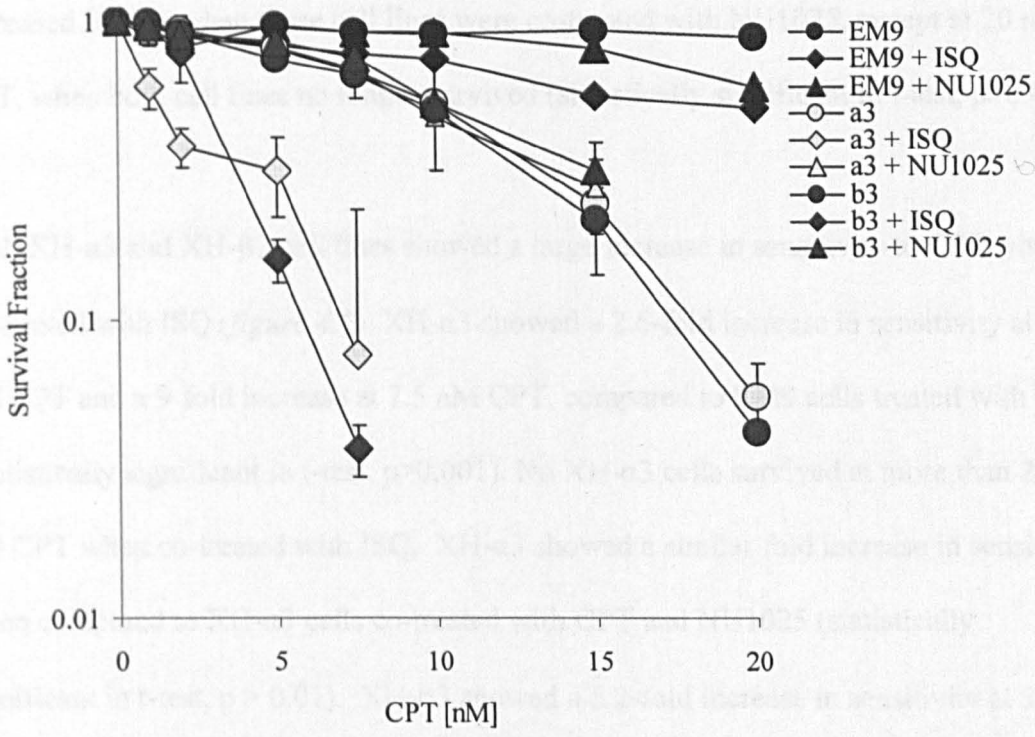

EM9 – XRCC1$^{-/-}$
XH-a3/b3 – EM9 complemented with hXRCC1 missing BRCT I

All cell lines were treated in increasing doses of CPT for 7 days at 37°C, under an atmosphere containing 5% CO2. Some cells were co-treated with 100 nM CPT and 0.6 mM ISQ, or 100 nM CPT and 10 μM NU1025. The effect of CPT on cells is expressed as a percentage of controls and the values are the mean ± S.E. of three independent experiments.

We found that as before both XH-α3 and XH-β3 cell lines were more sensitive to CPT treatment alone, compared to XRCC1^{defective} EM9 cells. XH-α3 cells showed a 1.7-fold increase in sensitivity to 10 nM CPT, a 3.8-fold increase at 15 nM CPT, and a 16-fold increase at 20 nM CPT. XH-β3 cells showed a similar increase in sensitivity, with a 1.8-fold increase at 10 nM CPT, a 4.3-fold increase at 15 nM CPT, and a 21-fold increase at 20 nM CPT (all statistically significant in t-test, $p>0.001$). This sensitivity was not increased further when these cell lines were co-treated with NU1025, except at 20 nM CPT, when both cell lines no longer survived (statistically significant in t-test, $p>0.05$).

Both XH-α3 and XH-β3 cell lines showed a large increase in sensitivity to CPT when co-treated with ISQ (*figure 4.9*). XH-α3 showed a 2.6-fold increase in sensitivity at 5 nM CPT and a 9-fold increase at 7.5 nM CPT, compared to EM9 cells treated with ISQ (statistically significant in t-test, $p>0.001$). No XH-α3 cells survived at more than 20 nM CPT when co-treated with ISQ. XH-α3 showed a similar fold increase in sensitivity when compared to XH-α3 cells co-treated with CPT and NU1025 (statistically significant in t-test, $p > 0.01$). XH-β3 showed a 5.2-fold increase in sensitivity at 5 nM CPT and a 21-fold increase at 7.5 nM CPT, compared to EM9 cells treated with ISQ (statistically significant in t-test, $p>0.001$). No XH-α3 cells survived at more than 20 nM CPT when co-treated with ISQ. XH-β3 showed a similar fold increase in sensitivity when compared to XH-β3 cells co-treated with CPT and NU1025 (statistically significant in t-test, $p>0.001$). Interestingly, XH-β3 cells seem to be more sensitive to CPT than XH-α3, there is a 2-fold increase in sensitivity in XH-β3 cells at 15 nM CPT and 20 nM CPT (statistically significant in t-test, $p > 0.05$). This data indicate that what

ever the effect mutating the BRCT I domain has it is mimicked but inhibition of PARP-1 by NU1025.

4.10 Chinese hamster cell line, SPD8 has decreased homologous recombination when co-treated with camptothecin and PARP-1 inhibitor, 1,5-dihydroisoquinoline.

We had already examined the level of HR in XRCC1^{wt} and XRCC1^{defective} cell lines, after treatment with CPT and ISQ, or after a co-treatment with CPT and ISQ, by examining the level of RAD51 foci in the cell. These foci form whenever the cell undergoes HR, and a measurement of these can be used as an indication of the amount of HR that is taking place within a cell. However, it is possible that the RAD51 foci form but that HR does not continue from this point. To be certain that HR does take place after CPT or ISQ treatment we used the HPRT gene system in the SPD8 cell line (**CHAPTER 2.4.5.1**).

We found that SPD8 cells are sensitive to high doses of CPT (*Figure 4.10*), when treated with increasing doses of CPT. 86% of cells survived at 20 nM CPT, which decreased to 13% at 50 nM CPT, 3% at 100 nM CPT and 1.5% at 200 nM CPT. Therefore, 100 nM CPT was chosen as a suitable dose for this cell line, as it was toxic but allowed enough survival for us to examine HR.

We found that SPD8 cells had a spontaneous reversion frequency of 5.9 cells per 100,000 cells. SPD8 cells treated with ISQ alone did not increase recombination above the spontaneous level, having a frequency of 6.5 cells per 100,000 cells. However, cells

co-treated with CPT and ISQ had a reduced level of recombination, compared to treatment with CPT alone (*figure 4.10.3*). Cells treated with CPT alone had a reversion frequency of 38 cells per 100,000 cells, but cells co-treated with CPT and ISQ had a reversion frequency of 6.8 cells per 100,000 cells.

Figure 4.10: Chinese hamster cell line, SPD8 has decreased homologous recombination when co-treated with camptothecin and PARP-1 inhibitor, 1,5-dihydroisoquinoline.

a)

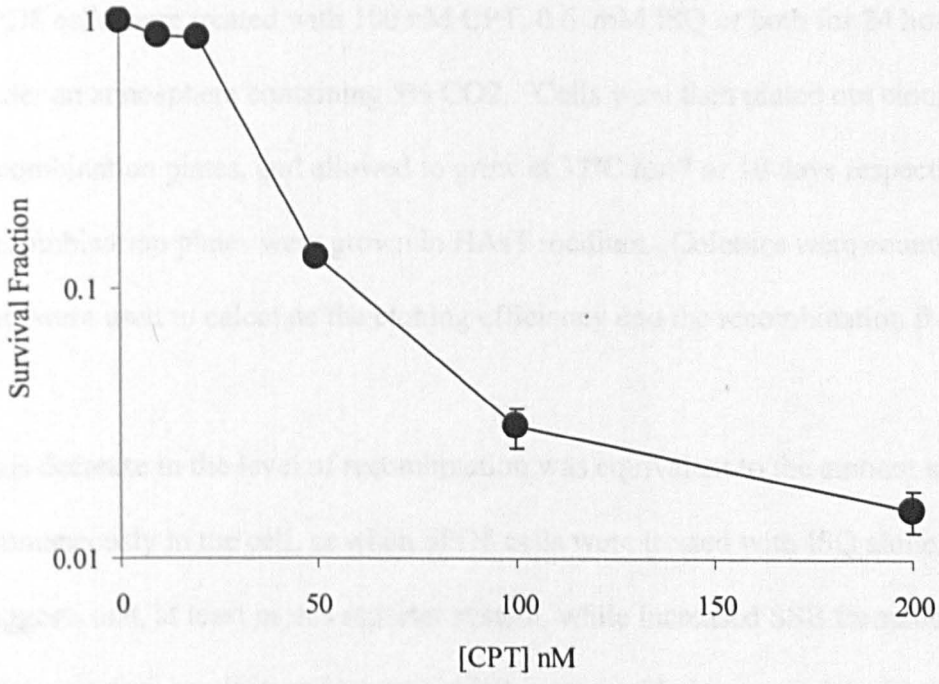

SPD8 cells were treated in increasing doses of CPT for 7 days at 37°C, under an atmosphere containing 5% CO2. The effect of CPT on cells is expressed as a percentage of controls and the values are the mean ± S.E. of three independent experiments.

b)

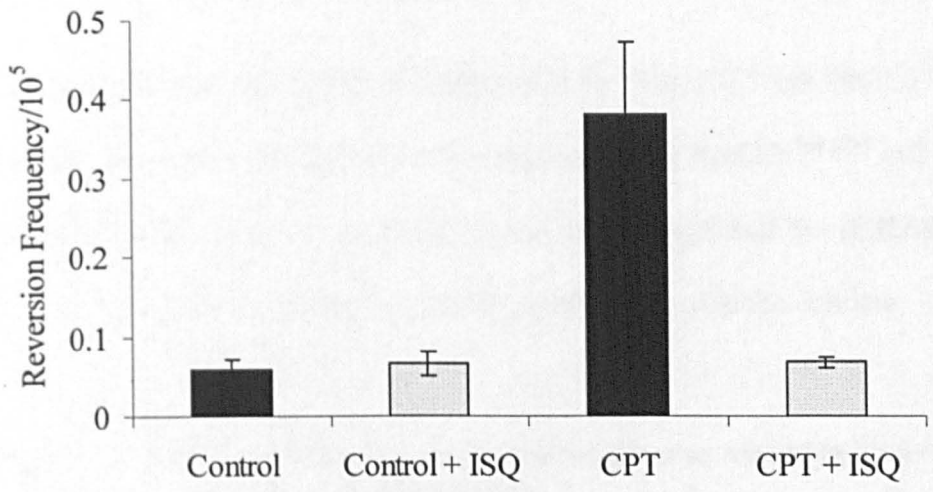

SPD8 cells were treated with 100 nM CPT, 0.6 mM ISQ or both for 24 hours at 37°C, under an atmosphere containing 5% CO2. Cells were then plated out cloning and recombination plates, and allowed to grow at 37°C for 7 or 10 days respectively. Recombination plates were grown in HAsT medium . Colonies were counted and these data were used to calculate the cloning efficiency and the recombination frequency.

This decrease in the level of recombination was equivalent to the amount seen spontaneously in the cell, or when SPD8 cells were treated with ISQ alone. This suggests that, at least in this reporter system, while increased SSB formation by CPT treatment does result in an increase in HR, presumably because of the increase in DSBs forming at replication forks, inhibition of PARP does not produce the same increase. This is the opposite to the effect seen when measuring HR by Rad51 foci formation. In addition, again in conflict with the RAD51 foci results, co-treatment of cells with CPT and PARP inhibitors decreases HR. Either the reporter system cannot pick up these HR events, or the foci are non-functional for HR.

4.11 S8SN.11 cells show increased homologous recombination when treated with camptothecin.

We wanted to examine the level of HR inside the XRCC1^{wt} and XRCC1^{defective} cell lines directly, so we used the SCneo vector transfected into XRCC1^{defective} cell lines, using SPD8 transfected with SCneo (S8SN.11) as the wildtype cell line (**CHAPTER 2.4.5.2**). We used Southern blotting to ensure the vector was inside the cell line.

Figure 4.11: S8SN.11 cells show increased homologous recombination when treated with camptothecin.

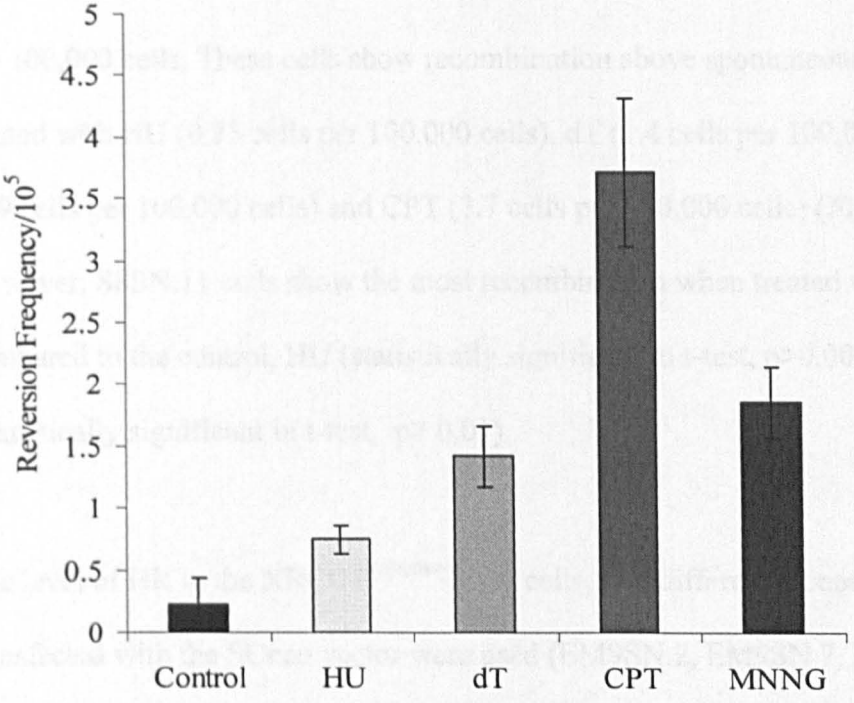

S8SN.11 cells were treated with 1 mM HU, 10 mM dT, 100 nM CPT or 10 μM MNNG for 24 hours under an atmosphere containing 5% CO2. Cells were then plated out cloning and recombination plates, and allowed to grow at 37°C for 7 or 10 days respectively. Recombination plates were grown in HAsT medium. Colonies were counted and these data were used to calculate the cloning efficiency and the recombination frequency.

S8SN.11 is sensitive to 100 nM CPT, so is a good control cell line for our experiments (*Figure 4.11*).In order to examine HR in S8SN.11 cells after treatments with a variety of drugs, we treated these cells with 1 mM hydroxyurea (HU), 10 mM thymidine (dT), 10 μM MNNG and 100 nM CPT for 24 hours. They were then grown in media containing 100 mg/ml geneticin. Cells that have not undergone HR will not survive in this media.

4.12 XRCC1^{defective} cells show homologous recombination when DSBs are induced using Sce-I endonuclease.

We found that S8SN.11 cells had a spontaneous recombination frequency of 0.23 cells per 100,000 cells. These cells show recombination above spontaneous levels when treated with HU (0.75 cells per 100,000 cells), dT (1.4 cells per 100,000 cells), MNNG (1.9 cells per 100,000 cells) and CPT (3.7 cells per 100,000 cells) (*Figure 4.11*). However, S8SN.11 cells show the most recombination when treated with CPT, compared to the control, HU (statistically significant in t-test, $p>0.001$), dT and MNNG (statistically significant in t-test, $p> 0.01$).

The level of HR in the XRCC1^{defective} EM9 cells, five different clones which had been transfected with the SCneo vector were used (EM9SN.2, EM9SN.7, EM9SN.11, EM9SN.12 and EM9SN.13). Each clone was treated with SceI endonuclease and we examined the level of HR.

Figure 4.12: XRCC1defective cells show homologous recombination when DNA double strand breaks are induced using Sce-I endonuclease.

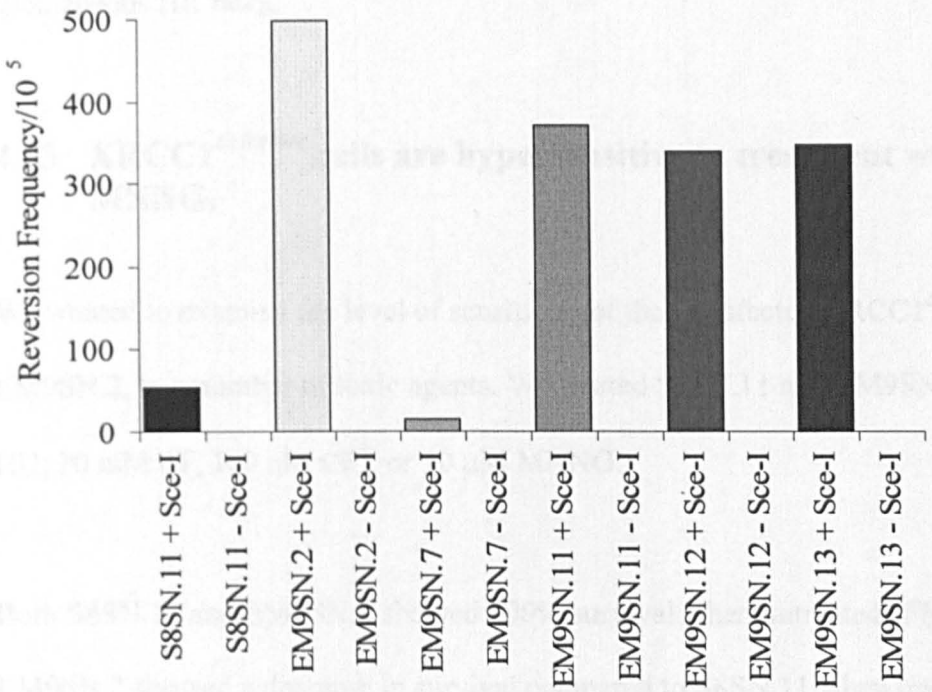

All cell lines were treated with Sce-I, with no treatment as a control. Cells were then plated out cloning and recombination plates, and allowed to grow at 37°C for 7 or 10 days respectively. Recombination plates were grown in medium containing G418. Colonies were counted and these data were used to calculate the cloning efficiency and the recombination frequency.

We observed that following Sce-I treatment four out of the five clones showed an increased amount of recombination compared to S8SN.11. EM9SN.7 showed only a small amount of recombination (*Figure 4.12*). S8SN.11 had a recombination frequency of 53 cells per 100,000 cells. EM9SN.2, EM9SN.11, EM9SN.12 and EM9SN.13 had a recombination frequency of 498, 371, 340 and 347 cells per 100,000 cells respectively. .

Spontaneous HR however was not any different to that seen in wildtype cells. This shows that lack of XRCC1 increases the amount of DSB induced HR but does not alter spontaneous HR rates.

4.13 XRCC1^{defective} cells are hypersensitive to treatment with CPT or MNNG.

We wanted to examine the level of sensitivity of the transfected XRCC1^{defective} cell line, EM9SN.2, to a number of toxic agents. We treated S8SN.11 and EM9SN.2 with 1 mM HU, 10 mM dT, 100 nM CPT or 10 μM MNNG.

Both S8SN.11 and EM9SN.2 showed 100% survival when untreated (*Figure 4.13*). EM9SN.2 showed a decrease in survival compared to S8SN.11 when treated with HU, 38% compared to 61% (statistically significant in t-test, $p>0.05$), and a smaller difference was seen between the two cell lines when treated with dT (50% in EM9SN.2, compared to 60% in S8SN.11), which was statistically significant in t-test, $p>0.05$. However, EM9SN.2 showed a huge decrease in survival when treated with CPT, compared to S8SN.11, showing only 0.6% survival, compared to 52% in S8SN.11 cells (statistically significant in t-test, $p > 0.001$). EM9SN.2 did not survive when treated with MNNG (statistically significant in t-test, $p > 0.01$). Thus XRCC1 appears to be important survival not only to CPT induced damage as we have seen previously but also to HU, thymidine and MNNG induced DNA damage.

Figure 4.13: XRCC1defective cells are hypersensitive to treatment with camptothecin or N-methyl-N-nitro-N-nitrosoguanidine

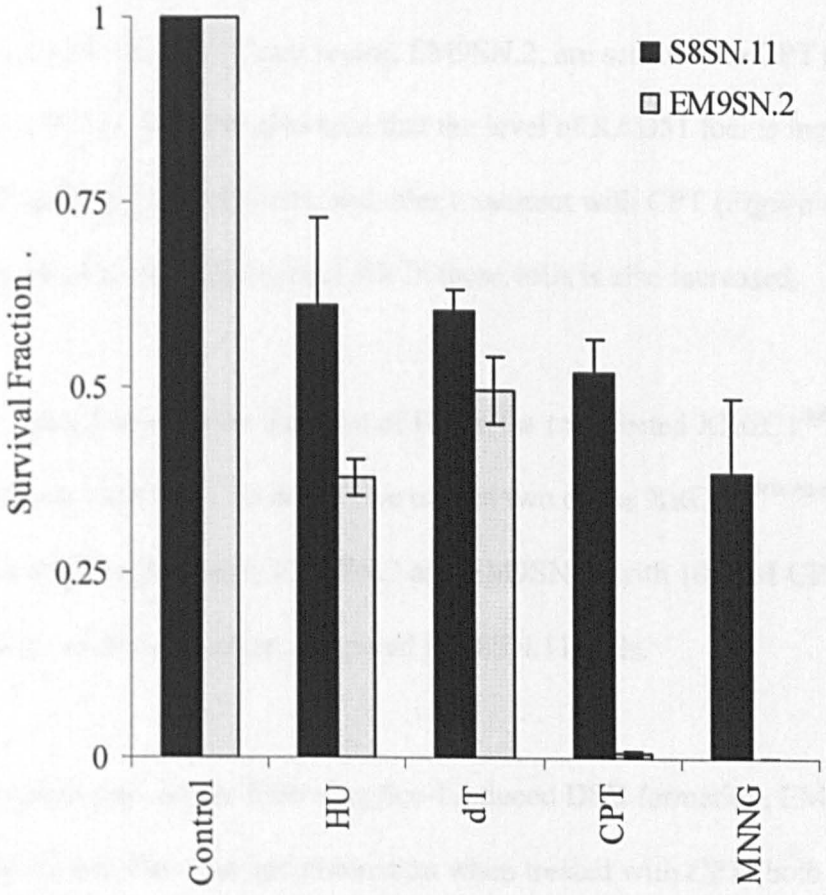

All cell lines were treated with 1 mM HU, 10 mM dT, 100 nM CPT or 10 μM MNNG for 7 days under an atmosphere containing 5% CO2. The effect of each drug on cells is expressed as a percentage of controls and the values are the mean ± S.E. of three independent experiments.

4.14 XRCC1^{defective} cells do not undergo homologous recombination when treated with CPT

We have already seen that that the XRCC1^{defective} EM9 cell line, and the same cell line transfected with the SCneo vector, EM9SN.2, are sensitive to CPT (*Figure 4.2* and *Figure 4.13*). We have also seen that the level of RAD51 foci is increased spontaneously in EM9 cells, and after treatment with CPT (*Figure 4.5* and *Figure 4.6*). This indicates that the level of HR in these cells is also increased.

We wanted to examine the level of HR in the transfected XRCC1^{defective} cell lines after treatment with CPT. To do this we treated two of the XRCC1^{defective} cell lines transfected with SCneo, EM9SN.2 and EM9SN.7, with 100 nM CPT, and examined the amount of recombination compared to S8SN.11 cells.

We found that, unlike following Sce-I induced DSB formation, EM9SN.7and EM9SN.2 cells did not show any recombination when treated with CPT (both statistically significant in t-test, $p>0.001$), while in wildtype cells, recombination was induced 20-fold (*Figure 4.14*). As previously seen, EM9SN.7 showed o spontaneous recombination but EM9SN.11 showed a small amount of spontaneous recombination, 0.025 cells per 100,000 cells. However this was still lower than the amount see in S8SN.11, which showed a spontaneous recombination frequency of 0.04 cells per 100,000 cells, and was not significant in the t-test. This experiment shows that while EM9 cells can undergo HR CPT does not induce HR in our reporter construct in the absence of XRCC1.

Figure 4.1.14: XRCC1defective cells do not undergo homologous recombination when treated with camptothecin.

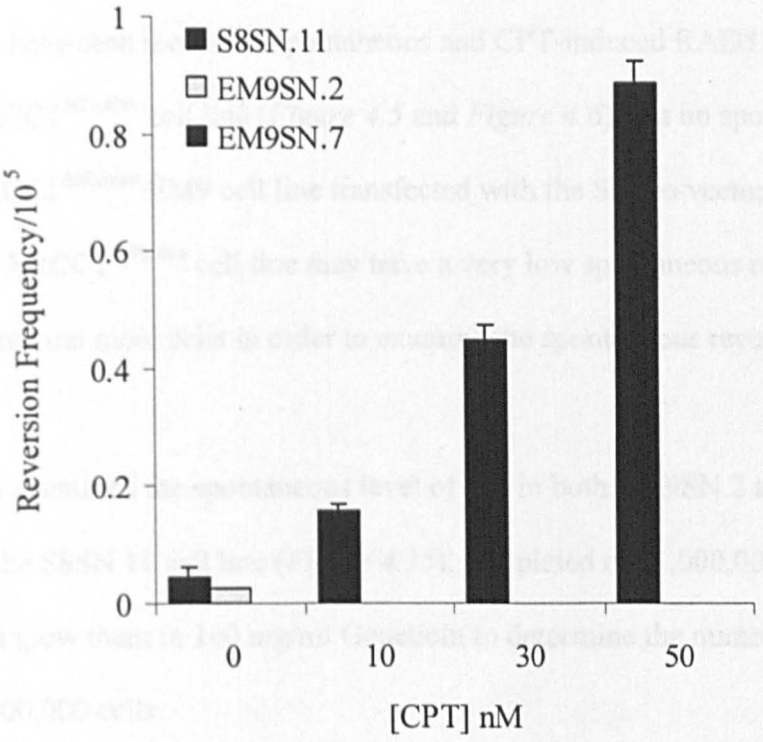

All cell lines were treated with 10 nM, 30 nM, or 50 nM CPT, with no treatment as a control., for 7 days under an atmosphere containing 5% CO2 Cells were then plated out cloning and recombination plates, and allowed to grow at 37°C for 7 or 10 days respectively. Recombination plates were grown in medium containing 6-tG. Colonies were counted and these data were used to calculate the cloning efficiency and the recombination frequency.

4.15 XRCC1^{defective} cells do not undergo spontaneous homologous recombination

We have seen increased spontaneous and CPT-induced RAD51 foci in the XRCC1^{defective} cell line (*Figure 4.5* and *Figure 4.6*), but no spontaneous HR in the XRCC1^{defective} EM9 cell line transfected with the SCneo vector. We hypothesised that the XRCC1^{defective} cell line may have a very low spontaneous recombination rate so we plated out more cells in order to examine the spontaneous recombination level.

We examined the spontaneous level of HR in both EM9SN.2 and EM9SN.11, compared to the S8SN.11 cell line (*Figure 4.15*). We plated out 1,000,000 cells from 1,000 cells and grew them in 100 mg/ml Geneticin to determine the number of revertants per 1,000,000 cells.

Figure 4.15: XRCC1^{defective} cells do not undergo spontaneous homologous recombination.

Cell line	Spontaneous recombination frequency
S8SN.11	6.4 x 10-7
EM9SN.2	0
EM9SN.7	0

We observed that S8SN.11 underwent a low level of spontaneous recombination, with only 6.4 cells per 1,000,000 undergoing recombination. No recombination was observed in EM9SN.2 and EM9SN.7 cells so we can conclude that the spontaneous recombination rate in these cells is less than 1 in 1,000,000 (statistically significant in t-test, $p > 0.01$).

4.16 Discussion

XRCC1^{defective} cells are more sensitive to CPT than XRCC1^{wt} cells, which suggests that XRCC1 has a role in the repair of SSBs. XRCC1 is believed to be a scaffold protein that is involved in the SSB repair pathway. In the defective cell lines, XRCC1 cannot bring the SSB repair proteins, DNA ligase III and DNA polymerase β to the site of the SSB, so it is likely that repair is slower. We have shown that CPT induces the formation of DSBs in both XRCC1^{defective} and XRCC1^{wt} cell lines, but that there are a greater number of DSBs in the deficient cell line. Our hypothesis is that as the repair of the SSBs in the XRCC1^{defective} cell line is slower SSBs encounter the replication machinery, at which point they are converted to DSBs, this is supported by the fact that if you inhibit replication, CPT-induced DSBs and HR is decreased (Saleh-Gohari *et al.*,2005) .

We see an increase in the amount of RAD51 foci formation in XRCC1^{defective} cells, suggesting that the level of HR repair is increased. This is not unexpected as we also see that DSB formation is increased and HR is the preferred mechanism for the repair of these DSB. HR is also shown to be increased in XRCC1^{wt} cells when treated with CPT. This suggests that HR is a major pathway for the repair of CPT-induced damage. The

increased spontaneous levels of RAD51 foci in SSB repair defective cells, suggests that a SSB is an important endogenous lesion for HR. This is supported by the fact that the spectrum of spontaneous recombinant products formed is highly similar to the CPT-induced spectrum of recombinants (Saleh-Gohari et al., 2005).

Co-treating XRCC1^{wt} cells with CPT and PARP inhibitors, NU1025 or ISQ, increased the sensitivity to CPT. This is probably because when PARP-1 is inhibited by NU1025, or ISQ, it cannot catalyse the production of poly(ADP-ribose) polymers. This may have two effects firstly XRCC1 may not be as strongly attracted to SSBs and secondly if PARP is not automodified it will not eventually be displaced and may block the access of other repair enzymes to the site of damage. It has been shown that when PARP-1 is inhibited by 3-aminobenzamine (3-AB), PARP-1 blocks access for BER proteins to the SSB (Parsons *et al*, 2005).

Another explanation could be that proteins involved in SSB repair, other than XRCC1 might be attracted to SSBs by PARP. In this scenario, additional inhibition of PARP, in XRCC1 defective cells, would result in further sensitivity to CPT. When we inhibited PARP in XRCC1 defective cells we saw that sensitivity was in deed further increased adding weight to this idea.

We observed that XRCC1^{wt} cells and XRCC1^{defective} cells were more sensitive to a co-treatment with CPT and ISQ, than CPT and NU1025. This may be explained by the different potencies of the two inhibitors.

In XRCC1^{defective} cells there is an increased amount of spontaneous HR. As discussed previously, this may be because the lack of XRCC1 results in slower SSB repair, so any endogenous SSBs in the DNA are repaired at a slower rate and can become DSBs when encountered by a replication fork. When XRCC1^{defective} cells are treated with ISQ, the amount cells with > 10 RAD51 foci (an indicator of HR) further increases to 97.5%. This is a drastic increase in the amount of HR, and could be because when there is no XRCC1 and PARP-1 is inhibited, SSB repair becomes even slower, or does not occur at all. In this case, all of the endogenous SSBs in the cell would become DSBs and result in a dramatically increased amount of HR.

We have seen how lack of XRCC1 in cells results in an increase in DSBs and homologous recombination, presumably as a reflection of less SSB repair occurring, we have also seen that inhibiting PARP in these deficient cells further enhances this effect, and have hypothesised that this is because SSB repair is even less efficient. In addition co-treatment of wt cells with either CPT or PARP inhibitors also increases Rad51 foci formation compared to none treated cells. When XRCC1^{wt} cells are treated with CPT, this drug stabilises the SSBs induced by Top1, so there will be more SSBs in the cell. Inhibition of PARP will also increase the number of SSBs in the cell by decreasing the efficiency of endogenous SSB repair. However, SSB repair is active in the cell and the SSBs can be repaired, so why do we see an increase in HR? It may be that there are too many SSBs for SSB repair to fix them all before they are encountered by the replication machinery and become DSBs, they then require HR for repair. When XRCC1^{wt} cells are co-treated with CPT and ISQ, there is still an increase in the number of SSBs due to the effect of CPT, but PARP-1 is also being inhibited by ISQ. This means that SSB repair is

likely to be slower, so there are both more SSBs formed and more left unrepaired. This further increases the number of SSBs becomes an increased number of DSBs when they encounter replication forks and so result in the further increase in HR, which we see. When XRCC1^{defective} cells are treated with CPT there is a similar level of HR to when they are treated with ISQ alone, 95% of cells contain > 10 RAD51 foci. This is the same as we observed previously, and is probably due to the increased amount of SSBs in the cell, caused by CPT, and SSB repair being slower due the lack of XRCC1 or inhibition of PARP. When XRCC1^{defective} cells are co-treated with CPT and ISQ, 100% of cells contain >10 RAD51 foci. This is probably because SSB repair is very slow, or does not happen at all when both XRCC1 and PARP-1 are not active in the cell. At the same time, CPT is causing lots of SSBs, which are not being repaired by SSB repair. This leads to SSBs becoming DSBs in the cell, and an increase in HR to repair them. If there are lots of SSBs due to the action of CPT, and no SSB repair this would increase the number of DSBs and would explain the dramatic increase in the amount of HR, as indicated by the increased number of cells containing > 10 RAD51 foci. The effect of inhibiting both PARP and XRCC1 together may be more detrimental than is reflected in the increase in foci as the damage response pathways may be saturated, once 100% of cells are seen to be containing foci we cannot record any more increase in HR. In the future, further Rad51 foci assays will be needed to ascertain whether there is an additive effect for CPT and ISQ in the PARP$^{-/-}$ cells. This could be dome by decreasing the dose of the CPT, so that the assay does not max out, or by treating the cells for less time.

The XRCC1 protein has been implicated in a DNA ligase III dependent and independent SSB repair (Taylor, 2002). The DNA ligase III dependent SSB repair

appears to be active throughout the cell cycle and involves the BRCT I motif of the XRCC1 protein, whilst DNA ligase III independent XRCC1 repair appears to be active at replication forks and involves the BRCT II motif of the XRCC1 protein. To test which repair pathway was involved in the repair of CPT-induced DNA damage, we used XRCC1 mutant cell lines that had one or both of the BRCT motifs removed. When the XRCC1^{defective} cell line was complemented with an empty vector, it had no effect on the sensitivity of the cell line to CPT. However, when the same cell line was complemented with the full XRCC1 protein, sensitivity was reverted back to the same levels as the wildtype cell line. Confirming that it is mutation of XRCC1 which is responsible for the sensitivity of the EM9 cells.

Both of the XRCC1^{defective} cell lines complemented with short XRCC1 had the same level of sensitivity to CPT as the deficient cell line. Therefore it seems that it is the lack of DNA ligase III at the site of the SSB that slows SSB repair. Short XRCC1 still carries DNA polymerase β to the site of the SSB, so it is not likely that this protein is the rate limiting step. The XRCC1^{defective} cell line complemented with XHα3 or XHβ3 showed even greater sensitivity to CPT. than EM9, thus the defect seems to have a dominant negative effect in cells. These cells lines have the BRCT I motif disrupted, XH-α3 has the third α-helix of the BRCT motif disrupted, and XH-β3 has the third β-sheet of the BRCT motif disrupted. The BRCT I motif is known to bind to the BRCT motif in the automodification domain of PARP-1, but we do not know what effect the disrupted XRCC1 BRCT I motif could have on the PARP-1 protein.

In the cell lines that have the XRCC1 BRCTI motif disrupted, we observed increased sensitivity to CPT, compared to XRCC1 defective cells, an increased number of cells displaying spontaneous and CPT- induced RAD51 foci and a further increase in sensitivity to CPT, when co-treated with ISQ. However, no significant increase in sensitivity to CPT was observed when these cell lines were co-treated with CPT and NU1025. This may be explained by the different potencies of the two inhibitors.
We can conclude that disruption of the BRCT I domain in XRCC1 has the same effect as inhibiting PARP-1 in XRCC1 defective cells. It is likely then that disrupting the BRCTI domain inhibits PARP activity in some way. It could be that the BRCT I motif binds PARP-1 as normal, but then PARP-1 cannot break away from XRCC1, inhibiting its activities. In this scenario, PARP-1 would be unable to bind to further SSBs and other SSB repair protein may be unable to access the site of damage.

Spontaneous and CPT-induced RAD51 foci formation is increased in both XH-α3 and XHβ3 cell lines, compared to XRCC1^{defective} cells. This could again be because PARP-1 is inhibited by the disrupted BRCT I motif, causing SSB repair to be slower. This in turn, would lead to more SSBs in the cells, which could encounter the replication machinery to become DSBs. Therefore, there would be more DSBs in the cell to be repaired. HR appears to be the major repair pathway for these single-ended DSBs, so the increase in cells containing RAD51 foci, could be an indication of a rise in HR repair. It may also be that HR repair is deficient in the absence of PARP-1 and XRCC1. This is supported by the fact that PARP-1 inhibitors reduce the number of CPT-induced recombinants.

While the RAD51 foci results suggest that that both spontaneous and CPT induced HR increases in XRCC1 defective and PARP inhibited cells, and that this level further increases if both are defective/inhibited, direct analysis of HR at the hprt loci or in the SCneo reporter assay did not agree. SPD8 cells show increased HR following treatment with 100 nM CPT, but no increase following PARP inhibition and in fact have decreased HR when co-treated with CPT and ISQ. One possible explanation could be that the HR event studied in SPD8 cells requires a recombination tract longer than 5 kb. Previously, it was found that recombination induced at replication forks is likely to involve short recombination tracts and will not be detected in the HR assay in the SPD8 cells (Lundin *et al.*, 2003). This could indicate that another recombination event is triggered in presence of an inhibitor of PARP. An alternative explanation could be that ISQ treatment may arrest cells in the G2 phase of the cell cycle (Schultz and Helleday, personal communication), which would result in fewer cells reaching the S phase of the cell cycle; the phase HR normally occurs (Saleh Gohari *et al.*, 2004).

S8SN.11 cells are SPD8 cells transfected with the SCneo vector. These cells show increased HR when treated with CPT, compared to treatments with HU, dT or MNNG. This indicates that CPT is a strong inducer of HR repair. XRCC1^{defective} cells, that have also been transfected with the SCneo vector, show HR when treated with Sce-I and are hypersensitive to CPT and MNNG. However they do not undergo HR when treated with CPT. The same cells undergo de creased spontaneous recombination. We see increased RAD51 foci in these cells, but the SCneo assay shows that HR does not take place. It could be that RAD51 foci form but cannot complete HR or that the HR event occurring

following CPT treatment in EM9 cells involves very short recombination tracts not detectable in the HR assay.

In conclusion, we suggest that the role of PARP-1 and XRCC1 in SSB repair of CPT lesions is likely to explain the results found. The inhibition of XRCC1 may slow the repair of CPT-induced SSBs, which in turn would lead to more SSBs collapsing at replication forks and thus more DSBs. This in turn would increase the amount of RAD51-foci forming for repair. When PARP-1 and XRCC1 were both inhibited or defective in the cell, sensitivity to CPT increases. This may be because there are two SSB repair pathways in the cell, one involving XRCC1 and PARP-1, the other involving PARP-1. When XRCC1 is defective in the cell, SSB repair is slower, but can be continued via the PARP-1 dependent pathway. When XRCC1 is defective and PARP-1 is inhibited neither pathways are viable, and no SSB repair takes place. This last hypothesis is reinforced by observations that sensitivity to CPT increases when both proteins are defective or inhibited in the cell.

CHAPTER 5: DISCUSSION

CHAPTER 5: DISCUSSION

5.1 The role of PARP-1 in CPT-induced damage

Co-treatment of PARP-$1^{+/+}$ and PARP-$1^{-/-}$ cells with camptothecin (CPT) and PARP-1 inhibitors increases the killing effect of CPT. This is probably because when PARP-1 is inhibited by NU1025, or 1,5-dihydroisoquinoline (ISQ), these drugs bind to the catalytic domain, preventing PARP-1 from catalysing the production of poly(ADP-ribose) polymers. PARP-1 can still bind to the single-strand break (SSB), but because it cannot automodify itself, PARP-1 remains bound to the SSB. Also, if PARP-1 is not automodified, XRCC1 will not bind to it, and bring the SSB repair proteins to the site of the SSB.

It has been shown that when PARP-1 is inhibited by 3-aminobenzamine (3-AB), PARP-1 blocks access for SSB repair proteins to the SSB (Parsons *et al*, 2005). However, it has also been shown that the presence of the PARP-1 protein in the cell offers some protection of the SSB from cellular nucleases.

We have seen that CPT has increased cytotoxicity in PARP-$1^{-/-}$ cells. This suggests that it is the loss of PARP-1 protein or its activity rather than an inability for PARP-1 to be displaced from DNA that is causing enhanced CPT sensitivity.

If the absence of PARP-1 from the cell increases the cytotoxicity of CPT, it must be the activity of PARP-1 rather than its presence at the SSB that is protecting the SSB from

becoming a double-strand break (DSB). This may happen when the SSB encounters the replication machinery. The activity of PARP-1 would recruit the SSB repair proteins to the site of DNA damage. Without this, the cell is more sensitive to CPT, probably because the repair of the SSB is slower. However, PARP-$1^{-/-}$ cells co-treated with CPT and PARP inhibitors, also showed an increase in sensitivity to CPT. This is likely to be because the presence of the PARP-1 protein, even though inhibited, does offer some protection and could explain why PARP-$1^{-/-}$ cells show more sensitivity to CPT than PARP-$1^{+/+}$ cells co-treated with CPT and PARP-1 inhibitors.

We observed that $PARP^{+/+}$ cells were more sensitive to a co-treatment with CPT and ISQ, than CPT and NU1025. This could be explained by the fact that NU1025 is active at a much lower concentration than ISQ, which likely increase substrate specificity. Also, treatments with ISQ alone arrests cells in the G2/M phase of the cell cycle (Schultz, Bryant and Helleday, personal communication), which is likely due to inhibition of also tankylase 1, which has a role in spindle assembly during mitosis (Chang *et al.*, 2005; Dynek & Smith, 2004). Treatments with NU1025 does not arrest cells in the G2/M phase of the cell cycle suggesting it is more specific inhibitor of PARP-1 (Schultz, Bryant and Helleday, personal communication).

PARP-like proteins have been discovered in humans, with 40% (PARP-2) and 31% (PARP-3) homology to PARP-1. Both of these proteins lack DNA-binding domains and automodification domains, but show strong homology with the catalytic domain (Johansson, 1999; Ame *et al.*, 2001). These proteins were discovered when it was observed that PARP knockout mice still showed residual PARP activity (Shall & de Murcia, 2000). PARP-2 and PARP-3 were able to synthesise pADPr polymers in

response to DNA damage, although these polymers were much shorter in length. Therefore it seems that these proteins are catalytically active, and may have an important role to play in some of the same pathways as PARP-1. Therefore, it would be beneficial to further our knowledge and define their exact roles. This however is a further study.

CPT increases the formation of DSBs in PARP-$1^{-/-}$ cells. The likely explanation for an increase in DSBs in these cells is that in the absence of PARP-1, the SSB repair proteins are not recruited to the site of the SSB via the interaction of PARP-1 with XRCC1. Therefore, SSB repair is slower. Since there are more unrepaired SSBs in the cell, it is more likely that they will encounter the replication machinery and form DSBs. This is probably why we see an increase in DSBs in these cells after treatment with CPT. DSBs are also increased in PARP-$1^{+/+}$ cells co-treated with CPT and PARP-1 inhibitors, NU1025 or ISQ. In this case, it is likely that inhibited PARP-1 may bind the SSB, even though it cannot recruit XRCC1 to the site by auto-ADP-ribosylating itself. Even thought the presence of PARP-1 in the cell may protect the SSBs from degradation from cellular nucleases, it may not protect them from becoming DSBs on encountering the replication machinery.

HR appears to be the major repair pathway for CPT-induced DSBs (Arnaudeau *et al.*, 2001). A measurement of the number of cells containing > 10 RAD51 foci per cells can be used as an indication of the amount of HR taking place within a cell. RAD51 foci are small nuclear foci containing all of the proteins involved HR. These foci form whenever the cell undergoes HR.

Spontaneous and CPT-induced RAD51 foci formation is increased in PARP-1$^{-/-}$ cells. These results suggest that HR is increased spontaneously in PARP$^{-/-}$ cells, probably because of an increase in SSBs leading to DSB formation when encountered by replication machinery, and that HR is the preferred mechanism for the repair of these DSB. HR is also shown to be increased in PARP-1$^{+/+}$ cells when treated with CPT. This suggests that HR is the major pathway for the repair of CPT-induced damage.

There is an increase in RAD51 foci in PARP$^{-/-}$ cells treated with CPT. This suggests that HR is increased in this cell line when treated with CPT. This increase in HR is above the level observed for CPT-treated PARP-1$^{+/+}$ cells. It has already been noted that there is an increased amount of spontaneous RAD51 foci in PARP$^{-/-}$ cells.

Co-treatment of PARP-1$^{+/+}$ and PARP$^{-/-}$ cells with CPT and ISQ significantly increases the amount of RAD51 foci formation in PARP-1$^{-/-}$ cells but not in PARP-1$^{+/+}$ cells. In the absence of PARP-1, there is an increase in CPT-induced DSBs, and a consequent increase in HR. When PARP-1 is inhibited by ISQ and treated with CPT, we seem to see the same effect. In PARP-1$^{-/-}$ cells, we already see an increase in CPT-induced DSBs, and an increase in HR. When PARP-1$^{-/-}$ cells are co-treated with ISQ, there is a further increase in spontaneous and CPT-induced HR. This may because of the possibility that ISQ may inhibit PARP-2 and PARP-3 as well. These two other PARPs are part of the PARP family but are less abundant in the cell. Their roles are still no well known, but they may offer some compensatory effect in cells where PARP-1 is inhibited. This may explain the further increase in HR.

5.2 The role of XRCC1 in CPT-induced damage

We have already showed that CPT has increased cytotoxicity in PARP-1$^{-/-}$ cells and that this is due to an increased amount of DSBs. We have also showed that RAD51 foci formation was increased in PARP-1$^{-/-}$ cells treated with CPT. This may indicate that HR is increased in these cells. It may also be that the high level of Rad51 foci is an indication of decreased HR repair in these cells. We see an increase in DSBs whether PARP-1 is absent or inhibited, so it is clear that it is the activity of the enzyme that is important for protection against CPT toxicity. In PARP-1$^{-/-}$ cells, there is no PARP-1 to bind to the SSBs and signal XRCC1 to the site of damage. Therefore, the inhibition of PARP-1 may decrease the repair of CPT-induced SSBs, which in turn leads to more SSBs collapsing at replication forks and more DSBs. An increase in collapsed forks would in turn lead to an increase in HR to repair the DSBs, which would explain the increase in RAD51 foci observed in PARP deficient or inhibited cells.

PARP-1 can bind the scaffold protein, XRCC1, and bring the SSB repair proteins to the site of the SSB. Here, we hypothesise that the role of XRCC1 in HR is linked to the affinity of XRCC1 to PARP-1 that has bound a SSB. XRCC1 can then bring other proteins to the site of the damage, and carry out repair. In the absence of PARP-1, XRCC1 cannot so easily relocate to the SSBs, and repair of CPT lesions is decreased. There is an increased cytotoxicity to CPT in XRCC1^{defective} cells. This is likely to be because even though PARP-1 can bind to the SSB and attract XRCC1 to the site of the damage, the XRCC1 in this cell line is defective, and cannot bring DNA ligase III and DNA polymerase β to the site of damage. Therefore, SSB repair will be slower, which

as in the case of PARP-1 inhibition, results in collapsed replication forks and an increase in toxicity. This hypothesis is supported by the increase in DSBs that we observe in EM9 cells.

Co-treatment of XRCC1^{wt} and XRCC1^{defective} cells with camptothecin and PARP-1 inhibitors increases the killing effect of camptothecin. In the XRCC1^{wt} cell line, if PARP-1 is inhibited, it may be binding to the site of the SSB, but cannot recruit XRCC1. In this case, SSB repair will be slower. In the XRCC1^{defective} cells, PARP-1 cannot recruit XRCC1, but there is no XRCC1 to recruit. Thus, one would not expect any further effect of inhibition of PARP-1 in these cells. The fact, there is a further synergistic effect suggests that either PARP-1 or XRCC1 has some other role in the cell that causes increased sensitivity to CPT when it is removed. We know that PARP-1 has many roles within the cell besides its role in SSB repair. It may be that there are two pathways for repair of SSBs; one involving XRCC1 and PARP-1, and the other involving PARP-1. In the absence of XRCC1, the other PARP-1 pathway can repair the SSB, perhaps by recruiting the SSB proteins itself. In the absence of PARP-1, XRCC1 can still recruit the SSB repair proteins to the site of the SSB, however more slowly. However, in the absence of both proteins, SSB repair cannot be carried out, or is carried out even more slowly. XRCC1^{defective} cells showed greater sensitivity to CPT when co-treated with ISQ, rather than NU1025. This is possibly explained by that NU1025 is an inhibitor specific for PARP-1, whereas ISQ inhibits PARP-2 and PARP-3 as well and removes any possible compensatory effects. There is an increased amount of DSB formation following CPT treatment in XRCC1^{defective} cells. This could be explained by the fact that the XRCC1^{wt} cell line has efficient SSB repair, and can repair methylated

adenine and guanine bases in the cell. It can also repair any SSBs stabilised by CPT. dT is not known to cause DSBs and does not form them in either cell line. In the XRCC1^{defective} cell line, SSB repair is slower because DNA ligase III and DNA polymerase β are not transported to the site of the SSB by XRCC1. The observation that CPT causes an increased amount of DSBs in the XRCC1^{defective} cells, could also be due to SSB repair being slower, leaving more unrepaired SSBs in the cell, which could potentially become DSBs.

Camptothecin-induced RAD51 foci formation is increased in XRCC1^{defective} cells. These results suggest that HR is spontaneously increased in XRCC1^{defective} cells, probably because of an increase in SSBs leading to DSB formation when encountered by the replication machinery, and that HR is the preferred mechanism for the repair of these DSB. HR is also shown to be increased in XRCC1^{wt} cells when treated with CPT. This suggests that HR is the major pathway for the repair of CPT-induced damage. Also, increased spontaneous levels of RAD51 foci in SSB repair defective cells, suggests that a SSB is an important endogenous lesion for HR. This is supported by that the spectrum of spontaneous recombinants is highly similar to the CPT-induced spectrum of recombinants, caused by SSBs (Saleh-Gohari et al., 2005). Camptothecin-induced RAD51 foci formation is significantly increased in XRCC1^{defective} cells, when co-treated with ISQ. This may be because in XRCC1^{wt} cells, there is an intact PARP-1 protein. When this is inhibited by ISQ, SSB repair still occurs, but at a slower rate, increasing the number of unrepaired SSBs. It could also be that the inhibited PARP-1 cannot destabilise the Top1-DNA-CPT complex, and remove Top1 from the DNA. PARP-1 also enhances religation of the DNA so that no SSB forms. If PARP-1 is inhibited, this

means that Tdp1 must remove Top1 from the DNA, leading to many SSBs. This increase in SSBs eventually results in an increase in DSBs, and hence an increase in HR to repair these.

Figure 5.2 Model of DSB formation in the presence and absence of PARP-1.

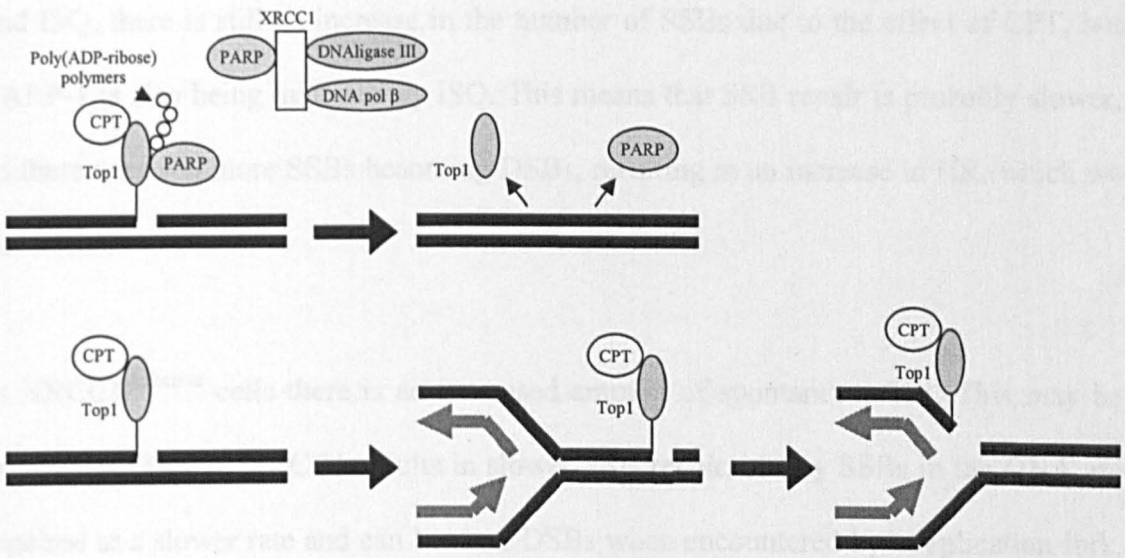

In the presence of CPT, Top1-DNA complexes are stabilised. When PARP-1 is present, it binds to Top1 and adds poly (ADP-ribose) polymers to it. This destabilises the Top1-DNA-CPT complex, removes Top1 and enhances DNA religation. Also, PARP-1 brings XRCC1 and the BER proteins to the site of the SSB. When PARP-1 is absent, the Top1-CPT complex is not destabilised or the Top1 protein is removed by Tdp1. Either way, this leaves a SSB to be repaired. When PARP-1 is not present, the BER repair proteins are not brought to the site of damage. On oncoming replication fork can then collide with the SSB to form a DSB.

When XRCC1^{wt} cells are treated with CPT, this drug stabilises the SSBs induced by Top1, so there are more of these in the cell. However, SSB repair is active in the cell and they can be repaired. It may be there are too many SSBs to repair them all before they are encountered by replication machinery and become DSBs. This may be why we see an increase in HR in this instance. When XRCC1^{wt} cells are co-treated with CPT and ISQ, there is still an increase in the number of SSBs due to the effect of CPT, but PARP-1 is also being inhibited by ISQ. This means that SSB repair is probably slower, so there are even more SSBs becoming DSBs, resulting in an increase in HR, which we have seen.

In XRCC1^{defective} cells there is an increased amount of spontaneous HR. This may be because the lack of XRCC1 results in slower SSB repair, so any SSBs in the DNA are repaired at a slower rate and can become DSBs when encountered by a replication fork. When XRCC1^{defective} cells are treated with ISQ, the amount cells with > 10 RAD51 foci (an indicator of HR) increases to 97.5%. This is a drastic increase in the amount of HR, and could be because when there is no XRCC1 and PARP-1 is inhibited, SSB repair becomes even slower, or does not occur at all. In this case, all of the SSBs in the cell would become DSBs and result in a dramatically increased amount of HR.

When XRCC1^{defective} cells are treated with CPT there is a similar level of HR to when they are treated with ISQ alone, 95% of cells contain > 10 RAD51 foci. This is the same as we observed previously, and is probably due to the increased amount of SSBs in the cell, caused by CPT, and SSB repair being slower due the lack of XRCC1. When XRCC1^{defective} cells are co-treated with CPT and ISQ, 100% of cells contain > 10

RAD51 foci. This further increase in HR when treated with CPT is probably a synergistic effect. There are more cells containing RAD51 foci in the XRCC1^{defective} cell line then would be expected from adding the effect of CPT in XRCC1^{wt} cells to the background level of RAD51 foci seen in the XRCC1^{defective} cells.

This is probably because SSB repair is very slow, or does not happen at all when both XRCC1 and PARP-1 are not active in the cell. At the same time, CPT is causing lots of SSBs, which are not being repaired by SSB repair. This leads to SSBs becoming DSBs in the cell, and an increase in HR to repair them. If there are lots of SSBs due to the action of CPT, and no SSB repair this would increase the number repair of DSBs and would explain the dramatic increase in the amount of HR, as indicated by the increased number of cells containing > 10 RAD51 foci.

5.3 The role of the XRCC1 BRCT motifs in CPT-induced damage

The XRCC1 protein has been implicated to be involved in a DNA ligase III dependent and independent SSB repair (Taylor, 2002). The DNA ligase III dependent SSB repair appears to be active throughout the cell cycle and involves the BRCT II motif of the XRCC1 protein, whilst DNA ligase III independent XRCC1 repair appears to be active at replication forks and involves the BRCT I motif of the XRCC1 protein. Here, we wanted to test which repair pathway was implicated in the repair of CPT-induced DNA damage. To do this we used XRCC1 mutant cell lines that had one or both of the BRCT motifs removed.

Expression of a mutated BRCT I motif increases sensitivity to camptothecin in XRCC1^{defective} cells. When the XRCC1^{defective} cell line was complemented with an empty vector, it had no effect on the sensitivity of the cell line to CPT. However, when the same cell line was complemented with the full XRCC1 protein, sensitivity was reverted back to the same levels as the wildtype cell line. Therefore it seems like complementing the XRCC1^{defective} cell line with full XRCC1 reverses the increased sensitivity seen in the deficient cell lines. Both of the XRCC1^{defective} cell lines complemented with short XRCC1 had the same level of sensitivity to CPT as the deficient cell line. Therefore it seems that it is the lack of DNA ligase III at the site of the SSB that slows SSB repair. Short XRCC1 still carries DNA polymerase β to the site of the SSB, so it is not likely that this protein is the rate limiting step. The XRCC1^{defective} cell line complemented with XHα3 or XHβ3 showed highest sensitivity to CPT.

It is likely that the disruption of the BRCT I domain in XRCC1 has some effect on PARP-1, although the nature of this effect is unknown. It could be that the BRCT I motif binds PARP-1 as normal, but then PARP-1 cannot break away from XRCC1, inhibiting its activities. In this scenario, PARP-1 would be unable to bind to further SSBs and attract SSB repair proteins to the site of the damage. It would be as if PARP-1 were inhibited.

Spontaneous and CPT-induced RAD51 foci formation is increased in both XH-α3 and XHβ3 cell lines, compared to XRCC1^{defective} cells. This could be because PARP-1 is inhibited by the disrupted BRCT I motif, causing SSB repair to be slower. This in turn, would lead to more SSBs in the cells, which could encounter the replication machinery

to become DSBs. Therefore, there would be more DSBs in the cell to be repaired. HR appears to be the major repair pathway for these single-ended DSBs, so we see an increase in cells containing RAD51 foci, indicating a rise in HR repair.

XRCC1^{defective} cells, complemented with XRCC1 that is missing the BRCT I motif, have increased sensitivity to camptothecin when co-treated with 1,5-dihydroisoquinoline, but not when co-treated with NU1025. This could be because of the different potencies of these two inhibitors.

5.4 The role of PARP-1 in CPT-induced HR

The Chinese hamster cell line, SPD8, was transfected with the SCneo vector (S8SN.11), in order to measure the amount of HR taking place within the cell. S8SN.11 cells show increased homologous recombination when treated with camptothecin. This indicates that CPT is a strong inducer of HR, probably through its stabilisation of Top1-induced SSBs, which then can become DSBs. This can then trigger HR repair.

SPD8 contains a partial duplication of the *hprt* gene, which creates a non-functional HPRT protein. A functional HPRT gene can be reverted to via HR, and this can also be used to measure the amount of HR occurring in the cell. SPD8 undergoes a large amount of HR after treatment with CPT, but has decreased homologous recombination when co-treated with camptothecin and PARP-1 inhibitor, ISQ. This contradicts the RAD51 foci data, which indicated that the amount of HR was increased in cells after treatment with CPT, and when co-treated with CPT and ISQ.

One possible explanation could be that the RAD51 foci do form, but that HR does not get past this stage. An alternative explanation could be the HR events studied in SPD8 cells require a recombination tract longer than 5 kb and that the CPT-induced recombination in PARP-1 inhibited cells trigger short tract recombination. Previously, it was found that overexpression of RAD51 results in an increase in RA51 foci, but a decrease in thymidine, etoposide or hydroxyurea-induced recombination (Lundin, 2003 JMB) which was explained by that recombination induced at replication forks is likely to involve short recombination tracts and will not be detected in the HR assay in the SPD8 cells. This could indicate that another recombination event is triggered in presence of an inhibitor of PARP.

An alternative explanation could be that ISQ treatment may arrest cells in the G2 phase of the cell cycle (Schultz, Bryant and Helleday, personal communication), which would result in fewer cells reaching the S phase of the cell cycle; the phase HR normally occurs (Saleh Gohari *et al.,* 2004).

5.5 The role of XRCC1 in CPT-induced HR

The XRCC1 defective EM9 cell line was transfected with the SCneo vector, and several clones were made (EM9SN.2, EM9SN.7, EM9SN.11, EM9SN.12 and EM9SN.13), in order to measure the amount of HR taking place within the cell. The transfected cell lines were treated with Sce-I endonuclease to test if they were capable of undergoing HR. They all show HR when DSBs are induced using Sce-I endonuclease. This endonuclease creates a double-ended DSB in the DNA Therefore, on encountering a

double-ended DSB in the DNA, XRCC1 defective cells are capable of repairing them via HR.

XRCC1^{defective} cells are hypersensitive to treatment with CPT or MNNG. This is probably because both of these compounds create SSBs in the DNA, and SSB repair appears to be slow in these cells. However, XRCC1^{defective} cells do not undergo HR when treated with CPT. These results on HR contrast the results on RAD51 foci formation. This could be explained either by RAD51 foci form but cannot complete HR or the HR event occurring following CPT treatment in EM9 cells involves very short recombination tracts not detectable in the HR assay.

XRCC1^{defective} cells do not undergo spontaneous homologous recombination. This indicates that it is not just the response to CPT that cannot be repaired by HR in these cells, but also any spontaneous SSBs arising in the cell. CPT-induced and spontaneous SSBs cause a similar lesion in the DNA; that is during replication, the SSB causes the replication fork to collapse. This is mainly repaired through sister chromatid exchange (SCE) (Saleh-Gohari *et al.*, 2005). Different DSBs are repaired through different kinds of HR, short tract gene conversion (STGE), long tract gene conversion (LTGC) or SCE. Double-ended DSBs, the type caused by Sce-I, is mostly repaired through STGC. In order for spontaneous and CPT-induced SSBs to collapse replication forks, the SSB must collide with DNA polymerase during replication. Since this takes place during the S-phase of the cell-cycle, it may be that these cells are arrested in S-phase and cannot undergo HR, because they cannot move through this phase of the cell cycle. Again, it is highly interesting to find lower HR events in XRCC1^{defective} cells. This is in line with

decreased CPT-induced HR in PARP defective cells and could be explained by the inability of the recombination reporter to pick up the recombination events occurring in the cells, as discussed earlier. However, it is also possible that both PARP-1 and XRCC1 plays a separate unique role in homologous recombination, maybe in a more downstream event following RAD51 foci formation. It is possible that the short-patch BER pathway is involved in recombination. Further support for such suggestion is that DNA polymerase β overexpressing cells show a general increase in homologous recombination levels and RAD51 foci formation (Cazaux, 2004).

5.6 Future perspectives

In the future, I would like to know if the disrupted BRCT I domain of XH-α3 and XH-β3 binds PARP-1, and if the level of PARP-1 activity changes in these cell lines. I would like to see the spontaneous levels of PARP-1 activity in both cell lines, and the activity after CPT treatment. I would also like to see if PARP-1 is capable of automodification, or the modification of other proteins via poly(ADP-ribosyl)ation. Both XH-α3 and XH-β3 cells are sensitive to CPT, which collapses replication forks. It would also be interesting to find out if XH-α3 and XH-β3 are sensitive to agents that stall replication forks, such as thymidine, or agents that inhibit replication fork progression, such as hydroxyurea. In cell lines lacking PARP-1, or where PARP-1 was inhibited, we have seen increased sensitivity to CPT, and an increase in DSBs. Therefore another future plan would be to find out if there is an increased amount of DSBs in the XH-α3 and XH-β3 cell lines. Also, it would be interesting to see if they

have also got an increased amount of RAD51 foci, or if like the XRCC1 defective cells, they do not seem to undergo HR.

5.7 Clinical applications

CPT is a very toxic chemotherapy drug, whose use was discontinued in the 1970s due to the severity of the side effects. Since then several less toxic analogues, such as irinotecan and topotecan, have been created and are in clinical use today. However, these drugs still have some strong side effects in some patients. For example, irinotecan can cause nausea, vomiting and diarrhoea, and in some cases has also caused colonic ulceration with gastro-intestinal bleeding. Also irinotecan commonly causes neutropenia (abnormally low number of neutrophils), leukopenia (abnormally low number of white blood cells), anaemia, asthenia (feeling of weakness), fever, abdominal pain and alopecia. Side effects to topotecan seem less severe, but still include nausea, loss of appetite, alopecia, asthenia and diarrhoea. PARP-1 inhibitors potentiate the cytotoxicity of several CPT-derivatives, including irinotecan and topotecan. This means that when PARP-1 inhibitors are applied clinically in conjunction with these drugs, the dose of the CPT-derived drugs may be lower, and will reduce the side-effects. Also, in understanding better, how the PARP-inhibitors are working in the cell, it may be possible to develop drugs against new targets within the cell that potentiate these drugs even further and improve their ability to kill cancer cells.

CHAPTER 6: REFERENCES

REFERENCES

Agrawal, A. & Schatz, D.G. (1997) RAG1 and RAG2 form a stable postcleavage synaptic complex with DNA containing signal ends in V(D)J recombination. *Cell*, 89 (1), 43-53.

Ame, J.C., Schreiber, V., Fraulob, V., Dolle, P., de Murcia, G. and Niedergang, C.P. (2001) A bidirectional promoter connects the poly(ADP-ribose) polymerase 2 (PARP-2) gene to the gene for RNase P RNA structure and expression of the mouse PARP-2 gene. *J Biol Chem.*, 276 (14), 11092-9.

Arnaudeau, C., Lundin, C. & Helleday, T. (2001). DNA double-strand breaks associated with replication forks are predominantly repaired by homologous recombination involving an exchange mechanism in mammalian cells. *J Mol Biol*, 307, 1235-45.

Avemann, K., Knippers, R., Koller, T. and Sogo, J.M. (1988) Camptothecin, a specific inhibitor of type I DNA topoisomerase, induces DNA breakage at replication forks. *Mol Cell Biol.*, 8 (8), 3026-34.

Banasik, M., Komura, H., Shimoyama, M. and Ueda, K. (1992) Specific inhibitors of PARP synthetase and mono(ADP-ribosyl) transferase. *J Biol Chem.*, 267 (3), 1569-1575.

Barrows, L.R., Holden, J.A., Anderson, M. and D'Arpa, P. (1998) The CHO XRCC1 mutant, EM9, deficient in DNA ligase III activity, exhibits hypersensitivity to camptothecin-independent of DNA replication. *Mutat Res.*, 408 (2), 103-10.

Bennett S.E., Umar, A., Oshima, J., Monnat, R.J. Jr, and Kunkel, T.A. (1997) Mismatch repair in extracts of Werner syndrome cell lines. *Cancer Res,* 57 (14), 2956-60.

Biedler, D.R. and Cheng, Y.C. (1995) Camptothecin induction of a time- and concentration-dependent decrease of topoisomerase I and its implication in camptothecin activity. *Mol Pharmacol,.* 47(5), 907-14.

Bjursell, G. & Reichard, P. (1973) Effects of thymidine on deoxyribonucleic triphosphate pools and deoxyribonucleic acid synthesis in Chinese hamster ovary cells. *J. Biol. Chem*, 248, 3904-3909.

Blount,S., Griffiths, H.R. and Lunec, J. (1989) Reactive oxygen species induce antigenic changes in DNA. *FEBS Lett*ers, 245 (1-2), 100-4.

Boulton, S. and Pemberton L. C. (1995). Potentiation of temozolomide-induced cytotoxicity: a comparative study of the biological effects of poly(ADP-ribose) polymerase inhibitors. *Br J Cancer,* 72 (4), 849-56

Bowman, K. J. and White, A. (1998). Potentiation of anti-cancer agent cytotoxicity by the potent poly(ADP-ribose) polymerase inhibitors NU1025 and NU1064. *Br J Cancer,* 78 (10), 1269-77.

Bowman, K.J., Newell, D.R., Calvert, A.H. & Curtin, N.J. (2001). Differential effects of the poly (ADP-ribose) polymerase (PARP) inhibitor NU1025 on topoisomerase I and II inhibitor cytotoxicity in L1210 cells in vitro. *Br J Cancer*, 84, 106-12.

Cadet, J. (1994) DNA damage caused by oxidation, deamination, ultraviolet radiation and photoexcited psoralens *IARC Sci Publ*, 125, 245-76

Calabrese, C., and Almassy, R.R.. (2004). Anticancer chemosensitization and radiosensitisation by the novel poly(ADP-ribose) polymerase-1 inhibitor AG14361. *J Natl Cancer Ins t,* 96 (1), 56-67.

Caldecott, K.W., Tucker, J.D. and Thompson, L.H. (1992) Construction of human XRCC1 minigenes that fully correct the CHO DNA repair mutant EM9. *Nucleic Acids Res.,* 20 (17), 4575-9.

Caldecott, K.W., McKeown, C.K., Tucker, J.D., Ljungquist, S. and Thompson, L.H.(1994) An interaction between the mammalian DNA repair protein XRCC1 and DNA ligase III. . *Mol Cell Biol.*, 14(1), 68-76.

Caldecott, K. W. (2003). DNA single-strand break repair and spinocerebellar ataxia. *Cell*, 112 (1), 7-10

Carrano A.V. & Wolff S. (1986) Distribution of sister chromatid exchanges in the euchromatin and heterochromatin of the Indian muntjac. *Chromosoma,* 1975 53 (4), 361-9.

Chadwick, K.H. & Leenhouts, H.P. (1978). The rejoining of DNA double-strand breaks and a model for the formation of chromosomal rearrangements. *Int J Radiat Biol Relat Stud Phys Chem Med*, 33, 517-29.

Chance, B., Sies, H. and Boveris, A. (1979) Hydroperoxide metabolism in mammalian organs. *Physiol Rev.*, 59 (3), 527-605.

Chang, W., Dynek J.N. and Smith S. (2005) NuMA is a major acceptor of poly(ADP-ribosyl)ation by tankyrase 1 in mitosis. *Biochem J.* 391(2), 177-84.

Ciccia, A, Constantinou, A. and West, S.C. (2003) Identification and characterization of the human mus81-eme1 endonuclease. *J Biol Chem.*, 278 (27),25172-8.

Clopton, D.A. and Saltman, P. (1995) Low-level oxidative stress causes cell-cycle specific arrest in cultured cells. *Biochem Biophys Res Commun,* 210 (1), 189-96.

Colleaux L., d'Auriol,L., Gailbert,F. and Dujon,B. (1988) Recognition and cleavage site of the intron-encoded omega transposase. *Proc. Natl Acad. Sci. USA*, 85, 6022–6026.

Cox, M.M. (1999) Recombinational DNA repair in bacteria and the RecA protein. *Prog Nucleic Acid Res Mol Biol.,* 63, 311-66.

Cox, M.M., Goodman, M.F., Kreuzer, K.N., Sherratt, D.J., Sandler, S.J. and Marians KJ. (2000) The importance of repairing stalled replication forks. *Nature*, 404 (6773), 37-41.

Cox, M.M. (2001) Recombinational DNA repair of damaged replication forks in Escherichia coli: questions. *Annu Rev Genet.,* 35, 53-82.

Curtin, N. J., and Wang, L.Z. (2004). Novel poly(ADP-ribose) polymerase-1 inhibitor, AG14361, restores sensitivity to temozolomide in mismatch repair-deficient cells. *Clin Cancer Res,* 10 (3), 881-9

d'Adda di Fagagna, F., Hande, M.P., Tong ,W.M., Lansdorp, P.M., Wang, Z.Q. and Jackson, S.P. (1999) Functions of poly(ADP-ribose) polymerase in controlling telomere length and chromosomal stability. *Nat Genet.,* 23 (1), 76-80.

D'Amours, D. & Desnoyers, S. (1999). Poly(ADP-ribosyl)ation reactions in the regulation of nuclear functions. *Biochem J.,* 342 (2), 249-68

D'Amours, D. & Jackson, S.P. (2002) The Mre11 complex: at the crossroads of DNA repair and checkpoint signalling. *Nat Rev Mol Cell Biol.*, 3 (5), 317-27.

Dantzer, F., and V. Schreiber (1999).Involvement of poly(ADP-ribose) polymerase in base excision repair *Biochimie,* 81 (1-2), 69-75.

de Bont, R. & van Larebeke, N. (2004). Endogenous DNA damage in humans: a review of quantitative data. *Mutagenesis*, 19, 169-85.

de Murcia, J.M., Niedergang, C., Trucco, C., Ricoul, M., Dutrillaux, B., Mark, M., Oliver, F.J., Masson, M., Dierich, A., LeMeur, M., Walztinger, C., Chambon, P. & de Murcia, G. (1997). Requirement of poly(ADP-ribose) polymerase in recovery from DNA damage in mice and in cells. *Proc Natl Acad Sci U S A*, 94, 7303-7.

Dianov, G.L., Sleeth, K.M., Dianova, I.I. and Allinson, S.L. (2003) Repair of abasic sites in DNA. *Mutat Res.*, 531 (1-2), 157-63.

Dizdaroglu, M. (2003) Substrate specificities and excision kinetics of DNA glycosylases involved in base-excision repair of oxidative DNA damage. *Mutat Res.,* 531 (1-2), 109-26.

Duckett, D.R., Drummond, J.T., Murchie, A.I., Reardon, J.T., Sancar, A., Lilley, D.M.and Modrich, P. (1996) Human MutSalpha recognizes damaged DNA base pairs containing O6-methylguanine, O4-methylthymine, or the cisplatin-d(GpG) adduct. *PNAS,* 93 (13), 6443-7.

Dynek, J.N. and Smith, S. (2004) Resolution of sister telomere association is required for progression through mitosis. *Science*, 304 (5667), 97-100.

Eckert, K.A. & Opresko, P.L. (1999). DNA polymerase mutagenic bypass and proofreading of endogenous DNA lesions. *Mutat Res*, 424, 221-36.

Frank-Vaillant, M. and Marcand, S.(2002) Transient stability of DNA ends allows nonhomologous end joining to precede homologous recombination. *Mol Cell*, 10 (5), 1189-99.

Friedberg, E.C., Walker, G.C. and Siede, W. (1995) DNA repair and mutagenesis. Washington DC: American Society of Microbiology Press.

Game, J.C. & Mortimer, R.K. (1974) A genetic study of x-ray sensitive mutants in yeast. *Mutat Res.*, 24 (3), 281-92.

Goldmacher, V.S., Cuzick, R.A. Jr. and Thilly, W.G. (1986) Isolation and partial characterization of human cell mutants differing in sensitivity to killing and mutation by methylnitrosourea and N-methyl-N'-nitro-N-nitrosoguanidine.*J Biol Chem.*, 261 (27), 12462-71.

Griffin, S., Branch, P., Xu, Y.Z. and Karran, P. (1994) DNA mismatch binding and incision at modified guanine bases by extracts of mammalian cells: implications for tolerance to DNA methylation damage. *Biochemistry,* 33 (16), 4787-93.

Haber, J.E. (1999) DNA recombination: the replication connection. *TIBS,* 24 (7), 271-5.

Hanakahi, L.A. & West S.C. (2002) Specific interaction of IP6 with human Ku70/80, the DNA-binding subunit of DNA-PK. *EMBO J*, 21 (8), 2038-44.

Hanawalt, P.C. (1966) The U.V. sensitivity of bacteria: its relation to the DNA replication cycle. *Photochem Photobiol.*, 5 (1), 1-12.

Helleday, T., Arnaudeau, C., and Jenssen, D. (1998) A partial *hprt* gene duplication generated by non-homologous recombination in V79 Chinese hamster cells is eliminated by homologous recombination. *J. Mol Biol.*, 279(4) 689-694.

Helleday, T. (2003) Pathways for mitotic homologous recombination in mammalian cells. *Mutat Res.*, 532 (1-2), 103-15.

Herceg, Z. and Wang, Z.Q. (2001) Functions of poly(ADP-ribose) polymerase (PARP) in DNA repair, genomic integrity and cell death. *Mutat Res.*, 477 (1-2), 97-110.

Hoeijmakers, J.H. (2001) Genome maintenance mechanisms for preventing cancer. *Nature*, 411 (6835), 366-74.

Holliday, R. (1964) The induction of mitotic recombination by mitomycin C in ustilago and saccharomyces. *Genetics,* 50, 323-35.

Holliday, R. & Ho, T. (1998). Gene silencing and endogenous DNA methylation in mammalian cells. *Mutat Res*, 400, 361-8.

Hsiang, Y.-H., Hertzberg, R., Hecht, S. & Lui, L.F. (1985). Camptothecin induces protein-linked DNA breaks via mammalian DNA topoisomerase I. *J.Biol. Chem*, 260, 14873-14878.

Huang, L.C., Clarkin, K.C. and Wahl, G.M. (1996) p53-dependent cell cycle arrests are preserved in DNA-activated protein kinase-deficient mouse fibroblasts. *Cancer Res.*, 56 (13), 2940-4.

Jackson, A.L. & Loeb, L.A. (2001). The contribution of endogenous sources of DNA damage to the multiple mutations in cancer. *Mutat Res*, 477, 7-21.

Johansson, M. (1999) A human poly(ADP-ribose) polymerase gene family (ADPRTL): cDNA cloning of two novel poly(ADP-ribose) polymerase homologues. *Genomics*, 57 (3), 442-5.

Kadyk, L.C. and Hartwell, L.H. (1992) Sister chromatids are preferred over homologues as substrates for recombinational repair in Saccharomyces cerevisiae. *Genetics,* 132 (2), 387-402.

Kanaar, R., Hoeijmakers, J.H. and van Gent, D.C. (1998) Molecular mechanisms of DNA double strand break repair. *Trends Cell Biol.,* 8 (12), 483-9.
Karran, P., Bignami, M. (1992) Self-destruction and tolerance in resistance of mammalian cells to alkylation damage. *Nucleic Acids Res.*, 20 (12), 2933-40.

Karran, P. & Lindahl, T. (1980). Hypoxanthine in deoxyribonucleic acid: generation by heat-induced hydrolysis of adenine residues and release in free form by a deoxyribonucleic acid glycosylase from calf thymus. *Biochemistry*, 19, 6005-11.

Khanna K.K. & Jackson S.P.(2001) DNA double-strand breaks: signalling, repair and the cancer connection. *Nat Genet.* 27 (3), 247-54.

Kogoma, T. (1996) Recombination by replication. *Cell,* 85 (5), 625-7.
Kuerbitz, S. J., Plunkett, B. S., Walsh, W. V. and Kastan, M. B. (1992) Wild-type p53 is a cell cycle checkpoint determinant following irradiation. PNAS, 89 (16), 7491-5.

Kraus,E, Leung, W.Y. and Haber, J.E. (2001) Break-induced replication: a review and an example in budding yeast. *PNAS*, 98 (15), 8255-62.

Kubota, Y., Nash, R.A., Klungland, A., Schar, P., Barnes, D.E. and Lindahl, T. (1996) Reconstitution of DNA base excision-repair with purified human proteins: interaction between DNA polymerase beta and the XRCC1 protein. *EMBO J.,* 15 (23), 6662-70.

LaFond, R.E. (1988) Cancer: the outlaw cell (2nd Ed.) Washington, DC: American Chemical Society.

Lehmann, A.R. (2000) Replication of UV-damaged DNA: new insights into links between DNA polymerases, mutagenesis and human disease. *Gene*, 253 (1), 1-12.

Lieber, M.R., Hesse, J.E., Lewis, S., Bosma, G.C., Rosenberg, N., Mizuuchi, K., Bosma, M.J. and Gellert, M. (1988) The defect in murine severe combined immune deficiency: joining of signal sequences but not coding segments in V(D)J recombination. *Cell,* 55 (1), 7-16.

Liehr, J.G. (2000). Role of DNA adducts in hormonal carcinogenesis. *Regul Toxicol Pharmacol*, 32, 276-82.

Lin, F.L., Sperle, K. and Sternberg, N. (1990) Repair of double-stranded DNA breaks by homologous DNA fragments during transfer of DNA into mouse L cells. *Mol Cell Biol.*, 10 (1), 113-9.

Lindahl, T., Karran, P., Demple, B., Sedgwick, B. and Harris, A. (1982) Inducible DNA repair enzymes involved in the adaptive response to alkylating agents. *Biochimie,* 64 (8-9), 581-3.

Lindahl, T. & Barnes, D.E. (1992). Mammalian DNA ligases. *Annu Rev Biochem*, 61, 251-81.

Lindahl, T. (1993). Instability and decay of the primary structure of DNA. *Nature*, 362, 709-15.

Lindahl, T., Satoh, M.S., Poirier, G.G. & Klungland, A. (1995). Post-translational modification of poly(ADP-ribose) polymerase induced by DNA strand breaks. *Trends Biochem Sci*, 20, 405-11.

Lundin, C., Erixon, K., Arnaudeau, C., Schultz, N., Jenssen, D., Meuth, M. and Helleday, T. (2002) Different roles for non-homologous end joining and homologous recombination following replication arrest in mammalian cells. *Mol Cell Biol*, 22 (16), 5869-5878.

Lundin, C., Schultz, N., Arnaudeau, C., Mohindra, A., Hansen, L.T. and Helleday, T. (2003) RAD51 is involved in repair of damage associated with DNA replication in mammalian cells. *J Mol Biol.,* 328 (3), 521-35.

Malanga, M. and Althaus, F.R. (2004) Poly(ADP-ribose) reactivates stalled DNA topoisomerase I and Induces DNA strand break resealing. *J Biol Chem.*, 279(7) 5244-8.

Marians, K.J. (2000) Replication and recombination intersect. *Curr Opin Genet Dev.*, 10 (2), 151-6.

Marintchev, A., Mullen, A.M., Maciejewski, M.W., Pan, B., Gryk, M.R., and Mullen G.P. (1999) *Nature Struct. Biol.*, 14, 68-76.

Marintchev, A., Robertson, A., Dimitriadis, E.K., Prasad, R., Wilson, S.H., and Mullen, G.P. (2000) Domain specific interaction in the XRCC1-DNA polymeraseβ complex. *Nucleic acid research*, 28 (10), 2049-2059.

Martin, D. S. & Schwartz, G. K. (1997) Chemotherapeutically induced DNA damage, ATP depletion, and the apoptotic biochemical cascade. *Oncol Res,* 9 (1), 1-5.

Maryon, E. and Carroll, D. (1991) Characterization of recombination intermediates from DNA injected into Xenopus laevis oocytes: evidence for a non-conservative mechanism of homologous recombination. *Mol Cell Biol.*, 11 (6), 3278-87.

Masson, M., Niedergang, C., Schreiber, V., Muller, S., Menissier-de Murcia, J. & de Murcia, G. (1998). XRCC1 is specifically associated with poly(ADP-ribose) polymerase and negatively regulates its activity following DNA damage. *Mol Cell Biol*, 18, 3563-71.

Masson, M., Rolli, V., Dantzer, F., Trucco, C., Schreiber, V., Fribourg, S., Molinete, M., Ruf, A., Miranda, E.A., Niedergang, C. & et al. (1995). Poly(ADP-ribose) polymerase: structure-function relationship. *Biochimie*, 77, 456-61.

McGlynn, P. & Lloyd, R.G. (2002) Replicating past lesions in DNA. *Mol Cell,* 10 (4), 700-1.

Meselson, M. and Weigle, J.J. (1961) Chromosome breakage accompanying genetic recombination in bacteriophage. *PNAS*, 47, 857-68.

Molinete, M., Vermeulen, W., Burkle, A., Menissier-de Murcia, J., Kupper, J.H., Hoeijmakers, J.H. & de Murcia, G. (1993). Overproduction of the poly(ADP-ribose) polymerase DNA-binding domain blocks alkylation-induced DNA repair synthesis in mammalian cells. *Embo J*, 12, 2109-17.

Morrison, C., Smith, G.C., Stingl, L., Jackson, S.P., Wagner, E.F. & Wang, Z.Q. (1997). Genetic interaction between PARP and DNA-PK in V(D)J recombination and tumorigenesis. *Nat Genet*, 17, 479-82.

Muiras, M.L. and Burkle, A. (2000) Defending genomic stability over life span: a proposed role for PARP-1. *Exp Gerontol.*, 35 (6-7), 703-9.

Neame, P.J., Young, C.N. & Treep, J.T. (1990). Isolation and primary structure of PARP, a 24-kDa proline- and arginine-rich protein from bovine cartilage closely related to the NH2-terminal domain in collagen alpha 1 (XI). *J Biol Chem*, 265, 20401-8.

O'Driscoll M. & Jeggo PA. (2002) Clinical impact of ATR checkpoint signalling failure in humans. *Cell Cycle,* 2 (3), 194-5.

Park, S.Y. and Cheng, Y.C. (2005) Poly(ADP-ribose) polymerase-1 could facilitate the religation of topoisomerase I-linked DNA inhibited by camptothecin. *Cancer Res.* 65(9) 3894-902.

Parsons, J.L., Dianova, I.I., Allinson, S.L. and Dianov, G.L. (2005) Poly(ADP-ribose) polymerase-1 protects excessive DNA strand breaks from deterioration during repair in human cell extracts. *FEBS J.* 272 (8) 2012-21.

Pierce, A.J., Hu, P., Han, M., Ellis, N. and Jasin, M. (2001).Ku DNA end-binding protein modulates homologous repair of double-strand breaks in mammalian cells. *Genes Dev.*, 15 (24), 3237-42.

Pommier, Y., Redon, C., Rao, V.A., Seiler, J.A., Sordet, O., Takemura, H., Antony, S., Meng, L., Liao, Z., Kohlhagen, G., Zhang, H. and Kohn, K.W. (2003) Repair of and checkpoint response to topoisomerase I-mediated DNA damage. *Mutat Res.*, 532 (1-2), 173-203.

Richardson, C., Moynahan, M.E. and Jasin, M. (1998) Double-strand break repair by interchromosomal recombination: suppression of chromosomal translocations. *Genes Dev.* 12 (24), 3831-42.

Roberts, M.J., Wondrak, G.T., Laurean, D.C., Jacobson, M.K. & Jacobson, E.L. (2003). DNA damage by carbonyl stress in human skin cells. *Mutat Res*, 522, 45-56.

Rothstein, R, Michel. B. and Gangloff, S. (2000) Replication fork pausing and recombination or "gimme a break". *Genes Dev.*, 14 (1), 1-10.

Ryan, A.J., Squires, S., Strutt, H.L. and Johnson, R.T. (1991) Camptothecin cytotoxicity in mammalian cells is associated with the induction of persistent double strand breaks in replicating DNA. *Nucleic Acids Res.*, 19 (12), 3295-300.
Saintigny, Y., Delacote, F., Vares, G., Petitot, F., Lambert, S., Averbeck, D. and Lopez, B.S. (2001) Characterization of homologous recombination induced by replication inhibition in mammalian cells. *EMBO J.*, 20 (14), 3861-70.

Saleh-Gohari ,N., Bryant, H.E., Schultz, N., Parker, K.M., Cassel, T.N. and Helleday, T. (2005) Spontaneous homologous recombination is induced by collapsed replication forks that are caused by endogenous DNA single-strand breaks. *Mol Cell Biol.*, 25 (16), 7158-69.

Sane, A.T. & Bertrand, R. (1999) Caspase activation in CPT-treated U-937 cells is coupled with a shift from apoptosis to transient G1 arrest followed by necrotic cell death. Cancer Res, 59, 3565-3569

Satoh, M.S. and Lindahl, T. (1994) Enzymatic repair of oxidative DNA damage. *Cancer Res.*, 54(7 Suppl), 1899-1901.

Sargent, R.G., Meservy, J.L., Perkins, B.D., Kilburn, A.E., Intody, Z., Adair, G.M., Nairn, R.S. and Wilson, J.H. (2000) Role of the nucleotide excision repair gene ERCC1 in formation of recombination-dependent rearrangements in mammalian cells. *Nucleic Acids Res.*, 28 (19), 3771-8.

Schmid, C.W. (1996) Alu: structure, origin, evolution, significance and function of one-tenth of human DNA. *Prog Nucleic Acid Res Mol Biol.*, 53, 283-319.

Schneider, E., Hsiang, Y.-H., & Lui, L.F. (1990) DNA topoisomerases as anti-cancer drug targets. *Adv. Pharmacol*, 21, 149-183

Schultz, N., Lopez, E., Saleh-Gohari, N. and Helleday, T. (2003) Poly(ADP-ribose) polymerase (PARP-1) has a controlling role in homologous recombination. *Nucleic Acids Res.*, 31(17), 4959-64.

Semionov, A., Cournoyer, D., and Chow, T.Y.-K. (1999) Inhibition of poly(ADP-ribose) polymerase stimulates extra-chromosomal homologous recombination in mouse-Ltk fibroblasts. *Nucleic Acid Res.*, 27(22), 4526-4531

Shall, S. and deMurcia, G. (2000) Poly(ADP-ribose) polymerase-1: what have we learned from the deficient mouse model? *Mutat Res.*, 460 (1), 1-15.

Shen, M.R., Zdzienicka, M.Z., Mohrenweiser, H., Thompson, L.H. and Thelen, M.P. (1998) Mutations in hamster single-strand break repair gene XRCC1 causing defective DNA repair. *Nucleic Acids Res.*, 26 (4), 1032-7.

Shao, R.-G., Cao, C.Z., Zhang H., Kohn, K.W., Wold, M.S., and Pommier ,S. (1999) Replication-mediated DNA damage by camptothecin induces phosphorylation of RPA by DNA-dependent protein kinase and dissociates RPA:DNA-PK complexes. *EMBO J.*, 18, 1397-1406.

Simbulan-Rosenthal, C.M., Haddad, B.R., Rosenthal, D.S., Weaver, Z., Coleman, A., Luo, R., Young, H.M., Wang, Z.Q., Ried, T. & Smulson, M.E. (1999). Chromosomal aberrations in PARP(-/-) mice: genome stabilization in immortalized cells by reintroduction of poly(ADP-ribose) polymerase cDNA. *Proc Natl Acad Sci U S A*, 96, 13191-6.

Smith, S. (2001) The world according to PARP. TIBS, 26 (3), 174-9.

Sonoda, E., Sasaki, M.S., Buerstedde, J.M., Bezzubova, O., Shinohara, A., Ogawa, H., Takata, M., Yamaguchi-Iwai, Y. and Takeda, S. (1998) Rad51-deficient vertebrate cells accumulate chromosomal breaks prior to cell death. *EMBO J.*, 17 (2), 598-608.

Strumberg, D., Pilon, A.A., Smith, M., Hickey, R., Malkas, L. and Pommier, Y. (2000) Conversion of topoisomerase I cleavage complexes on the leading strand of ribosomal DNA into 5'-phosphorylated DNA double-strand breaks by replication runoff. *Mol Cell Biol.*, 20 (11), 3977-87.

Szostak, J.W., Orr-Weaver, T.L., Rothstein, R.J. and Stahl, F.W. (1983) The double-strand-break repair model for recombination. *Cell.* 33 (1), 25-35.

Takata ,M., Sasaki, M.S., Sonoda, E., Morrison, C., Hashimotom M., Utsumi, H., Yamaguchi-Iwai, Y., Shinohara, A. and Takeda, S. (1998) Homologous recombination and non-homologous end-joining pathways of DNA double-strand break repair have overlapping roles in the maintenance of chromosomal integrity in vertebrate cells. *EMBO J.*, 17 (18), 5497-508.

Taylor, R.M., Wickstead, B., Cronin, S. and Caldecott, K.W. (1998) Role of a BRCT domain in the interaction of DNA ligase III-alpha with the DNA repair protein XRCC1. *Curr Biol.*, 8 (15), 877-80.

Taylor, R.M., Moore, D.J., Whitehouse, J., Johnson, P. and Caldecott, K.W. (2000) A cell cycle-specific requirement for the XRCC1 BRCT II domain during mammalian DNA strand break repair. *Mol Cell Biol.*, 20 (2), 735-40.

Taylor, R.M., Thistlethwaite, A. and Caldecott, K,W. (2002) Central role for the XRCC1 BRCT I domain in mammalian DNA single-strand break repair. *Mol Cell Biol.*, 22 (8), 2556-63.

Tebbs, R.S., Flannery, M.L., Meneses, J.J., Hartmann, A., Tucker, J.D.,Thompson, L.H., Cleaver, J.E. and Pedersen, R.A. (1999) Requirement for the Xrcc1 DNA base excision repair gene during early mouse development. *Dev Biol.*, 208 (2), 513-29.

Tentori, L, Orlando, L., Lacal, P.M., Benincasa, E., Faraoni, I., Bonmassar, E., D'Atri, S. and Graziani, G. (1997) Inhibition of O6-alkylguanine DNA-alkyltransferase or poly(ADP-ribose) polymerase increases susceptibility of leukemic cells to apoptosis induced by temozolomide. *Mol Pharmacol.*, 52 (2), 249-58.

Tentori, L., Lacal, P.M., Benincasa, E., Franco, D., Faraoni, I., Bonmassar, E. and Graziani, G. (1998) Role of wild-type p53 on the antineoplastic activity of temozolomide alone or combined with inhibitors of poly(ADP-ribose) polymerase. *J Pharmacol Exp Ther.*, 285 (2), 884-93.

Tentori, L., Portarena, I., Bonmassar, E. and Graziani, G. (2001) Combined effects of adenovirus-mediated wild-type p53 transduction, temozolomide and poly (ADP-ribose) polymerase inhibitor in mismatch repair deficient and non-proliferating tumour cells. *Cell Death Differ.*, 8 (5), 457-69.

Thelander, L. & Reichard, P. (1979) Reduction of ribonucleotides. *Annu Rev Biochem*, 48, 135-158.

Thompson, L.H., Brookman, K.W., Dillehay, L.E., Carrano, A.V., Mazrimas, J.A., Mooney, C.L. and Minkler, J.L. (1982) A CHO-cell strain having hypersensitivity to mutagens, a defect in DNA strand-break repair, and an extraordinary baseline frequency of sister-chromatid exchange. *Mutat Res.*, 95 (2-3), 427-40.

Thompson, L.H., Brookman, K.W., Jones, N.J., Allen, S.A. and Carrano, A.V.(1990) Molecular cloning of the human XRCC1 gene, which corrects defective DNA strand break repair and sister chromatid exchange. *Mol Cell Biol.*, 10 (12), 6160-71.

Thompson, L.H. (1991) Properties and applications of human DNA repair genes. *Mutat Res.*, 247 (2), 213-9.

Tornaletti, S. and. Pfeiffer, G. P (1996) UV damage and repair mechanisms in mammalian cells. *Bioessays,* 18, 221–228.

Trucco, C., Oliver F.J., de Murcia G., and Menissier-de Murcia J. (1998) DNA repair defect in poly(ADP-ribose) polymerase-deficient cell lines. *Nucleic Acids Res.,* 26 (11), 2644-9

Tsao, Y.P., Russo, A., Nyamuswa, G., Silber, R.and Liu, L.F. (1993) Interaction between replication forks and topoisomerase I-DNA cleavable complexes: studies in a cell-free SV40 DNA replication system. *Cancer Res.,* 53 (24), 5908-14.

Umar A., Buermeyer, A.B., Simon, J.A., Thomas, D.C., Clark, A.B., Liskay, R.M. and Kunkel, T.A.(1996) Requirement for PCNA in DNA mismatch repair at a step preceding DNA resynthesis. *Cell,* 87 (1), 65-73.

Vance, J.R. and Wilson, T.E. (2001) Repair of DNA strand breaks by the overlapping functions of lesion-specific and non-lesion-specific DNA 3' phosphatases. *Mol Cell Biol.* 21(21) 7191-8.

Van Dyck, E., Stasiak, A.Z., Stasiak, A. and West, S.C. (1997) Visualization of recombination intermediates produced by RAD52-mediated single-strand annealing. *EMBO Rep.*, 2 (10), 905-9.

van Gent, D.C, Hoeijmakers, J.H. and Kanaar, R. (2001) Chromosomal stability and the DNA double-stranded break connection. *Nat Rev Genet.*, 2 (3), 196-206.

Veuger, S.J., Curtin, N.J., Smith, G.C. and Durkacz, B.W. (2004) Effects of novel inhibitors of poly(ADP-ribose) polymerase-1 and the DNA-dependent protein kinase on enzyme activities and DNA repair. *Oncogene*, 23 (44), 7322-9.

Verschraegen, C. F, Jaeckle, K,, Giovanella, B., Knight, V. and Gilbert, B.E. (2000) Alternative administration of camptothecin analogues. *Ann N Y Acad Sci.*, 922, 237-46.

Vodenicharov, M.D., Sallmann, F.R., Satoh, M.S., and Poirier, G.G. (2000) Base excision repair is efficient in cells lacking poly(ADP-ribose) polymerase 1. *Nucleic Acids Res.,* 28 (20), 3887-96.

Wang, J.C. (2002). Cellular roles of DNA topoisomerases: A molecular perspective. *Nature Reviews Molecular cell biology*, 3, 430-440

Wang, Z.Q., Stingl, L., Morrison, C., Jantsch, M., Los, M., Schulze-Osthoff, K. & Wagner, E.F. (1997). PARP is important for genomic stability but dispensable in apoptosis. *Genes Dev*, 11, 2347-58.

Wedge, S.R. and Newlands, E.S. (1996) O6-benzylguanine enhances the sensitivity of a glioma xenograft with low O6-alkylguanine-DNA alkyltransferase activity to temozolomide and BCNU. *Br J Cancer.*, 73 (9), 1049-52.

Whitehouse, C.J., Taylor, R.M., Thistlethwaite, A., Zhang, H., Karimi-Busheri, F., Lasko, D.D., Weinfeld, M. and Caldecott, K.W. (2001) XRCC1 stimulates human polynucleotide kinase activity at damaged DNA termini and accelerates DNA single-strand break repair. *Cell,* 104 (1), 107-17.

Wiesel, J.M., Gamiel, H., Vlodavsky, I., Gay, I. and Ben-Bassat, H. (1983) Cell attachment, growth characteristics and surface morphology of human upper-respiratory tract epithelium cultured on extracellular matrix. *Eur J Clin Invest*, 13 (1), 57-63

Yager, J.D. & Liehr, J.G. (1996). Molecular mechanisms of estrogen carcinogenesis. *Annu Rev Pharmacol Toxicol*, 36, 203-32.
Yamada, A., Masutani, C., Iwai, S. and Hanaoka, F. (2000) Complementation of defective translesion synthesis and UV light sensitivity in xeroderma pigmentosum variant cells by human and mouse DNA polymerase eta. *Nucleic Acids Res*, 28 (13):2473-80.

Yang, Y.G., Cortes, U., Patnaik, S., Jasin, M. and Wang, Z.Q. (2004) Ablation of PARP-1 does not interfere with the repair of DNA double-strand breaks, but compromises the reactivation of stalled replication forks. *Oncogene,* 23 (21), 3872-82.

Yung, T.M., Sato, S. and Satoh, M.S. (2004) Poly(ADP-ribosyl)ation as a DNA damage-induced post-translational modification regulating poly(ADP-ribose) polymerase-1-topoisomerase I interaction. *J Biol Chem.*, 279(38) 39686-96.

Zhou, B.B. & Elledge, S.J. (2000) The DNA damage response: putting checkpoints in perspective. *Nature,* 408 (6811), 433-9.

CHAPTER 7: APPENDICES

APPENDIX 1: Addresses of companies

3M
3M United Kingdom PLC, 3M Centre, Cain Road, Bracknell, RG12 8HT, UK
Tel: 08705 360036 Web: www.3m.com

Adams Healthcare
Lotherton Way, Garforth, Leeds, West Yorkshire, United Kingdom, LS25 2JY, UK
Tel: (0113) 2320066 Fax: (0113) 2871317 Web: www.adams-healthcare.co.uk

Amersham Biosciences
Amersham Biosciences UK Limited, Amersham Place, Little Chalfont, Buckinghamshire HP7 9NA
Tel: 0870 606 1921 Fax: 01494 544350 Web: www.amershambiosciences.com

Amity U.K. Limited
Amity UK Ltd, Friendship House, Dodworth Business Park
Barnsley, South Yorkshire, S75 3SP
Tel: (01226) 770787 Fax: (01226) 770757 Email: sales@amityinternational.com
Web: wwwamityinternational.com

Apple
Apple (UK), 2 Furzeground Way, Stockley Park East, Uxbridge, Middlesex, UB11 1BB, UK
Tel: 0800 039 1010 Web: www.apple.com/uk

Azlon
RealLabware, Unit 33, Moor Park Industrial Centre, Tolpits Lane, Watford Herts, WD1 8SP, UK
Tel: (019230 249492 Fax: (01923) 249751 Email: info@reallabware.com
Web: reallabware.com

BDH
Merck House, Poole, Dorset, BH15 1TD, England
Tel: +44 1202 660444 Fax: +44 1202 666856 Email: pat.simmons@uk.vwr.com.
Web: www.bdh.com

BD UK Ltd
Medical Pharmaceutical Systems, 21 Between Towns Road, Cowley, Oxford OX4 3LY, UK
Tel: (01865) 781555 Fax: (01865) 781596 Email: bdpharma@eurpe.bd.com
Web: www.bdpharma.com

Becton Dickenson Immunocytometry Systems
2350 Qume Drive, San Jose, CA 95131, USA
Tel: 408-223-8226

Bibby Sterilin
Bibby Sterilin Ltd. Tilling Drive Stone, Staffordshire, United Kingdom. ST15 0SA, UK
Tel: (01785) 812121 Fax: (01785) 815066 bsl@bibby-sterilin.com
Web: www.bibby-sterilin.co.uk

BioRad
Bio-Rad Laboratories Ltd, Bio-Rad House, Maylands Avenue, Hemel Hempstead, Hertfordshire HP2 7TD, United Kingdom
Tel: 020 8328 2000 Fax: 020 8328 2550 E-mail: uk.lsg.marketing@bio-rad.com
Web: www.bio-rad.com

BOC gases
The Priestly Centre, 10 Priestly Road, Surrey Research Park, Guildford, Surry, GU2 7XY, UK
Tel: (01483) 579857 Web: www.boc.com

Bodyguards
Medisavers, Harrier Park, Southgate Way, Orton Southgate, Peterborough, Cambs, PE2 6YQ, UK
Tel: (01733) 361414 Fax: (01733) 361121 Email: sales@medisavers.co.uk
Web: www.medisavers.co.uk

Cambrex
Cambrex Bio Science Wokingham, Ltd., 1 Ashville Way, Wokingham, Berkshire, RG41 2PL, England
Tel: 0118 979 5234 Fax: 0118 979 5231 Email: sales.uk@cambrex.com
Web: www.cambrex.com

Caterwrap
Chef's Trolley Ltd, Hillcroft Business Park, Whisby Road, Lincoln LN6 3QT
Tel: (01522) 888188 Fax: (01522) 888190 Email: enquiries@chefs-trolley.co.uk
Web: www.chefs-trolley.co.uk

Chemlab
Chemlab Scientific Products Ltd, Construction House, Grenfall Avenue, Hornchurch, Essex, RM12 4EH, United Kingdom
Tel: (01708) 476162

Continental Lab Products
CLP, 4 Carousel Way, Riverside Business Park East, Northampton NN3 9VV, UK
Tel: (01604) 417900 Fax: (01604) 417909 Email: mail@clpdirect.com
Web: www.clpdirect.com

ConTaFree Liquids
Quest Biomedical, The Exchange, 24 Haslucks Green Road, Shirley, Solihull, West Midlands, UK
B90 2EL
Tel: 00 44 (0)121 744 7674 Fax: 00 44 (0)121 744 0775 Email: sales@questbiomedical.com Web: www.questbiomedical.com

Corning Incorporated
Corning Limited , The Guildway, Old Portsmouth Road, Artington, Surrey GU3 1LR
Tel: (01483) 526520 Fax: (01483) 526798
Web: www.corning.com

Denver Instruments
Denver House, Sovereign Way, Trafalgar Business Park, Downham Market, Norfolk. PE38 9SW
Tel: 0044 1366 386242 Fax: 0044 1366 386204
Email: sales@denverinstrument.co.uk

Drummond Scientific
Alpha Laboratories Ltd.
Tel: 44 23 8048 3000 Email: alpha@alphalabs.co.uk
Web: www.alphalabs.co.uk

ENM Company
5617 Northwest Highway Chicago, IL 60646-6135
Tel: 773 775-8400 Fax: 773 775-5968 Email: support@enmco.com
Web: www.enmco.com

Eppendorf
Eppendorf UK Limited Endurance House Chivers Way Histon Cambridge CB4 9ZR
Tel: (01223) 200 440 Fax (01223) 200 441
Web: www.eppendorf.com.uk

Equibio Limited
The Wheelwrights The Green Boughton Maidstone Kent, ME17 4LT
Web site: http://www.equibio.com

Fisher Scientific
Fisher Scientific UK Ltd Bishop Meadow Road, Loughborough, Leicestershire LE11 5RG
Tel: 01509 231166 Fax: 01509 231893
Web: www.fisher.co.uk

FMC BioProducts Europe
Risingevej 1, DK-2665, Vallensbaek Strand, Denmark
Tel: 42 73 11 22 Fax: 42 73 56 92
Web: www.bioproducts.com/

Fujifilm
PO Box 015, Leamington Spa, Warwickshire, CV 31 YA, England
Tel: 01926 335537 Fax: 01926 887793
Web: www.fujifilm-europe.com/

Gilson
3000 W. Beltline Hwy., PO Box 620027, Middleton, WI 53562
Tel: 608 836 1551, 800 445 7661 Fax: 608 831 4451
Web: www.gilson.com

Grant
Barrington, Cambridge, CB2 5QZ, England
Tel: 01763 260811 Fax: 01763 26241 Email: Marketing@grantinst.co.uk
Web: www.grant.co.uk

Greiner Bio-One
Greiner Bio-One, Inc, 1205 Sarah St, Longwood, FL 32750, USA
Tel: 407.333.2800 Fax: 407.333.3001 Email: INFO@greinerbiooneinc.com
Web: www.greinerbioone.com

Harvard Instruments
22 Pleasant St., South Natick, MA 01760
Tel; 508 655 7000, 800 272 2775 Fax: 508 655 6029

Iiyama
First Floor, Unit 9 Meadway Court Meadway Technology Park Rutherford Close
Stevenage Herts SG1 2EF
Tel: (01438) 745482 Fax: (01438) 745483
Web: www.iiyama.co.uk/

IKA
Janke & Kunkel-Str. 10 D-79219 Staufen Germany / Deutschland
Tel: +49-7633-831-0 Fax: +49-7633-831-98 Email: sales@ika.de
Web: www.ika.net/ika/home.html

Invitrogen
1600 Faraday Avenue, Carlsbad, CA 92008
Tel: 800-955-6288 Fax: 750-603-7201 Email: tech_service@invitrogen.com
Web: www.invitrogen.com

Johnson & Johnson Medical Limited
Coronation Road, Ascot, Berks. SL5 9EY, England
Tel: 01344 871 000 Fax: 01344 872 599

Kimberley Clark
1 Tower View Kings Hill West Malling, Kent ME19 4HA England, U.K.
Tel: (0800) 626008 Fax: (01732)594910
E-mail: consumeruk@kcc.com Web: www.kimberly-clark.com

Labcold
Unit F The Loddon Centre Wade Road Basinstoke Hampshire RG24 8FL
Tel: (o870) 300 1010 Fax: (0870) 300 1004 Email:website@labcold.com
Web: www.labcold.co.uk

Lotus Professional
Sovereign Publications Limited Meridien House 42 Upper Berkeley Street
London W1H 5QJ
Tel: +44 (0)20 7616 0800 Fax: +44 (0)20 7724 1444
Email: webmaster@sovereign-publications.com
Web: www.sovereign-publications.com

LTE Scientific Ltd.
Address: Greenbridge Lane, Greenfield, Oldham, OL3 7EN, England
Tel: 01457 876221 Fax: 01457 870131 Email: mktg@lte.u.net.com

Maple
2414 Major Mackenzie Dr. W. P.O. Box 645 Maple, Ontario L6A 1W5
Tel: 416.410-3128 E-mail: sales@maplecomputers.com
Web: www.maplecomputers.com

Marvel
Nestle UK
Tel: 00800 63785385
Web: www.nestle.co.uk

MD Biosciences
Tel: 0800 0197 200 Email: info@mdbiosciences.com
Web: www.mdbiosciences.com

Mettler
Mettler-Toledo Ltd., 64 Boston Road, Beaumont Leys Leicester, LE4 1AW
Tel: (0116) 235 7070 Email: enquire.mtuk@mt.com
Web: www.mt.com/mthomepage

MSE
97 Avenue Road Beckenham Kent BR3 4RX United Kingdom
Tel: +44 (0)20 8402 4426 Fax: +44 (0)20 8778 7571 Email: info@mseuk.co.uk
Web: www.mseuk.co.uk

New Brunswick Scientific (UK) Ltd.
Edison House, 163 Dixons Hill Road, North Mimms, Hatfield AL9 7JE, England
Tel: 01707 75733 Fax: 01707 67859
Web: www.nbsc.com

New England Biolabs
Knowl Piece, Wilbury Way, Hitchin, Herts SG4 OTY, England
Tel: (01462) 420 616, 0800 318486 Fax: (01462) 421 057, 0800 435682
Email: info@uk.neb.com Web: www.uk.neb.com

Nikon UK Ltd.
Nikon House, 380 Richmond Road, Kingston upon Thames, Surrey KT2 5PR, England
Tel: 0181 541 4440 Fax: 0181 541 4584
Web: www.nikon.co.uk

Nunc
Nalge Nunc International 2000 N. Aurora Rd., Naperville, IL 60563-1796
Tel : 630 983 5700, 800 288 6862, 800 416 6862 Fax: 630 416 2556, 630 416 2519
Web: www.nalgenunc.com

Olympus
8 Honduras Street, London, EC1Y 0TX, England
Tel: 0171 250 4069 Fax: 0171 250 4677 Email: SimonShelley@compuserve.com
Web: www.olympus.europa.com

Panasonic
Panasonic House Willoughby Road Bracknell Berkshire RG12 8FP
United Kingdom
Web: www.panasonic.co.uk

Pechiney Plastic Packaging
Email: contactpharma_europe@alcan.com
Web: www.pechineyplasticpackagingcom

Perbio
Medical Supply Co. Ltd Damastown Mulhuddart Dublin 15 Ireland
Tel: +35318224222 Fax: +35318224100 Email: info@medicalsupply.ie
Web: www.pewrbio.com

Perkin Elmer
549 Albany Street Boston, MA 02118, USA
Tel: 617-482-9595 Email: ProductInfo@perkinelmer.com
Web: www.perkinelmer.com

Pierce
Perbio Science UK Ltd. Century House, High Street, Tattenhall, Cheshire CH3 9RJ, United Kingdom
Tel: (01829) 771 744 Fax: (01829) 771 644 Email: uk.info@perbio.com
Web: www.piercenet.com

Plastibrand
BiocomDirect, 6 Lomond Crescent, Bridge of Weir, PA11 3HJ, United Kingdom
Tel: +44 1505 615973 Fax: +44 1505 615976 Email: info@biocomdirect.com

Qiagen
Qiagen House Fleming Way Crawley West Sussex RH10 9NQ
Tel: 01293-422-922 Email: customercare-uk@qiagen.com
Web: www1.quigen.com

Rodwell Scientific Instruments
Rodwell Scientific Instruments Bentalls Pipps Hill Industrial Estate Basildon Essex SS14 3SD England
Tel: +44 (0)1268 286646 Fax: +44 (0)1268 287799
Email: sales@rodwell-autoclave.com Web: www.rodwell-autoclave.com

Sanyo Gallenkamp PLC
Park House, Meridian East, Meridian Business Park, Leicester LE3 2UZ, England
Tel: 0116 2630530 Fax: 0116 2630353 Email: 100633.127@compuserv.com

Sarstedt
68 Boston Road Beaumont Leys Leicester LE4 1AW United Kingdom
Tel.: +44 1162 359023 Fax: +44 1162 366099 E-mail: info@sarstedt.com
Web: www.sarstedt.com

Schott Duran
Schott Corp. 3 Odell Plaza, Yonkers, NY 10701
Tel: 914 968 8900, 800 633 4505 Fax: 914 968 8585

Scientific Industries
Jencons-PLS Unit 6, Forest Row Business Park Station Road Forest Row East Sussex RH18 5DW UK
Tel: (01342) 826836 Fax: (01342) 826771 Email: uksales@jencons.co.uk
Web: http://www.scientificindustries.com

Scientific Laboratory Supplies
Wilford Industrial Estate Ruddington Lane Wilford Nottingham NG11 7EP
Tel: +44 (0)115 982 1111 Fax: +44 (0)115 982 5275
Web: http://www.scientific-labs.net

Scotsman
Frimont S.p.a. - Via Puccini, 22 20010 Bettolino di Pogliano - Milan - Italy
Tel: +39-02-939601 Fax: +39-02-93550500 Email: scotsman.europe@frimont.it
Web: http://www.scotsman-ice.com

Seiko Instruments Inc
Micro Printer Division 2990 West Lomita Blvd. Torrance CA 90505
Tel: (800) 553-6570 Fax: (310) 517-8154 E-mail: siumpd.id@salessupport.com
Web: www.seikoinstruments.com

Sigma
Sigma-Aldrich Company Ltd., The Old Brickyard, New Road, Gillingham, Dorset, SP8 4XT
Tel: 0800 717181 Fax: 0800 378785 E-mail: ukorders@eurnotes.sial.com
Web: www.sigma-aldrich.com

Sony
Email: sales.gb@sonystyle-europe.com
Web: www.sony.co.uk

Starlab
4 Tanners Drive Blakelands Milton Keynes MK14 5NA Great Britain
Tel: (01908) 283800 Fax: (01908) 283802 E-mail: info@starlab.co.uk
Web: www.starlab.de/uk/corp

Stuart Scientific
Beacon Road Stone Staffordshire ST15 0SA UK
Tel: +44 (0) 1785 – 812121 Fax: +44 (0) 1785 – 813748
E-mail: bsl@barloworld-scientific.com Web: www.barloworld-scientific.com

Swann-Morton
Owlerton Green Sheffield S6 2BJ
Tel: +44 (0)114 234 4231 Fax: +44 (0)114 231 4966 Email: info@swann-morton.com
Web: www.swannmorton.com

Techne
Barloworld Scientific Ltd Beacon Road Stone Staffordshire ST15 0SA UK
Tel: +44 (0)1785 812121 Fax: +44 (0)1785 813748
Web: www.techne.com

Terinex
Terinex Limited Hammond Road Elms Estate Bedford MK41 0ND England
Tel: +44 (0) 1234 364411 Fax: +44 (0) 1234 271486 Email: info@terinex.co.uk
Web: http://www.terinex.co.uk

Walker Safety Cabinets Limited
Unit 1, Howard Town Mills Mill Street Glossop Derbyshire SK13 8PT
Tel: (001457) 864936 Fax: (01457) 857377 Email: sales@walkersafetycabinets.co.uk
Web: www.walkersafetycabinets.co.uk